

APPENDIX B

**CONCEPTUAL MODEL FOR THE HOUSTON-GALVESTON-
BRAZORIA NONATTAINMENT AREA FOR THE 2015 EIGHT-
HOUR OZONE NATIONAL AMBIENT AIR QUALITY
STANDARD**

Houston-Galveston-Brazoria Moderate Area Attainment
Demonstration State Implementation Plan Revision for the
2015 Eight-Hour Ozone National Ambient Air Quality Standard
Project Number 2022-022-SIP-NR

Proposal
May 31, 2023

EXECUTIVE SUMMARY

This conceptual model provides a detailed examination of ozone formation in the Houston-Galveston-Brazoria (HGB) area with a focus on ozone levels above 70 parts per billion (ppb). Ozone is not directly emitted into the atmosphere, but rather formed through a photochemical reaction with nitrogen oxides (NO_x) and volatile organic compounds (VOC). Most of the analyses in this conceptual model focus on ten years of ozone season (March through October) data from 2012 through 2021. The analyses focus on changes in how, when, and where ozone forms in the HGB area.

From 2012 through 2021, ozone concentrations in the HGB area decreased by 13%, with most decreases occurring prior to 2014. Over that same time, there was almost no change in ambient NO_x concentrations and increases in ambient VOC concentrations, including highly reactive VOC (HRVOC). Emissions of NO_x, VOC, and HRVOC also show little change.

The analyses in the conceptual model support the following conclusions regarding ozone formation in the HGB area.

- Ozone formation peaks from April through June and then again from August through October, with a mid-summer minimum occurring in July.
- High ozone typically occurs on hot sunny days with dry conditions and slow recirculating winds.
- Wind direction plays an important role in the location of high ozone, with monitors downwind of the urban area or the Houston Ship Channel observing the highest ozone concentrations. This causes the location of the highest ozone, which often occurs at Manvel, Bayland Park, and Aldine, to change from year to year.
- Point source emissions in the Houston Ship Channel combine with urban area emissions to create ozone at downwind monitors.
- Although the HGB area produces much of its own ozone, there are also high ozone days that are associated with continental transport from the north and northeast.
- Increases in NO_x and VOC were observed in 2021 in the Houston Ship Channel, indicating possible increases in emissions from sources in the area.
- The reactivity weighted composition of VOC in the HGB area is composed of mostly HRVOC; reductions in these compounds are likely to be more impactful on the ozone concentrations compared to equal reductions in less reactive VOC.
- The HGB area measures mostly transitional ozone chemistry, meaning reductions in either VOC or NO_x could reduce ozone concentrations. It is likely that controlling NO_x would be more effective at influencing the HGB area design value, although ozone formation may respond to VOC (in particular HRVOC) emission reductions in some parts of the metro area and at certain times of day.

TABLE OF CONTENTS

Executive Summary	i
Table of Contents	ii
List of Tables.....	iv
List of Figures	v
Chapter 1: Introduction.....	1-1
1.1 General Description of Ozone Formation.....	1-1
1.2 Previous Understanding of Ozone Formation in the Houston-Galveston-Brazoria Area	1-1
1.3 Air Monitors in the Houston-Galveston-Brazoria Area.....	1-2
Chapter 2: Ozone Concentrations and Trends	2-1
2.1 Eight-Hour Ozone Design Values.....	2-1
2.2 Fourth-Highest Eight-Hour Ozone	2-4
2.3 Ozone Exceedance Days.....	2-6
2.4 Ozone Season	2-7
2.5 Time of Peak Ozone.....	2-8
2.6 Background Ozone.....	2-10
2.7 Rapid Ozone Formation	2-14
Chapter 3: Ozone Precursor Concentrations and Trends	3-1
3.1 Ambient NO _x Trends.....	3-1
3.2 Ambient VOC Composition and Trends.....	3-5
3.2.1 Ambient VOC and HRVOC Trends	3-5
3.2.2 HRVOC Concentrations by Wind Direction.....	3-12
3.2.3 VOC Composition Trends	3-14
3.3 Ozone Precursor Emissions	3-17
3.3.1 On-Road and Non-Road Emissions Trends	3-17
3.3.2 Point Source Emissions Trends.....	3-18
3.3.3 Point Source Locations.....	3-20
Chapter 4: Ozone Chemistry.....	4-1
4.1 VOC and NO _x Limitations	4-1
4.2 Weekday versus Weekend Analysis.....	4-6
Chapter 5: Meteorology and its Affect on Ozone.....	5-1

5.1 Temperature	5-1
5.2 Relative Humidity	5-2
5.3 Solar Radiation	5-4
5.4 Winds.....	5-4
5.4.1 Wind Speed	5-5
5.4.2 Surface Winds on High Ozone Days	5-7
5.4.3 Upper-Level Winds	5-9
5.4.4 Ozone Concentrations versus Winds.....	5-12
5.5 Meteorologically Adjusted Ozone Concentrations	5-14
Chapter 6: Conclusions	6-1
Chapter 7: References.....	7-1
Chapter 8: Data Sources.....	8-1

LIST OF TABLES

Table 1-1: 2021 Monitor Information for the HGB Area.....	1-4
Table 2-1: Average Time of Maximum One-Hour Ozone in the HGB Area.....	2-9
Table 3-1: VOC Group Definitions	3-14
Table 5-1: Eight-Hour Ozone Statistics in ppb by HYSPLIT Cluster.....	5-12

LIST OF FIGURES

Figure 1-1: 2021 Ozone Monitors in the HGB Area.....	1-3
Figure 2-1: Eight-Hour Ozone Design Values in the HGB Area.....	2-2
Figure 2-2: Eight-Hour Ozone Design Values by Monitor in HGB Area	2-3
Figure 2-3: Eight-Hour Ozone Design Value Maps for the HGB Area.....	2-4
Figure 2-4: Fourth-Highest MDA8 Ozone Concentration by Monitor in the HGB Area	2-6
Figure 2-5: Eight-Hour Ozone Exceedance Days in the HGB Area	2-7
Figure 2-6: Ozone Exceedance Days by Month from 2012 through 2021 in the HGB Area	2-8
Figure 2-7: Average Time of Maximum One-Hour Ozone on Low versus High Eight- Hour Ozone Days in the HGB from 2012 through 2021	2-10
Figure 2-8: Ozone Season Trends in MDA8 Ozone, Background Ozone, and Locally Produced Ozone for High versus Low Ozone Days in the HGB Area.....	2-12
Figure 2-9: Background Ozone versus MDA8 Ozone for the Ozone Season in the HGB Area from 2012 through 2021	2-13
Figure 2-10: Background Ozone, MDA8 Ozone, and Locally Produced Ozone by Month from 2012 through 2021 in the HGB Area.....	2-14
Figure 2-11: Ozone Season Daily-Maximum One-Hour Ozone Increases for High versus Low Ozone Days in the HGB Area	2-15
Figure 2-12: Ozone Season Daily-Maximum One-Hour Ozone Increase versus MDA8 Ozone in the HGB Area from 2012 through 2021	2-16
Figure 2-13: Number of Hours with a One-Hour Ozone Increase of 30 ppb or Greater for the Ozone Season in the HGB Area from 2012 through 2021	2-17
Figure 3-1: Ozone Season NO _x Trends in the HGB Area.....	3-2
Figure 3-2: Monthly NO _x Trends in the HGB Area	3-3
Figure 3-3: Ozone Season Hourly NO _x Trends in the HGB Area.....	3-3
Figure 3-4: Ozone Season NO _x Trends by Monitor in the HGB Area	3-4
Figure 3-5: 2021 Ozone Season NO _x Concentrations and the Change from 2012 Values in the HGB Area	3-5
Figure 3-6: Ozone Season Median and 95th Percentile TNMOC and HRVOC Trends in the HGB Area.....	3-7
Figure 3-7: Monthly TNMOC (top) and HRVOC (bottom) Trends in the HGB Area	3-8
Figure 3-8: Ozone Season Hourly TNMOC (top) and HRVOC (bottom) Trends in the HGB Area	3-9
Figure 3-9: Ozone Season TNMOC (top) and HRVOC (bottom) Concentrations by Monitor in the HGB Area.....	3-10
Figure 3-10: 2021 Ozone Season TNMOC and HRVOC Concentrations and the Change from 2012 Values in the HGB Area.....	3-12

Figure 3-11: Geometric Mean Wind Speed Weighted HRVOC Concentrations by Shifting Wind Bin for the 2021 Ozone Season in the HGB Area	3-14
Figure 3-12: Ozone Season VOC Composition in the HGB Area from 2012 through 2021	3-16
Figure 3-13: Ozone Season MIR Weighted VOC Composition Trends in the HGB Area... 3-17	
Figure 3-14: HGB Area Point Source NO _x Emissions by Site	3-19
Figure 3-15: HGB Area Point Source VOC Emissions by Site	3-19
Figure 3-16: HGB Area Point Source HRVOC Emissions by Site.....	3-20
Figure 3-17: Maps of the 2021 Point Source NO _x Emissions in the HGB Area	3-21
Figure 3-18: Maps of the 2021 Point Source VOC Emissions in the HGB Area	3-22
Figure 3-19: Maps of the 2021 HRVOC Point Source Emissions in the HGB Area.....	3-23
Figure 4-1: Median VOC-to-NO _x Ratios During the Ozone Season in the HGB Area	4-3
Figure 4-2: Median Hourly VOC-to-NO _x Ratios During the Ozone Season from 2012 through 2021 in the HGB Area.....	4-4
Figure 4-3: Frequency of VOC Limited, NO _x Limited, and Transitional Regimes During Ozone Season Mornings from 2012 through 2021 in the HGB Area	4-5
Figure 4-4: Number of Eight-Hour Ozone Exceedance Days by Day of the Week in the HGB Area from 2012 through 2021	4-7
Figure 4-5: Average Ozone Exceedance Days on the Weekdays versus the Weekends from 2012 through 2021 in the HGB Area	4-8
Figure 4-6: Ozone Season 95th Percentile Concentrations by Day of the Week from 2012 through 2021	4-9
Figure 5-1: Ozone Season Daily-Maximum Temperature versus MDA8 Ozone in the HGB Area from 2012 through 2021	5-2
Figure 5-2: Ozone Season Average Mid-Day Relative Humidity versus MDA8 Ozone in the HGB Area from 2012 through 2021	5-3
Figure 5-3: Ozone Season Average Daytime Solar Radiation Versus MDA8 Ozone in the HGB Area from 2012 through 2021	5-4
Figure 5-4: Ozone Season Average Morning Resultant Wind Speed Versus MDA8 Ozone in the HGB Area from 2012 through 2021	5-6
Figure 5-5: Average Morning Resultant Wind Speed in the HGB area from 2012 through 2021.....	5-7
Figure 5-6: Ozone Season Wind Roses on High and Low Ozone Days in the HGB Area from 2012 through 2021	5-8
Figure 5-7: Surface-Level Back-Trajectories at on Ozone Exceedance Days at Four Monitors in the HGB Area from 2017 through 2021	5-9
Figure 5-8: Mean of 72-Hour HYSPLIT Back Trajectory Clusters and Ozone Exceedance Days for the Ozone Season in the HGB Area from 2012 through 2021 ...	5-11
Figure 5-9: One-Hour Ozone Bivariate Polar Plots for the Ozone Season from 2012 through 2021 at Select Monitors in the HGB Area	5-14

Figure 5-10: Meteorologically Adjusted 98th Percentile MDA8 Ozone for May through September at Select Monitors in the HGB Area5-16

Figure 5-11: Meteorologically Adjusted Ozone Trends for May through September in the HGB Area5-17

Figure 5-12: Difference Between Meteorological Adjusted and Observed 98th Percentile MDA8 Ozone Concentrations from May through September in the HGB Area5-18

Disclaimer: Maps in this document were generated by the Air Quality Division of the Texas Commission on Environmental Quality. The products are for informational purposes and may not have been prepared for or be suitable for legal, engineering, or surveying purposes. They do not represent an on-the-ground survey and represent only the approximate relative location of property boundaries. For more information concerning these maps, contact the Air Quality Division at 512-239-1459.

CHAPTER 1: INTRODUCTION

Ozone formation conceptual models characterize ozone trends, precursors, formation, and transport in a geographic area. This information provides a comprehensive picture of not only where and when ozone forms, but also how and why ozone forms in a geographic area. Conceptual models, also known as conceptual descriptions, are required by the United States (U.S.) Environmental Protection Agency (EPA) to accompany ozone photochemical modeling performed for State Implementation Plans (SIP) (EPA 2018). This conceptual model will focus on ozone formation for the Houston-Galveston-Brazoria (HGB) area for the 2015 eight-hour ozone National Ambient Air Quality Standard (NAAQS) of 0.070 parts per million (ppm). This section discusses general ozone formation and includes a summary of previous conceptual models for the HGB area.

1.1 GENERAL DESCRIPTION OF OZONE FORMATION

Ozone is not directly emitted into the atmosphere; it is formed through a complex series of chemical reactions of nitrogen oxide (NO_x) and volatile organic compounds (VOC) in the presence of sunlight. Ozone production is generally associated with relatively clear skies, light winds, abundant sunshine, and warm temperatures. Typically, these meteorological conditions are associated with high-pressure areas that migrate across the U.S. during the summer season. High-pressure areas have two characteristics that encourage ozone formation: light winds and subsidence inversions. Typically, winds circulating around a high-pressure system are too weak to ventilate the urban area well, so local emissions tend to accumulate. Subsidence inversions cap the vertical mixing, further aggravating the situation by concentrating local pollutants near the surface. These meteorological conditions are further affected by the area's geography. Areas near the coast may experience air-mass flow reversals and valleys near mountainous areas may experience air inversions that trap pollution in the air near the surface.

1.2 PREVIOUS UNDERSTANDING OF OZONE FORMATION IN THE HOUSTON-GALVESTON-BRAZORIA AREA

The HGB area, located on the coast of Texas, has exhibited a steadily increasing population and in 2021 had a population of just over seven million (Census Bureau 2022). Eight counties in the HGB area were designated as nonattainment of the original 1979 one-hour ozone NAAQS of 0.12 ppm. Those counties were Brazoria, Chambers, Fort Bend, Galveston, Harris, Liberty, Montgomery, and Waller. Those same eight counties were designated nonattainment for both the 1997 eight-hour ozone NAAQS of 0.08 ppm and the 2008 eight-hour ozone NAAQS of 0.075 ppm. Only six of those eight counties were designated as nonattainment of the 2015 eight-hour ozone NAAQS of 0.070 ppm: Brazoria, Chambers, Fort Bend, Galveston, Harris, and Montgomery.

Although the area has a steadily increasing population, it has shown improvements in ozone and is currently monitoring attainment of the 1979 one-hour ozone NAAQS and the 1997 eight-hour ozone NAAQS. Work remains to achieve attainment of both the 2008 eight-hour ozone NAAQS and the 2015 eight-hour ozone NAAQS.

The previous conceptual model for the HGB area was prepared as part of the serious classification attainment demonstration SIP revision for the 2008 eight-hour ozone NAAQS (TCEQ 2019a). That conceptual model, which focused on data from 2007 through 2016, reached the following conclusions regarding ozone formation in the HGB area.

- Like many other areas in Texas, ozone formation peaks in May and June and then again in August and September, with a mid-summer minimum occurring in July.
- Background ozone concentrations range from 20 parts per billion (ppb) to 30 ppb and have been slowly trending downward.
- Rapid ozone formation is occurring less frequently compared to the early 2000's, likely due to VOC reactivity and ozone production rates decreasing across the area.
- The area around the Houston Ship Channel exhibits more VOC limited conditions while other parts of the HGB area exhibit more transitional to NO_x limited conditions.
- The meteorological characteristics associated with high ozone days include low relative humidity, high temperatures, low wind speeds, and clear skies.
- Recirculation of surface-level winds throughout the day leads to high ozone formation and accumulation.
- Locations downwind of the Houston Ship Channel experience the highest ozone concentrations.

1.3 AIR MONITORS IN THE HOUSTON-GALVESTON-BRAZORIA AREA

The HGB area is the most extensively monitored area in Texas. This conceptual model focuses on monitors in operation in 2021 that measure ozone, ozone precursors, or meteorological parameters. For ozone, the analysis only used data from monitors that report to the EPA, also referred to as regulatory monitors. In 2021, the HGB area had 45 monitors measuring some combination of ozone, ozone precursors and meteorology, with 21 of those monitors measuring regulatory quality ozone data. The location of the ozone monitors is shown in Figure 1-1: *2021 Ozone Monitors in the HGB Area*. Details on each monitor, including the parameters measured, are in Table 1-1: *2021 Monitor Information for the HGB Area*. More detail on nonregulatory monitors, monitor locations, and other parameters measured per monitor can be found on the Texas Commission on Environmental Quality (TCEQ) [Air Monitoring Sites](https://www.tceq.texas.gov/airquality/monops/sites/air-mon-sites) webpage (<https://www.tceq.texas.gov/airquality/monops/sites/air-mon-sites>). Monitors will be referenced by their monitor abbreviation for the rest of the conceptual model. The conceptual model uses regulatory ozone data from EPA's Air Quality System (AQS) data mart and all other data is from TCEQ's Texas Air Monitoring Information System (TAMIS).

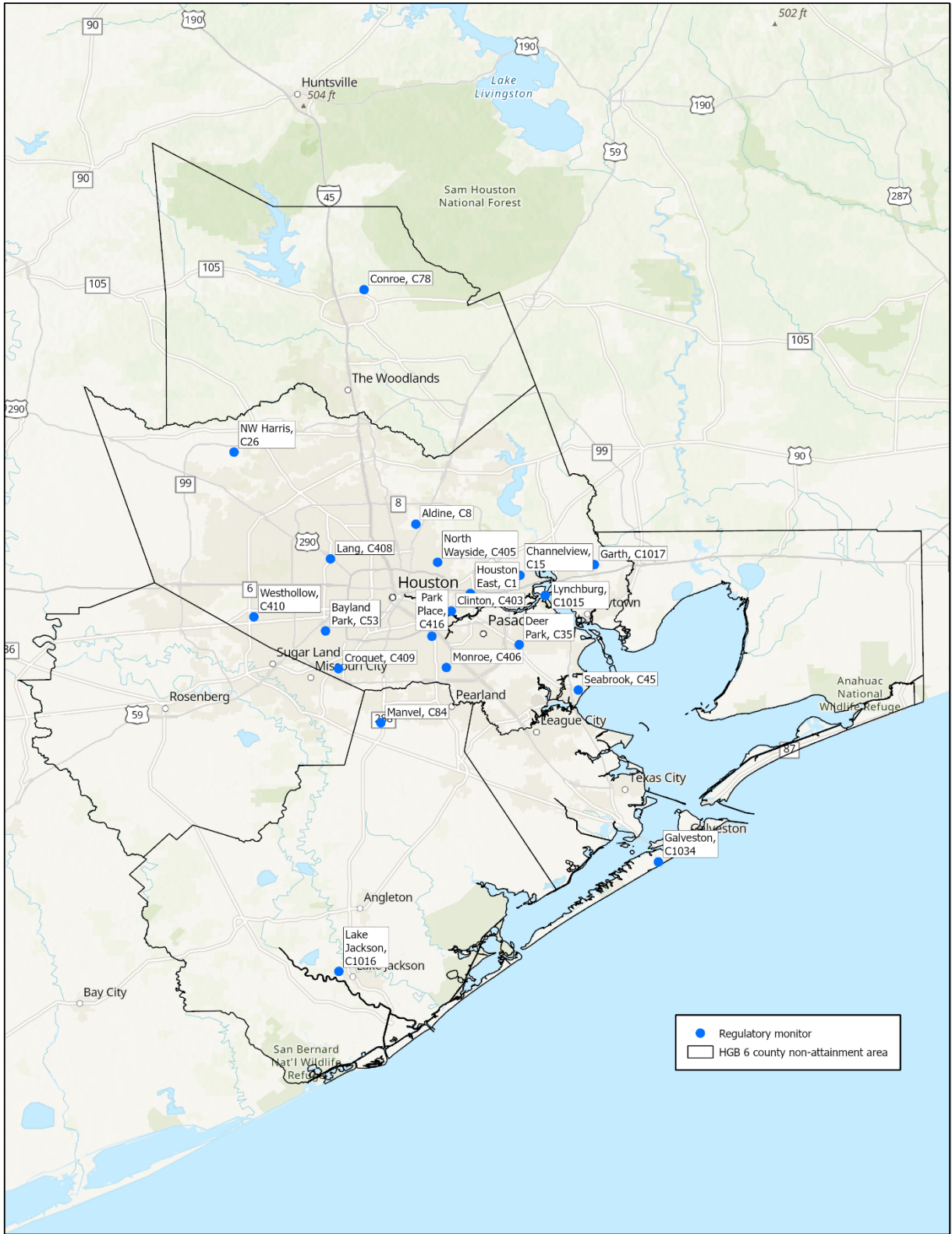


Figure 1-1: 2021 Ozone Monitors in the HGB Area

Table 1-1: 2021 Monitor Information for the HGB Area

Monitor Name	Abbreviation	AQS No.	CAMS No. ¹	Regulatory for Ozone	Compounds or Parameters Measured
Clute	Clute	480391003	0011		Temperature, Wind Direction, Wind Speed, VOC (Canister)
Manvel Croix Park	Manvel	480391004	0084	Y	Ozone, NO _x , NO, NO ₂ , Temperature, Wind Direction, Wind Speed
Freeport South Avenue I	Freeport	480391012	1012		Temperature, Wind Direction, Wind Speed
Lake Jackson	Lake Jackson	480391016	1016	Y	Ozone, NO _x , NO, NO ₂ , Temperature, Solar Radiation, Wind Direction, Wind Speed, VOC (auto-GC)
Oyster Creek	Oyster Creek	480391607	1607		NO _x , NO, NO ₂ , Temperature, Wind Direction, Wind Speed, VOC auto-GC)
Smith Point Hawkins Camp	Smith Point	480710013	0096, 0638		Temperature, Wind Direction, Wind Speed
Texas City Ball Park	Texas City Ball Park	481670005	0147, 1022		Temperature, Wind Direction, Wind Speed, VOC (Canister)
Texas City 34th Street	Texas City	481670056	0620		NO _x , NO _x , NO ₂ , Net Radiation, Temperature, Wind Direction, Wind Speed, VOC (auto-GC)
Galveston 99th Street	Galveston	481671034	1034	Y	Ozone, NO _x , NO, NO ₂ , Dew Point, Temperature, Relative Humidity, Solar Radiation, Wind Direction, Wind Speed
Galveston Airport KGLS	Galveston Airport	481675005	5005		Dew Point

Monitor Name	Abbreviation	AQS No.	CAMS No. ¹	Regulatory for Ozone	Compounds or Parameters Measured
Houston Aldine	Aldine	482010024	0008, 0108, 0150	Y	Ozone, NO _x , NO _y , NO, NO ₂ , Pressure, Dew Point, Temperature, Relative Humidity, Solar Radiation, Wind Direction, Wind Speed
Channelview	Channelview	482010026	0015, 0115	Y	Ozone, NO _x , NO, NO ₂ , Dew Point, Temperature, Relative Humidity, Solar Radiation, Wind Direction, Wind Speed, VOC (auto-GC)
Northwest Harris County	NW Harris	482010029	0026, 0110, 0154	Y	Ozone, NO _x , NO, NO ₂ , Dew Point, Temperature, Relative Humidity, Solar Radiation, Wind Direction, Wind Speed
Channelview Drive Water Tower	CView Water Tower	482010036	1036		Temperature, Wind Direction, Wind Speed, VOC (Canister), VOC (auto-GC)
Houston North Wayside	North Wayside	482010046	0405, 1033	Y	Ozone, Temperature, Wind Direction, Wind Speed
Lang	Lang	482010047	0408	Y	Ozone, NO _x , NO, NO ₂
Houston Croquet	Croquet	482010051	0409	Y	Ozone, Temperature, Wind Direction, Wind Speed
Houston Bayland Park	Bayland Park	482010055	0053, 0146, 0181	Y	Ozone, NO _x , NO, NO ₂ , Temperature, Solar Radiation, Wind Direction, Wind Speed, VOC (Canister)
Galena Park	Galena Park	482010057	0167, 1667		Temperature, Wind Direction, Wind Speed, VOC (Canister), VOC (auto-GC)

Monitor Name	Abbreviation	AQS No.	CAMS No. ¹	Regulatory for Ozone	Compounds or Parameters Measured
Baytown	Baytown	482010058	0148		Temperature, Wind Direction, Wind Speed, VOC (Canister)
Houston Kirkpatrick	Kirkpatrick	482010060	0404		Temperature, Wind Direction, Wind Speed
Shore Acres	Shore Acres	482010061	0145		Temperature, Wind Direction, Wind Speed, VOC (Canister)
Houston Monroe	Monroe	482010062	0406	Y	Ozone, Precipitation
Houston Westhollow	Westhollow	482010066	0410, 3003	Y	Ozone, Temperature, Wind Direction, Wind Speed
Milby Park	Milby Park	482010069	0169		Temperature, Wind Direction, Wind Speed, VOC (auto-GC)
Manchester East Avenue N	Manchester	482010307	1029		Temperature, Wind Direction, Wind Speed, VOC (Canister)
Park Place	Park Place	482010416	0416	Y	Ozone, NO _x , NO, NO ₂ , Pressure, Dew Point, Temperature, Precipitation, Relative Humidity, Solar Radiation, UV Radiation, Wind Direction, Wind Speed
Houston Harvard Street	Harvard	482010417	0417	Y	Ozone, NO _x , NO, NO ₂
Wallisville Road	Wallisville	482010617	0617		NO _x , NO, NO ₂ , Net Radiation, Temperature, Wind Direction, Wind Speed, VOC (auto-GC)
HRM #3 Haden Rd	HRM 3	482010803	0114, 0603		NO _x , NO, NO ₂ , Net Radiation, Temperature, Wind Direction, Wind Speed, VOC (Canister), VOC (auto-GC)

Monitor Name	Abbreviation	AQS No.	CAMS No. ¹	Regulatory for Ozone	Compounds or Parameters Measured
HRM 7 Baytown	HRM 7	482010807	0607		Temperature, Wind Direction, Wind Speed, VOC (auto-GC)
Lynchburg Ferry	Lynchburg	482011015	0165, 1015	Y	Ozone, NO _x , NO, NO ₂ , Temperature, Solar Radiation, Wind Direction, Wind Speed, VOC (Canister), VOC (auto-GC)
Baytown Garth	Garth	482011017	1017	Y	Ozone, Temperature, Solar Radiation, Wind Direction, Wind Speed
Houston East	Houston East	482011034	0001	Y	Ozone, NO _x , NO, NO ₂ , Temperature, Wind Direction, Wind Speed
Clinton	Clinton	482011035	0055, 0113, 0304, 0403	Y	Ozone, NO _x , NO, NO ₂ , Pressure, Dew Point, Temperature, Precipitation, Relative Humidity, Solar Radiation, UV Radiation, Wind Direction, Wind Speed, Formaldehyde, VOC (auto-GC)
Houston Deer Park #2	Deer Park	482011039	0035, 0139, 0235, 1001, 3000	Y	Ozone, NO _x , NO, NO ₂ , Pressure, Dew Point, Temperature, Precipitation, Relative Humidity, Solar Radiation, UV Radiation, Wind Direction, Wind Speed, VOC (Canister), Formaldehyde, VOC (auto-GC)
La Porte Airport C243	La Porte	482011043	0243		Temperature, Precipitation, Wind Direction, Wind Speed

Monitor Name	Abbreviation	AQS No.	CAMS No. ¹	Regulatory for Ozone	Compounds or Parameters Measured
Pasadena North	Pasadena	482011049	1049		Temperature, Wind Direction, Wind Speed, VOC (Canister)
Seabrook Friendship Park	Seabrook	482011050	0045	Y	Ozone, NO _x , NO, NO ₂ , Temperature, Solar Radiation, Wind Direction, Wind Speed
Houston North Loop	North Loop	482011052	1052		NO _x , NO, NO ₂ , Temperature, Wind Direction, Wind Speed
Houston Southwest Freeway	Southwest Freeway	482011066	1066		NO _x , NO, NO ₂ , Temperature, Wind Direction, Wind Speed
HRM 16-Deer Park	HRM 16	482011614	1614		Temperature, Wind Direction, Wind Speed, VOC (auto-GC)
Cesar Chavez	Cesar Chavez	482016000	0078		Temperature, Wind Direction, Wind Speed, VOC (auto-GC)
Conroe Relocated	Conroe	483390078	0078	Y	Ozone, NO _x , NO, NO ₂ , Temperature, Solar Radiation, Wind Direction, Wind Speed

1: CAMS: Continuous Air Monitors System

CHAPTER 2: OZONE CONCENTRATIONS AND TRENDS

To characterize the current ozone situation in the HGB area, this conceptual model focuses on ozone concentrations from 2012 through 2021. This section reviews ozone data in various forms to characterize where, when, and how ozone forms in the HGB area.

2.1 EIGHT-HOUR OZONE DESIGN VALUES

Ozone design values are statistics used to compare an area's ozone concentration to the ozone National Ambient Air Quality Standards (NAAQS). The design value for the 2015 eight-hour ozone NAAQS is calculated by averaging the fourth-highest daily-maximum eight-hour averaged (MDA8) ozone concentration over three years. Ozone design values are calculated for each monitor, and then the monitor with the highest design value sets the design value for the area. A monitor exceeds the 2015 eight-hour ozone NAAQS when its design value exceeds 0.070 parts per million (ppm), or 70 parts per billion (ppb), and a monitor exceeds the 2008 eight-hour ozone NAAQS when its design value exceeds 0.075 ppm, or 75 ppb.

The eight-hour ozone design value trend for the HGB area is displayed in Figure 2-1: *Eight-Hour Ozone Design Values in the HGB Area*. The 2021 eight-hour ozone design value for the HGB nonattainment area is 77 ppb, which is the lowest eight-hour ozone design value ever recorded in the HGB area. This design value represents a 13% decrease from the 2012 design value of 88 ppb. Between 2012 and 2021, the largest decrease in the HGB design value occurred from 2013 to 2014, when it dropped by 7 ppb. After 2014, the HGB area design value decreases slowed. Decreases may be due to changes in meteorology, background ozone, and/or emissions, which will be examined in later chapters.

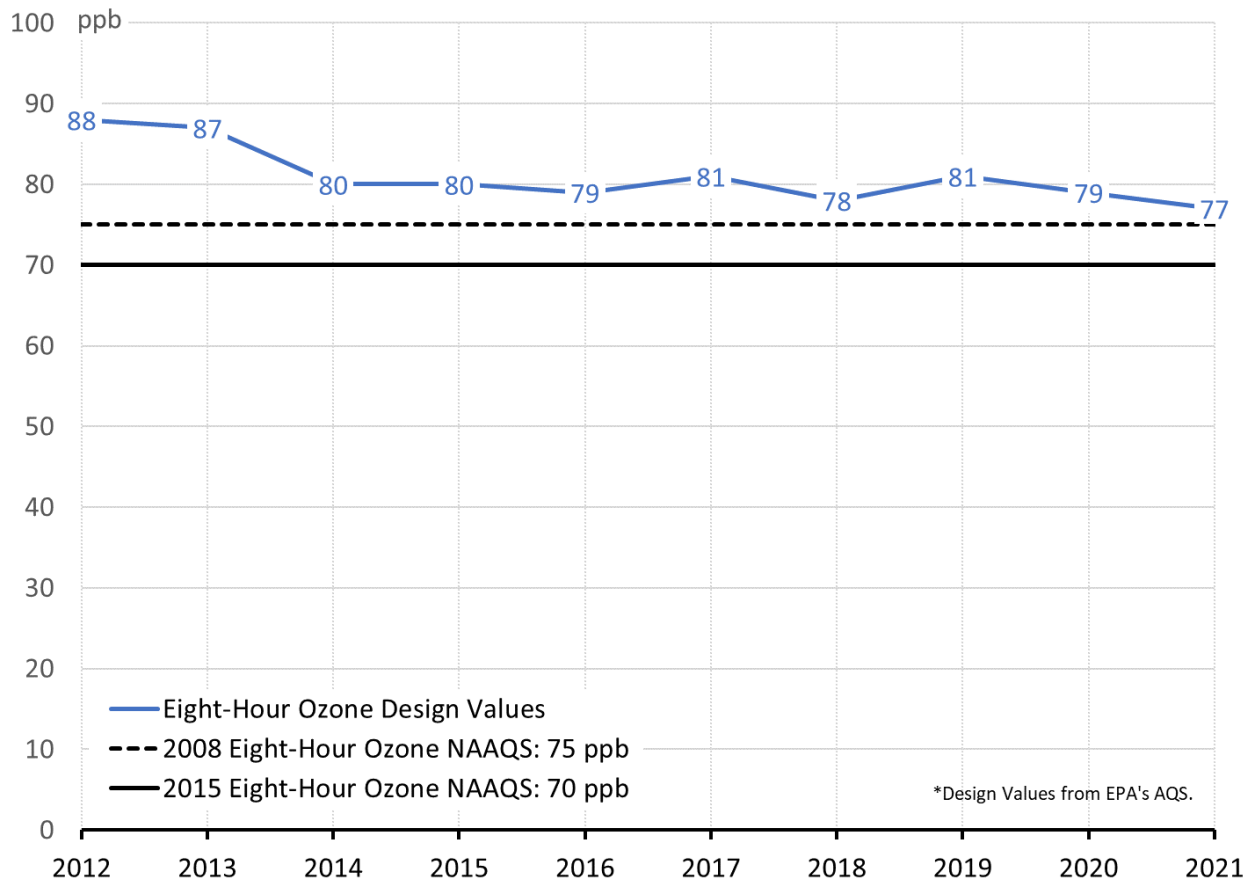


Figure 2-1: Eight-Hour Ozone Design Values in the HGB Area

Because ozone varies spatially, it is also prudent to investigate trends at all monitors in an area. Figure 2-2: *Eight-Hour Ozone Design Values by Monitor in the HGB Area* displays the eight-hour design values from 2012 through 2021 at each monitor in the HGB area. The individual monitors’ trends are less important for assessing trends than the overall range in design values across the area. Figure 2-2 demonstrates that design values have been decreasing across the HGB area and not only at the monitor with the highest design value. Prior to 2013, no monitors in the HGB area measured below the 2015 eight-hour ozone NAAQS. As of 2021, over half of the monitors in the HGB area measure below the 2015 eight-hour ozone NAAQS.

Figure 2-2 also shows how the monitor with the highest eight-hour ozone design value in the HGB area has changed over time. From 2012 through 2015, Manvel observed eight-hour ozone design values several ppb higher than other monitors. From 2016 to 2020, the highest design value was at Aldine. Bayland Park observed the highest eight-hour ozone design value in 2021. Most years show a difference of several ppb between the maximum design value and the second highest design value.

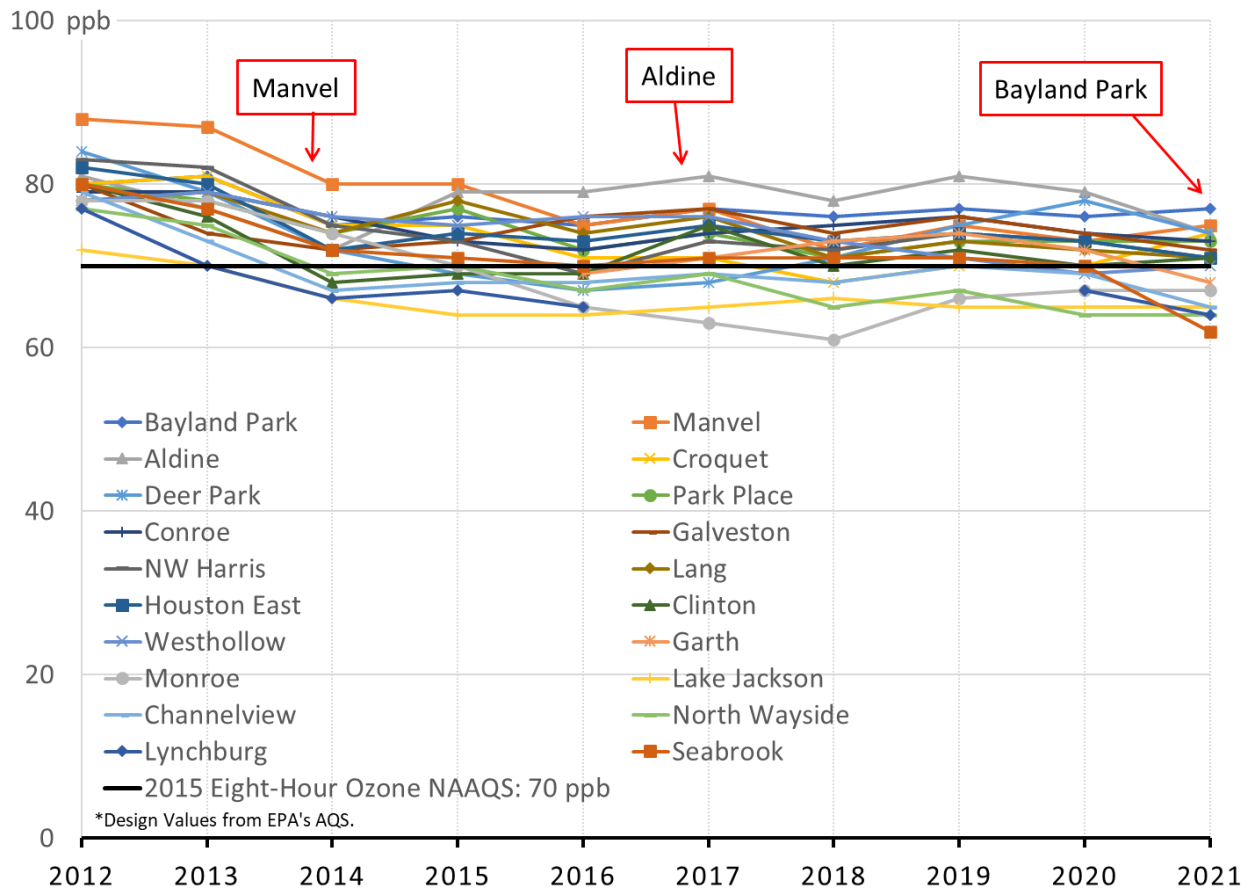


Figure 2-2: Eight-Hour Ozone Design Values by Monitor in HGB Area

Displaying monitor level eight-hour ozone design values on a map can give better insight into ozone formation patterns within the HGB area. Kriging interpolation was used to determine the spatial variation of eight-hour ozone design values across the HGB area for 2012, 2016, and 2021.¹ The maps of those values for three different years are displayed in Figure 2-3: *Eight-Hour Ozone Design Value Maps for the HGB Area*. Only the monitors with the maximum eight-hour ozone design value in the HGB area for each year are labeled on the maps. The maps demonstrate how much eight-hour ozone design values have decreased across the entire HGB area. All monitors in 2012 were above the 2015 ozone NAAQS, but by 2021 many monitors were below the 2015 ozone NAAQS and only one monitor was above the 2008 ozone NAAQS of 75 ppb.

In addition to the level of the design values, the maps also illustrate the changing location of the minimum and maximum eight-hour ozone design values. The monitor with the maximum design value in 2012, Manvel, is located southwest of the Houston Ship Channel, an area with a large amount of industrial activity. In 2016, the maximum design value was located at Aldine, located north of the Houston Ship Channel. In 2021, the maximum eight-hour ozone design value was located at Bayland Park, north of Manvel and west of the Houston Ship Channel. The location of the minimum eight-

¹ Kriging interpolation is a method of spatial interpolation that uses a limited set of sampled data points to estimate the value of a variable over a continuous spatial field.

hour ozone design value has also changed; however, lower design values for all three of the years shown are observed to the south and in the east central portion of the area. In 2012, higher ozone design values were observed in areas closer to the Houston Ship Channel, such as Deer Park. Design values near the ship channel were much lower in 2016 and 2021, with low design values at Monroe and Lynchburg in 2016 and at Seabrook in 2021. These spatial patterns seem consistent with wind flows in the area and ozone formation dynamics, with lower values observed either upwind or closer to emissions sources and high values observed downwind.

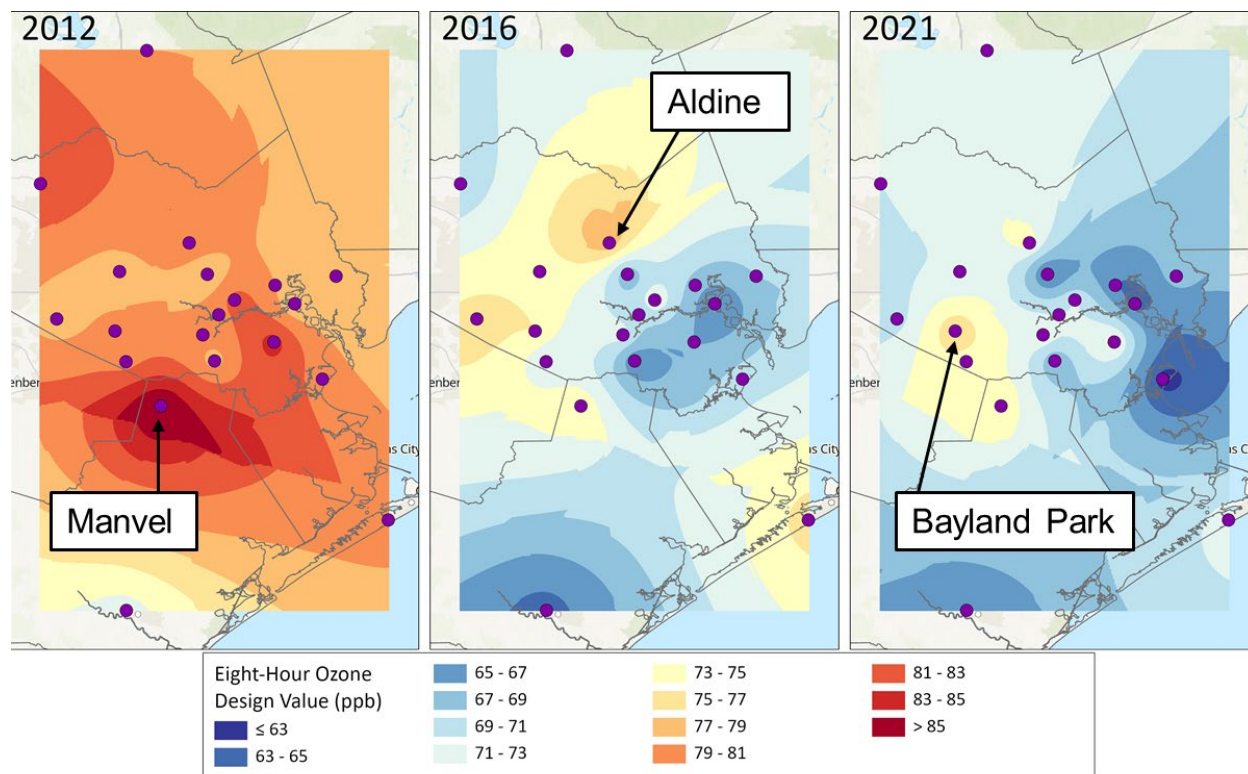


Figure 2-3: Eight-Hour Ozone Design Value Maps for the HGB Area

2.2 FOURTH-HIGHEST EIGHT-HOUR OZONE

Because eight-hour ozone design values are three-year averages, trends tend to be smoother, making year-to-year variations in ozone concentrations due to factors such as meteorology less apparent. Trends in the yearly fourth-highest MDA8 ozone concentrations provide more insight into each individual year. Variability in fourth-highest MDA8 ozone concentrations may indicate what years are more affected by unusual events such as ozone conducive meteorology.

Area-wide fourth-highest MDA8 ozone trends are not very instructive because design values are calculated on a per monitor basis. Instead, fourth-highest MDA8 ozone trends are investigated at each monitor in the HGB area in Figure 2-4: *Fourth-Highest MDA8 Ozone Concentration by Monitor in the HGB Area*. The fourth-highest MDA8 ozone trends span from 2010 though 2021 in order to encompass all years used in the design value trends.

Trends show that there is more variability present in fourth-highest MDA8 ozone values when compared to design values. Fourth-highest MDA8 ozone values decreased from 2010 through 2014, and then stagnated from 2014 through 2021. Most monitors showed an overall decrease in fourth-highest MDA8 ozone from 2010 through 2021, except for Bayland Park, which showed no change, and Croquet, which showed an increase. The fourth-highest MDA8 ozone at Croquet in 2021, 83 ppb, was the highest measured at that monitor since 2011. More data are needed to investigate the high value at Croquet, but it could be due to unusual meteorology or an anomalous event.

The monitor with the maximum fourth-highest MDA8 ozone concentration changes from year to year and is not always the same as the monitor with the areawide maximum design value. This indicates that overall, ozone in the area is not changing very much and that changes at individual monitors are likely due to changes in shifting wind directions on high ozone days rather than changes in emissions.

For most years, individual monitors did not exhibit similar trends and different monitors may have had increasing or decreasing fourth-highest MDA8 ozone values from year to year. This indicates that there may be more local factors influencing ozone concentrations. In 2014 and 2015, almost all monitors exhibit similar trends, with values decreasing area-wide in 2014 and increasing area-wide in 2015. This indicates that ozone concentrations in those years may be strongly influenced by non-local factors such as meteorology. Another notable year in the trend is 2020. Although 2020 did not observe fourth-highest MDA8 ozone values as low as those in 2014, they were lower compared to recent years.

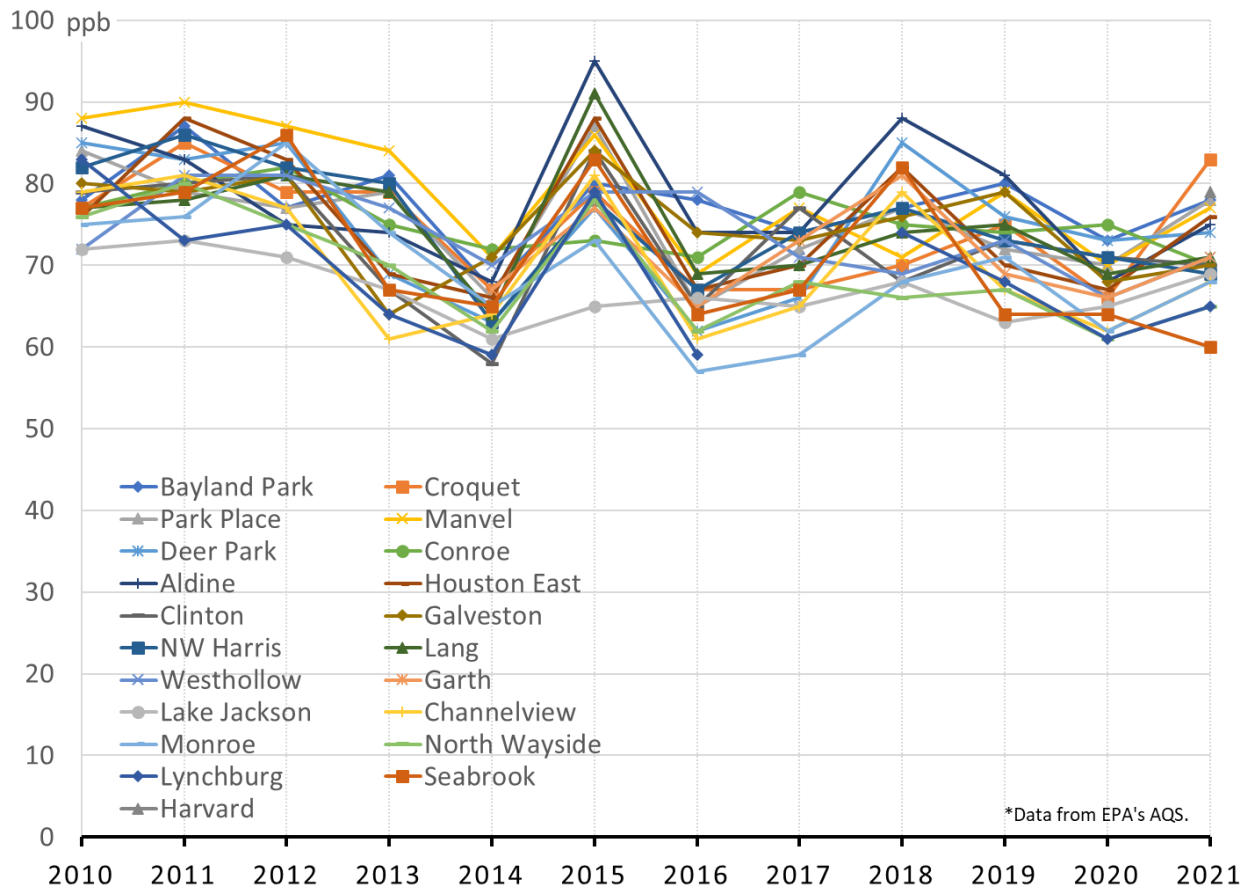


Figure 2-4: Fourth-Highest MDA8 Ozone Concentration by Monitor in the HGB Area

2.3 OZONE EXCEEDANCE DAYS

Ozone trends can also be investigated by looking at the number of days that MDA8 ozone levels were above a NAAQS threshold, termed an ozone exceedance day. For the 2015 eight-hour ozone NAAQS, any day that any monitor in the area measures an MDA8 ozone value greater than 70 ppb is considered an eight-hour ozone exceedance day. Because the number of monitors can influence the number of exceedance days, it is important to look at the number of ozone exceedance days at each individual monitor. When exceedances are calculated for the area, days with multiple monitors with ozone exceedances are only counted as one day.

The number of eight-hour ozone exceedance days for the HGB area is displayed in Figure 2-5: *Eight-Hour Ozone Exceedance Days in the HGB Area*. Although there was an area-wide decrease in exceedance days from 2012 through 2021 of 40%, there was almost no change in exceedance days after 2012. Area-wide trends appear to correlate well with trends at the monitor level. Like with the fourth-highest MDA8 ozone values, there is not a monitor that consistently has the most ozone exceedances. Most monitors observed an overall decrease in ozone exceedance days from 2012 through 2021, but most of that change occurred prior to 2014. After 2014, ozone exceedance day trends have stagnated.

The ozone exceedance day trends vary from year to year with each monitor but in 2014 and 2015 all the monitors exhibited similar trends, as was observed with the fourth-highest MDA8 ozone values. This is further evidence that there was a non-local factor, such as meteorology, that affected the ozone concentrations in those years. The second lowest number of exceedance days was in 2020.

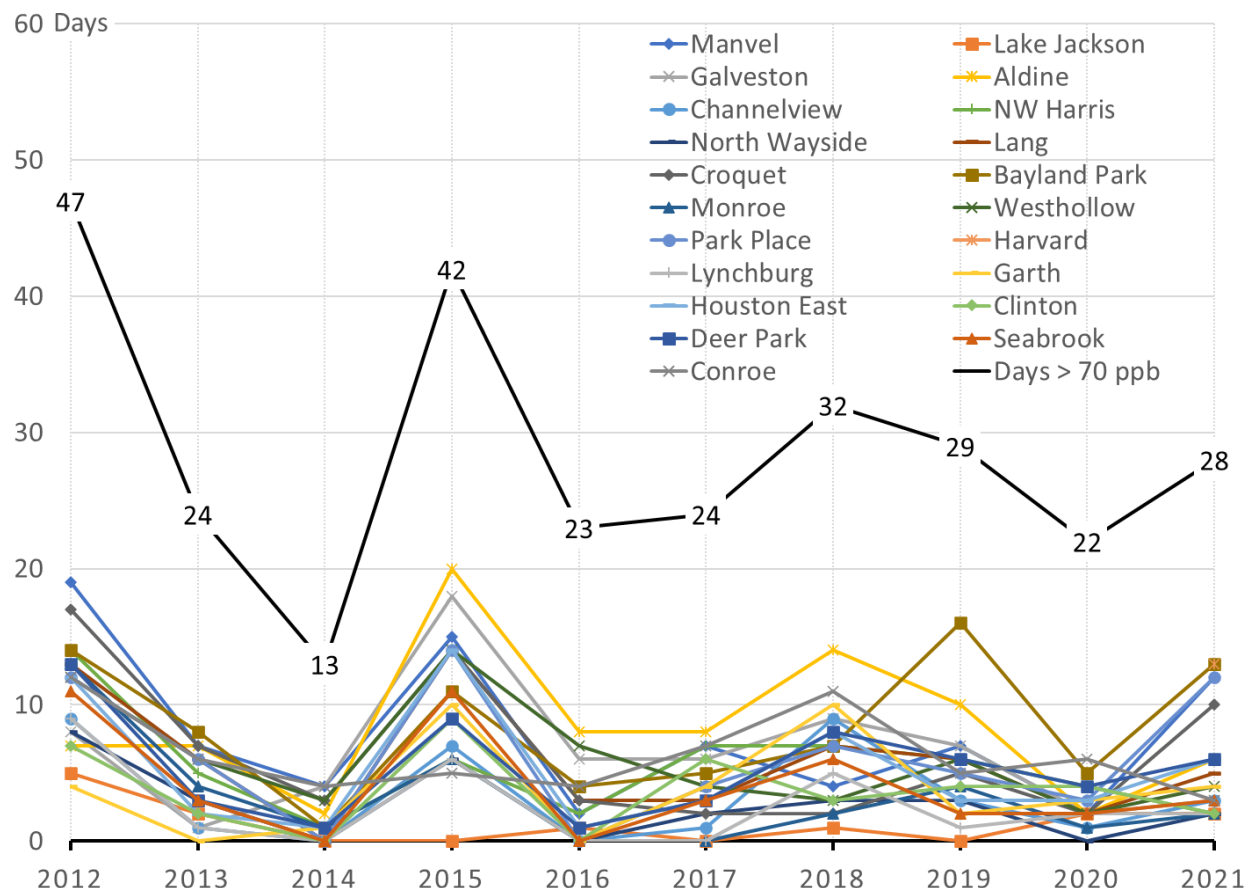


Figure 2-5: Eight-Hour Ozone Exceedance Days in the HGB Area

2.4 OZONE SEASON

Analysis of the ozone season can provide insight into when ozone forms in the HGB area. One way to examine the ozone season is to determine what months observe the most ozone exceedance days. Previous conceptual models for the HGB area and the Dallas-Fort Worth (DFW) area have shown that the ozone season in many areas of Texas has two peaks in ozone exceedance days (TCEQ 2019a, TCEQ 2019b). The first peak occurs in the late spring/early summer months of April through June, and the second peak occurs in the late summer/early fall months of August through October. These areas also exhibit a decrease in high ozone days in July, commonly referred to as the mid-summer minimum in ozone concentrations. This mid-summer minimum is likely caused by the dominance of high pressure in the southeast United States (U.S.), which results in air flow from the Gulf of Mexico over eastern Texas, and hence low background concentrations (Davis et al. 1998, Chan and Vet 2010, Smith et al. 2013). Other things such as the El Nino Southern Oscillation can affect the ozone season

(Edwards 2018). Compared to neutral years, ozone season is worse in the spring during El Nino years and worse in October during La Nina years.

Since the ozone season has been well established in previous conceptual models, this analysis will use newer data to compare eight-hour ozone exceedance days at three ozone levels, which will correspond to the three different eight-hour ozone standards. Results are shown in Figure 2-6: *Ozone Exceedance Days by Month from 2012 through 2021 in the HGB Area*. Results show that in more recent years at all three ozone levels, the ozone season continues to exhibit two peaks with the mid-summer minimum occurring in July. MDA8 ozone values at all three levels are observed from March through October. High ozone occurs most frequently in August at lower ozone levels, but the highest ozone values, those greater than or equal to 85 ppb, occur more frequently in June. This analysis shows that, although the official ozone season in the HGB area occurs year-round, the area is mostly likely to experience high ozone values in March through October. The remainder of this conceptual model will use the months of March through October when referring to the ozone season.

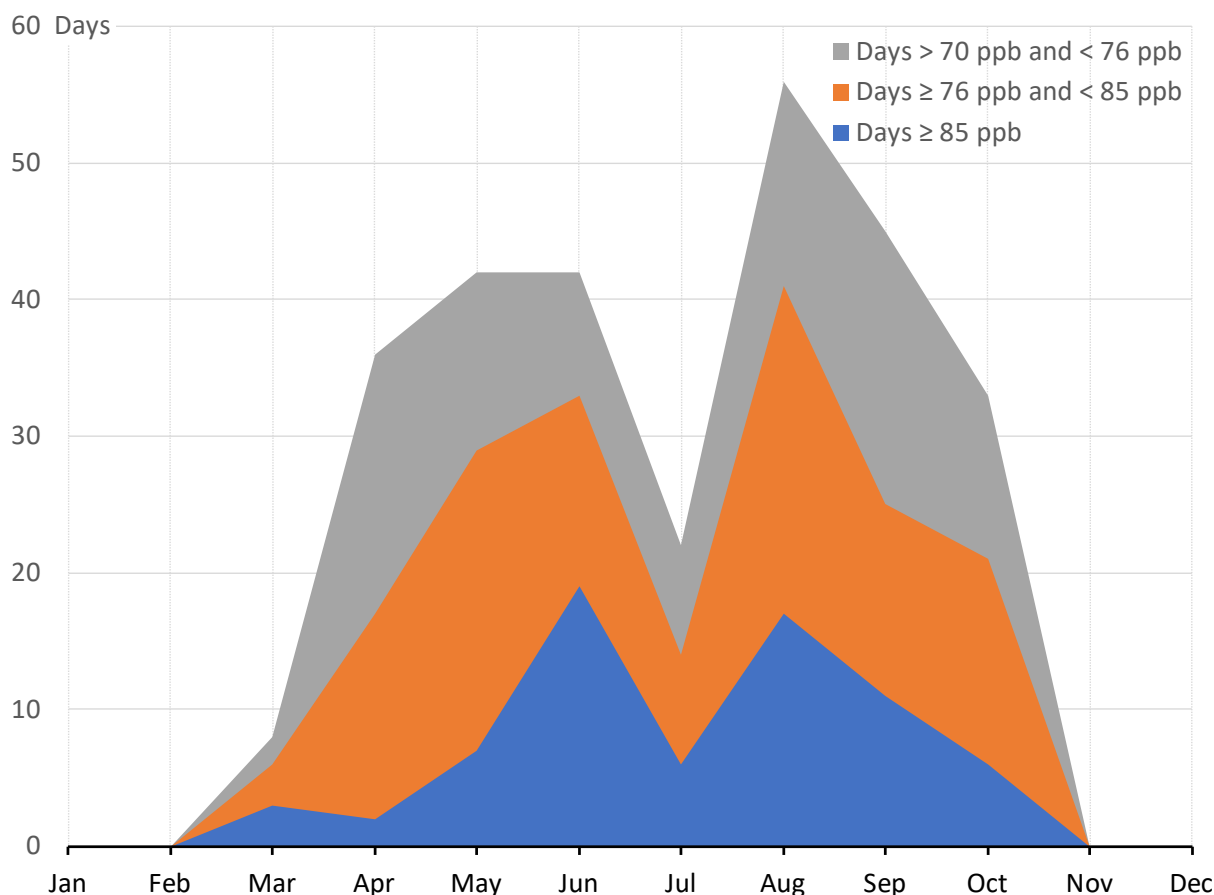


Figure 2-6: Ozone Exceedance Days by Month from 2012 through 2021 in the HGB Area

2.5 TIME OF PEAK OZONE

Another way to investigate when ozone occurs is to look at the time of day that peak ozone occurs. In addition, differences in the time of peak ozone by monitor may give

insight into the origins of ozone formation in the area. This conceptual model used one-hour ozone to determine when the peak occurs. Differences in peak ozone between high ozone days and low ozone days was also investigated, with high ozone days defined as any day with an ozone exceedance, as defined in section 2.3. This definition of high ozone days will be used throughout the remainder of the conceptual model.

The average time of peak one-hour ozone during the ozone season was calculated from 2012 through 2021 for both high and low eight-hour ozone days. The analysis used time values in local standard time (LST). Results are listed in Table 2-1: *Average Time of Maximum One-Hour Ozone in the HGB Area*. Although peak ozone times vary each year, there has not been an overall change in the time of peak ozone over the past ten years. More notable is that ozone peaks later in the day on high ozone days compared to low ozone days. On average, ozone peaks around 12:54 LST on low ozone days but on high ozone days it peaks at around 13:40 LST. This is an indication of slower winds that are typical on high ozone days, which would allow for longer accumulation times for ozone.

Table 2-1: Average Time of Maximum One-Hour Ozone in the HGB Area

Year	Low Ozone Days (LST)	High Ozone Days (LST)	Difference (LST)
2012	12:52	13:33	0:40
2013	12:56	13:26	0:29
2014	13:00	13:33	0:33
2015	12:53	13:49	0:55
2016	13:02	14:01	0:58
2017	13:01	13:31	0:30
2018	12:46	13:37	0:51
2019	12:45	13:50	1:04
2020	13:06	13:43	0:37
2021	12:41	13:39	0:58
Average	12:54	13:40	0:46

Kriging interpolation was used to determine if the time of peak ozone on high versus low ozone days varies spatially. The results are displayed in Figure 2-7: *Average Time of Maximum One-Hour Ozone on Low versus High Eight-Hour Ozone Days in the HGB from 2012 through 2021*. On low ozone days, ozone first peaks around 12:00 LST in the coastal areas near Galveston. On these days, ozone subsequently peaks in a southeast to northwest pattern across the HGB area, with the latest peak occurring around 14:00 LST near Conroe. On high ozone days, ozone peaks almost an hour later area-wide. Instead of the first peak occurring near the coast, on high ozone days, ozone first peaks near the center of the HGB area around the Monroe and Park Place monitors. Ozone then peaks later in the day at the monitors surrounding the HGB area, with the latest peak occurring to the northwest of the area at NW Harris. This may indicate that on high ozone days, ozone is first formed in the center of the HGB area and then transported to the outskirts of the city. These patterns seem consistent with what was observed in previous conceptual models for the HGB area.

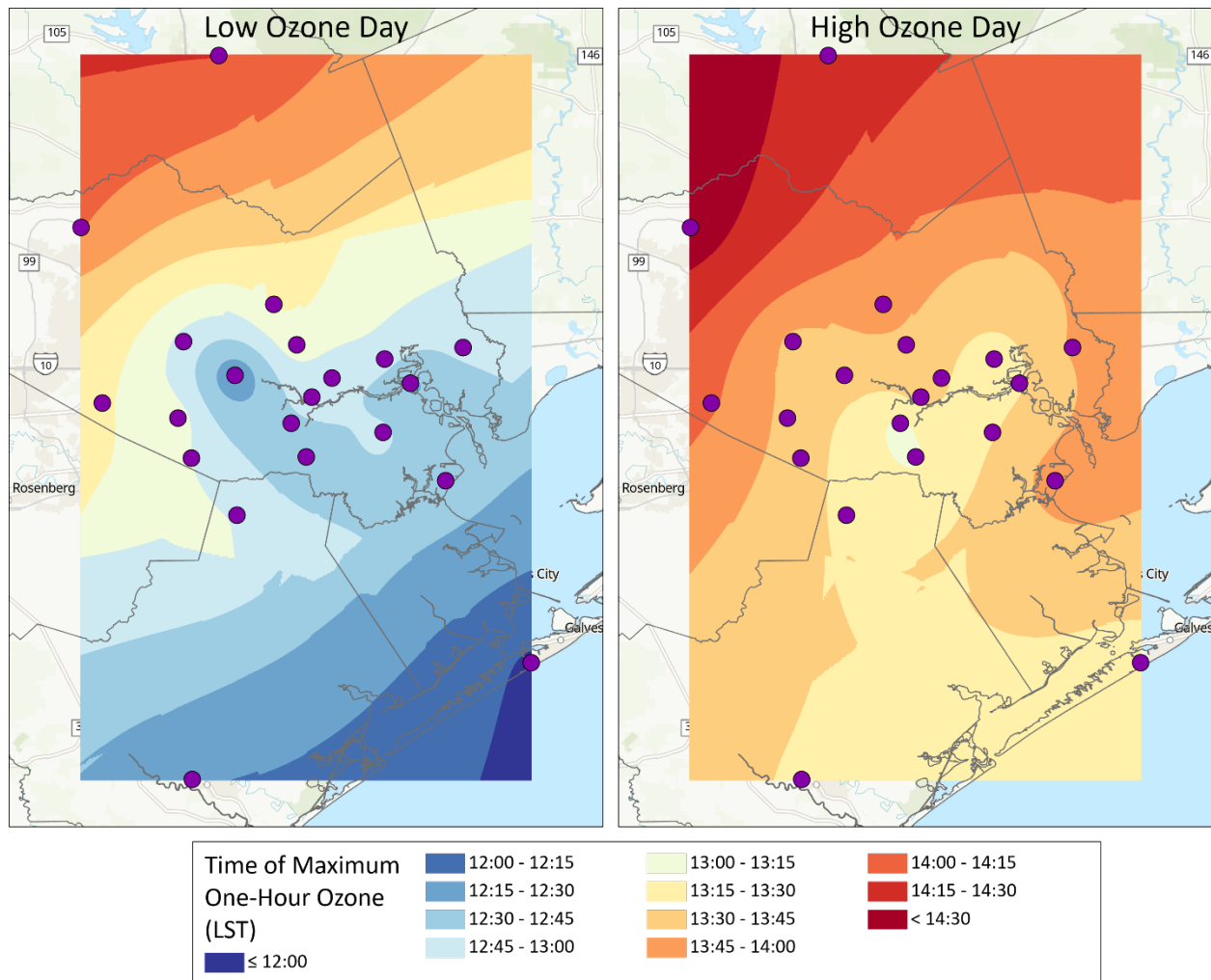


Figure 2-7: Average Time of Maximum One-Hour Ozone on Low versus High Eight-Hour Ozone Days in the HGB from 2012 through 2021

2.6 BACKGROUND OZONE

Regional background ozone, which will be referred to as background ozone for the remainder of this document, reflects the ozone produced from all sources outside of the six-county HGB 2015 ozone NAAQS nonattainment area. There are several ways to estimate regional background ozone, but none of those techniques are a perfectly accurate measure of ozone that would be present in the absence of local emissions. Nonetheless, examination of background ozone provides insight into whether observed ozone changes are from locally produced ozone or from transported ozone. Since background ozone concentrations are not easily controlled, the local component of ozone formation is then the amount of ozone that the area could potentially control to meet the 2015 eight-hour ozone NAAQS.

The technique for estimating background ozone concentrations is similar to methods used by Nielsen-Gammon et al. (2005) and described by Berlin et al. (2013). To estimate background ozone concentrations, monitoring sites capable of measuring background ozone were selected based upon their distance from local emissions sources in the urban core and industrial areas of the HGB area. Each selected site is expected to

receive air with regional background ozone when it is upwind (or at least, not downwind) of the urban and industrial areas. For this analysis, selected sites included Lake Jackson, Manvel, Galveston, Aldine, Channelview, NW Harris, North Wayside, Croquet, Bayland Park, Monroe, Westhollow, Garth, Seabrook, and Conroe. This technique is conservative, in that if a gradient exists in background ozone, the technique will choose the low end of the gradient. In other words, based on observational data, the background ozone cannot be lower than the chosen value.

Background ozone was then estimated as the lowest MDA8 ozone value observed at the selected background sites for each ozone season day from 2012 through 2021. In addition to daily background ozone, locally produced ozone (within the HGB area) was also calculated by subtracting the background ozone concentration from the highest MDA8 ozone value for the area. Results were then separated into low ozone days and high ozone days to investigate if high ozone is due to changes in background ozone or changes in local ozone.

Because ozone data are so skewed, the median is a better summary statistic to use to investigate the central tendency of the background ozone data. The median MDA8 ozone, background ozone, and locally produced ozone was calculated for the ozone season of each year. Figure 2-8: *Ozone Season Trends in MDA8 Ozone, Background Ozone, and Locally Produced Ozone for High versus Low Ozone Days in the HGB Area* shows that the area-wide median background ozone is 26 ppb on low ozone days and 48 ppb on high ozone days. Although background ozone is higher on high ozone days, local ozone production also increases at a proportional rate on these days. For both high and low ozone days background ozone accounts for approximately 60% of the MDA8 ozone and locally produced ozone accounts for approximately 40% of the MDA8 ozone. These findings are corroborated by other studies that used positive matrix factorization to show that background ozone can contribute 59% to 70% of the MDA8 ozone (Soleimanian et al. 2022).

There does not appear to be any trend in either background ozone, MDA8 ozone, or locally produced ozone on low ozone days. On high ozone days, there appears to be a small decrease in background ozone concentrations and a small increase in locally produced ozone concentrations; this results in a flat trend for MDA8 ozone. Low ozone values observed in 2014 appear to be driven by a decrease in background ozone since that same year observed the highest local production on high ozone days from 2012 through 2021. It may be that changes in ozone transport patterns due to meteorology caused lower ozone concentrations in 2014.

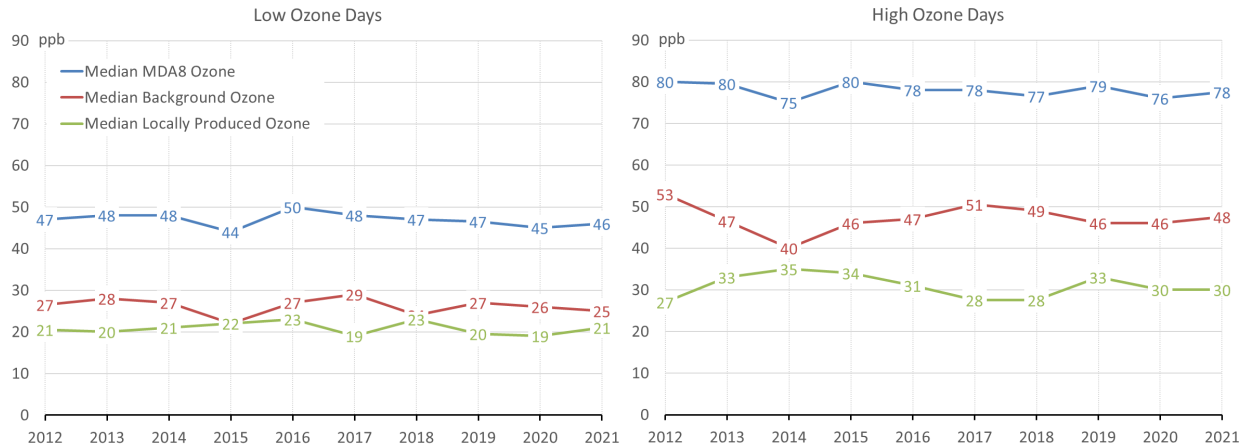


Figure 2-8: Ozone Season Trends in MDA8 Ozone, Background Ozone, and Locally Produced Ozone for High versus Low Ozone Days in the HGB Area

Trends in background ozone for both high and low ozone days show little correlation with MDA8 ozone. This is seen in Figure 2-9: *Background Ozone versus MDA8 Ozone for the Ozone Season in the HGB Area from 2012 through 2021*. Days with an ozone exceedance are marked in red. Ozone data from 2012 through 2021 show that background ozone and MDA8 ozone have little correlation on low ozone days, with a correlation coefficient of 0.56 for low ozone. High ozone days are even less correlated with background ozone, with a correlation coefficient of only 0.08. This indicates that ozone formation in the HGB area is not only driven by transported, or regional background ozone, but that there is a large amount of local ozone formation in the area as well.

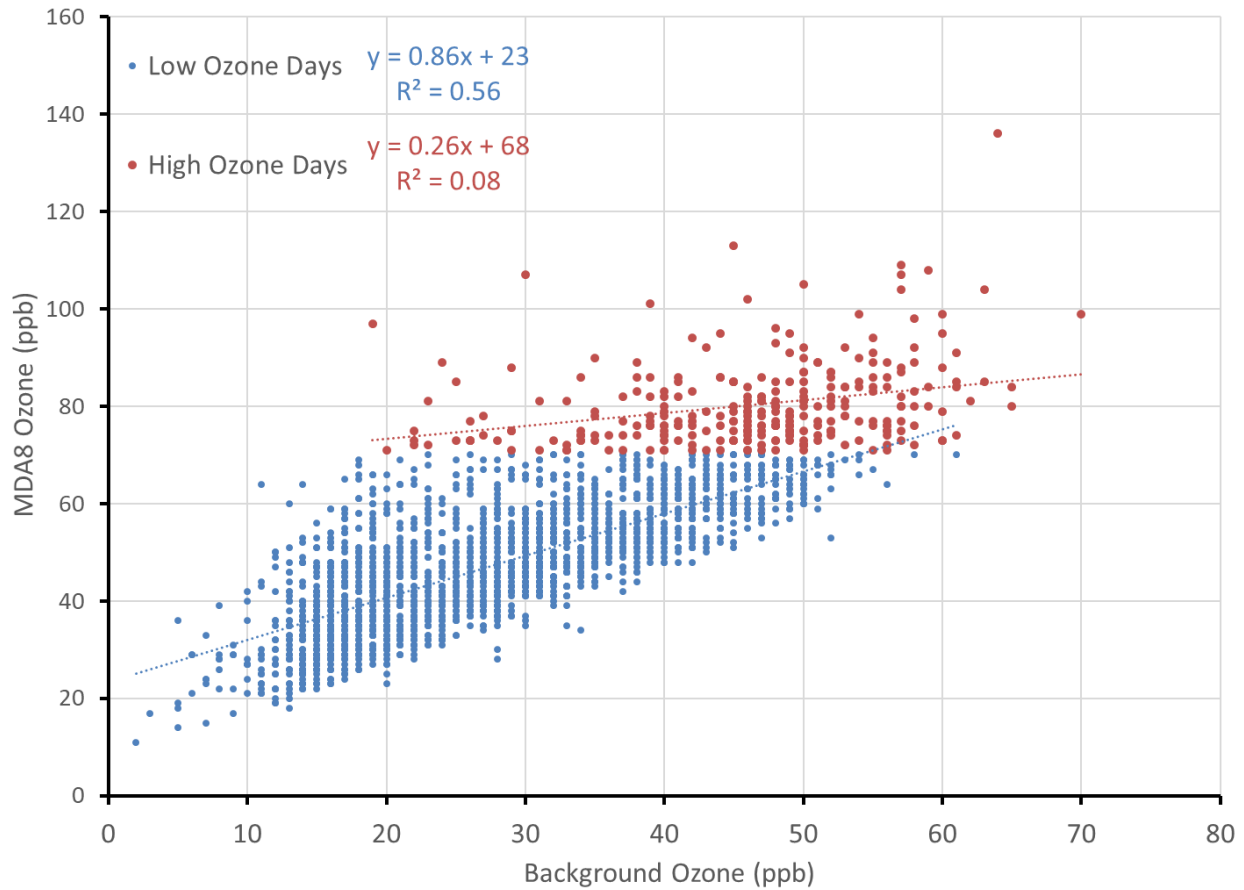


Figure 2-9: Background Ozone versus MDA8 Ozone for the Ozone Season in the HGB Area from 2012 through 2021

Past conceptual models for the HGB area have also found a seasonality in background ozone concentrations, which was also corroborated by other studies (Mountain 2022). To investigate how background ozone may change throughout the ozone season, the median background ozone, median MDA8 ozone, and median locally produced eight-hour ozone in the HGB area was calculated for each ozone season month from 2012 through 2021. Results were then further divided into high and low ozone days to explore possibly differences on ozone exceedance days.

Results are displayed in Figure 2-10: *Background Ozone, MDA8 Ozone, and Locally Produced Ozone by Month from 2012 through 2021 in the HGB Area*. There appear to be similar seasonal patterns for both high and low ozone days. The background ozone appears highest in the spring and early fall, with the lowest background levels observed in July and August. For low ozone days, locally produced ozone is larger than the background during the summer (June through August). This same pattern is observed on high ozone days as well, but the local ozone production on high ozone days in the summer is slightly lower than the background. These trends indicate that high ozone levels in the early part of the ozone season are driven by transported ozone rather than locally produced ozone. High ozone levels in the later part of the ozone season, most notably in August, appear to be driven more by local ozone production.

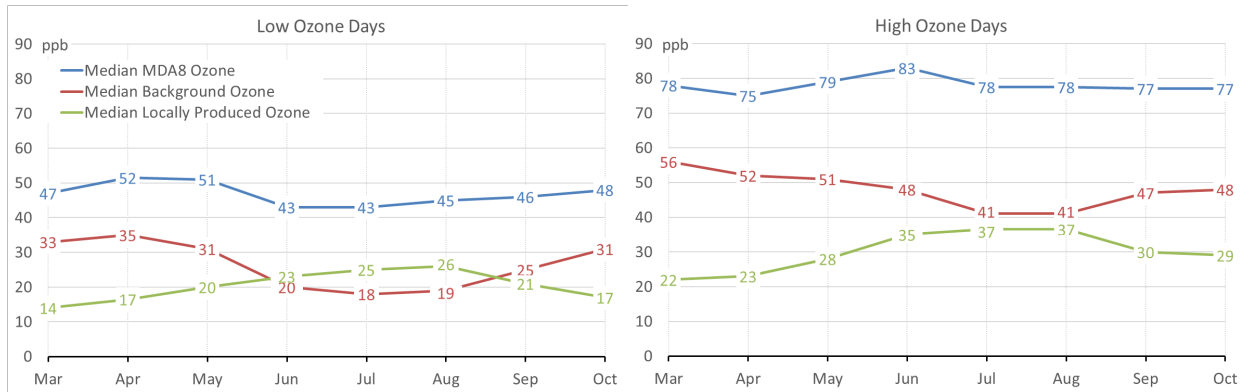


Figure 2-10: Background Ozone, MDA8 Ozone, and Locally Produced Ozone by Month from 2012 through 2021 in the HGB Area

2.7 RAPID OZONE FORMATION

Monitors in the HGB area can record large increases in ozone concentrations over the course of a single hour. These rapid ozone events have two possible causes, a concentrated ozone plume that passes over an ozone monitor or rapid ozone formation occurs near a monitor. Multiple studies of ozone production rates indicated that rapid ozone formation near a monitor was due to large quantities of highly reactive volatile organic compounds (HRVOCs) and NO_x from industrial facilities (Ge et al. 2020, Kleinman et al. 2002, Ryerson et al. 2003, Webster et al. 2007).

To investigate rapid ozone formation in the HGB area, the one-hour ozone change was calculated for every hour during the ozone season at each monitor in the HGB area. The daily-maximum one-hour ozone increase was then calculated for the HGB area. The results were further divided into high and low ozone days. Results are displayed in Figure 2-11: *Ozone Season Daily-Maximum One-Hour Ozone Increases for High versus Low Ozone Days in the HGB Area*. Analysis from the early 2000's found that the median increase on high ozone days was about 40 ppb (TCEQ 2002). Data from 2012 to 2021 show that this value is now around 30 ppb. Although the rate of ozone formation in the HGB area has decreased from the early 2000's, the area still observes hourly increases of 40 ppb or more, but these values now fall within the top 5% of high ozone days.

Data from 2012 to 2021 show the rate that ozone increases is larger on high ozone days compared to low ozone days. Half of the low ozone days observe an hourly increase of about 16 ppb and 5% observe an increase of about 30 ppb. On high ozone days, hourly increases of about 28 ppb occur half of the time, while increases of about 43 ppb occur 5% of the time. When these rates are compared to data from the early 2000's, it appears that the HGB area does not produce ozone as rapidly as in the past. This is likely due to the large reductions in ozone precursors that occurred since the early 2000's.

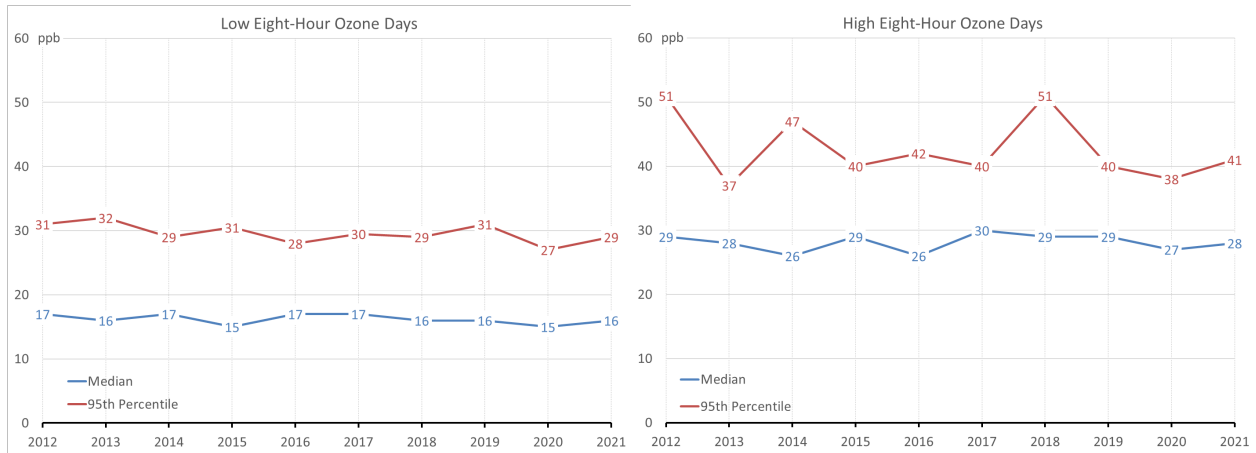


Figure 2-11: Ozone Season Daily-Maximum One-Hour Ozone Increases for High versus Low Ozone Days in the HGB Area

Another way to look at rapid ozone changes in HGB is to compare the daily-maximum one-hour ozone increase to the MDA8 ozone value. This will show if high ozone days are well correlated with one-hour ozone increases. Results are displayed in Figure 2-12: *Ozone Season Daily-Maximum One-Hour Ozone Increase versus MDA8 Ozone in the HGB Area from 2012 through 2021*. There does appear to be some correlation between ozone exceedance days, which are represented in red, and daily-maximum one-hour ozone increases, but large increases are not always associated with high MDA8 ozone. A 30 ppb or greater daily-maximum one-hour ozone increase occurs on high MDA8 ozone days about half of the time. Only daily-maximum one-hour ozone increases of 50 ppb and above are associated with an ozone exceedance day for all occurrences. No ozone exceedance days occur on days when the daily-maximum one-hour ozone increase is 13 ppb or less. These correlations show that the highest rapid ozone increases consistently lead to ozone exceedances, but mid-range rates of hourly ozone increases can occur on days with high or low ozone levels.

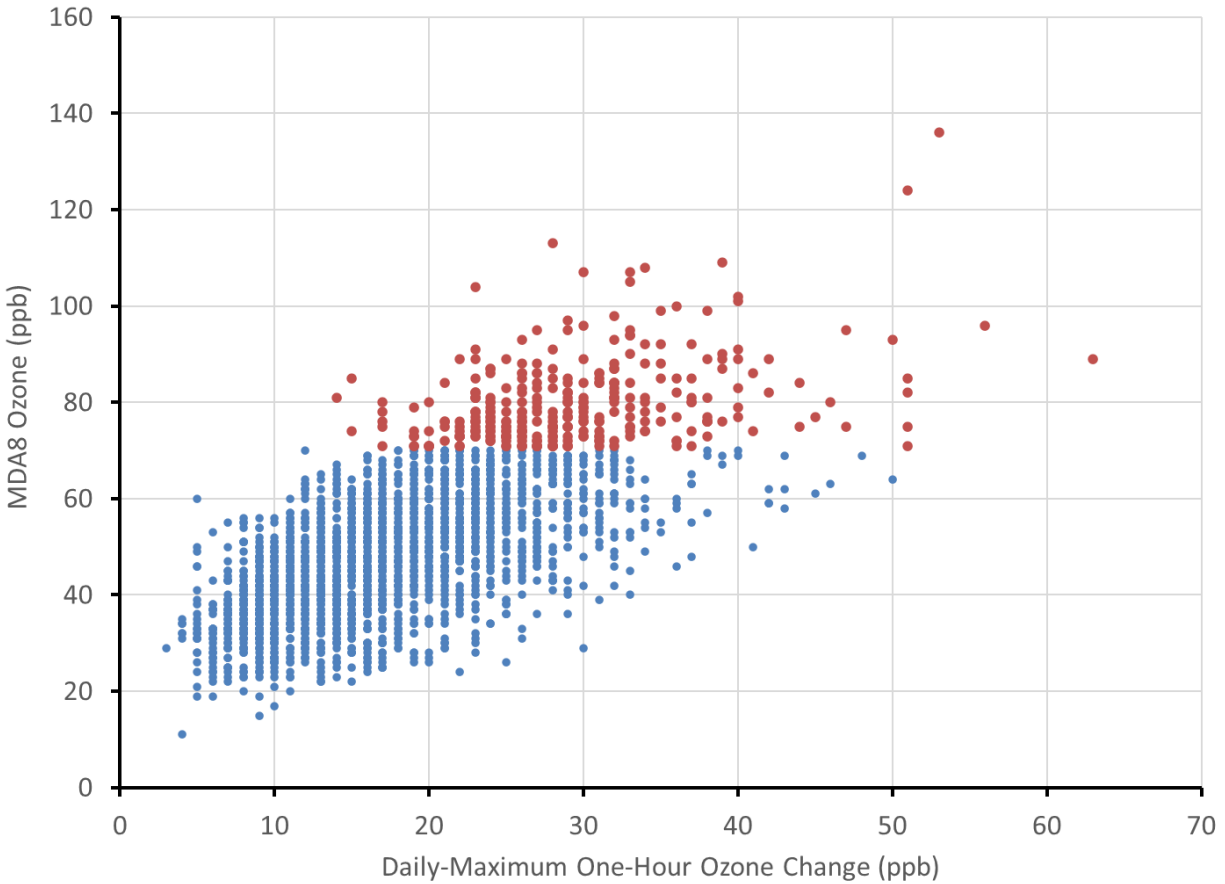


Figure 2-12: Ozone Season Daily-Maximum One-Hour Ozone Increase versus MDA8 Ozone in the HGB Area from 2012 through 2021

To determine if these rapid increases vary by location, the frequency at which these events occur was investigated at each monitor. The frequency of hours with a one-hour ozone increase of 30 ppb or greater was determined at each monitor for the ozone season from 2012 through 2021. A map of the results is shown in Figure 2-13: *Number of Hours with a One-Hour Ozone Increase of 30 ppb or Greater for the Ozone Season in the HGB Area from 2012 through 2021*. The two monitors that measure the most rapid ozone formation are Houston East and Seabrook, both near to numerous urban and industrial sources. In general, monitors closer to the Houston Ship Channel typically measure more frequent rapid ozone formation and monitors further from the urban core of the HGB area measure less rapid ozone formation. The Harvard monitor only has one year of valid data, so the number of hours at that monitor may be skewed low.

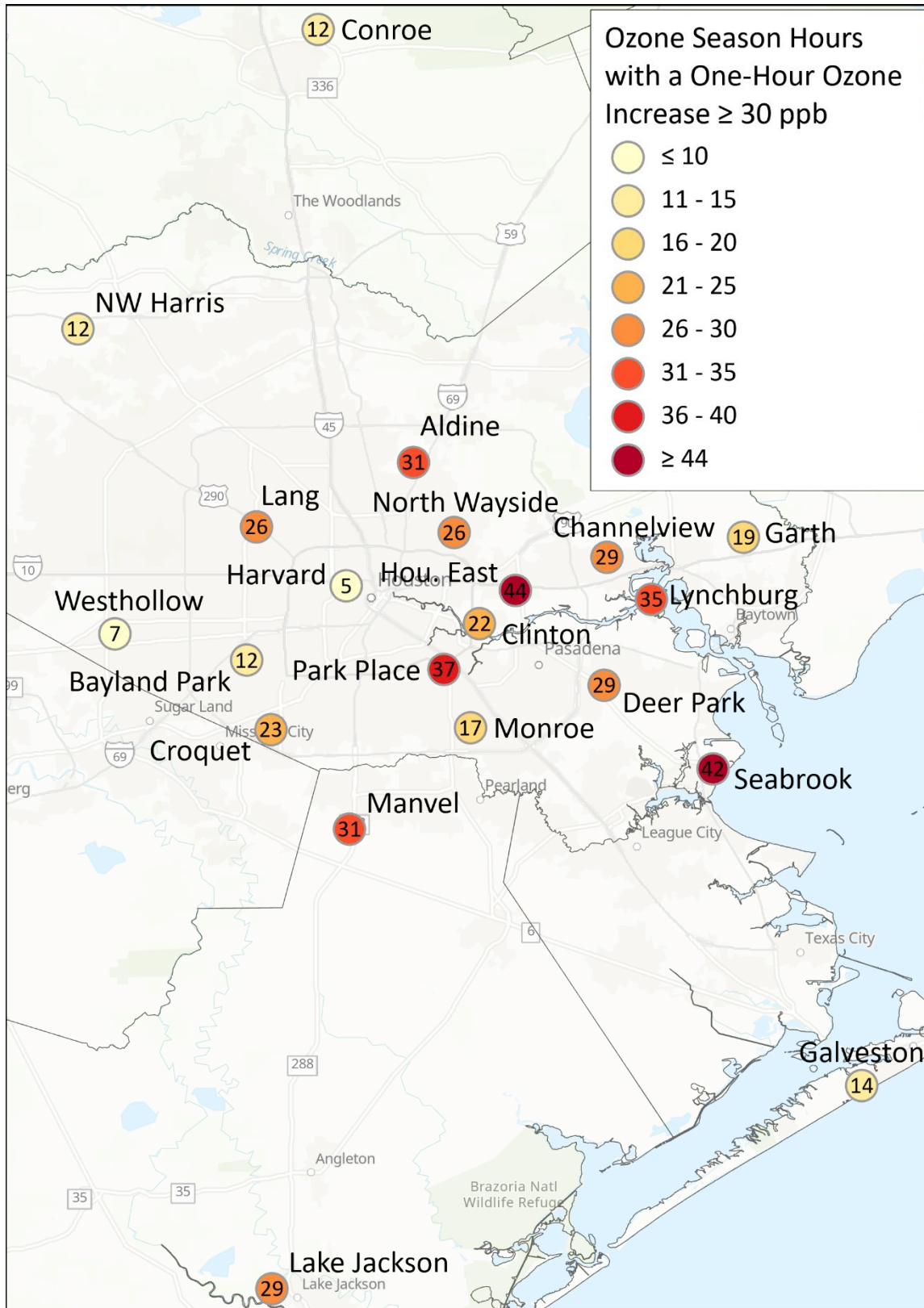


Figure 2-13: Number of Hours with a One-Hour Ozone Increase of 30 ppb or Greater for the Ozone Season in the HGB Area from 2012 through 2021

CHAPTER 3: OZONE PRECURSOR CONCENTRATIONS AND TRENDS

As mentioned previously, ozone is not directly emitted into the atmosphere but formed through photochemical reactions with nitrogen oxide (NO_x) and volatile organic compounds (VOC). The complexity of ozone formation requires a comprehensive examination of these precursors to ozone formation. This section will focus on NO_x and VOC concentration trends, emissions trends, and locations of sources within the Houston-Galveston-Brazoria (HGB) area.

3.1 AMBIENT NO_x TRENDS

NO_x , a precursor to ozone formation, is a variable mixture of nitric oxide (NO) and nitrogen dioxide (NO_2). NO_x is primarily emitted by fossil fuel combustion, lightning, biomass burning, and soil. Examples of common NO_x emissions sources, which occur in all urban areas, are automobile, diesel, and small engines; residential water heaters; industrial heaters and flares; and industrial and commercial boilers. Mobile, residential, and commercial NO_x sources are usually numerous, smaller sources distributed over a large geographic area, while industrial sources are usually large point sources, or numerous small sources, clustered in a small geographic area. Sources of NO_x that are important to air quality in the HGB area are mobile sources, large electric generation units (EGUs), and industrial processes. These sources can produce large, concentrated plumes of emissions that can enhance ozone generation.

The HGB area currently has 21 NO_x monitors, including two near-road monitors. There are four additional NO_x monitors that were in operation in 2012 but have ceased operations prior to 2021. Those four monitors are Danciger (CAMS 0618), Deer Park, Houston Texas Avenue (CAMS 0411), and Mustang Bayou (CAMS 0619). To remove effects of incomplete data on NO_x trends the data were first checked for validity. Only monitors that had eight or more valid years of data for the ozone seasons from 2012 through 2021 were used in this analysis. A year was considered valid if there were at least 75% valid days of NO_x data during the ozone season and a day was considered valid if there were at least 75% of valid hours of NO_x data recorded for that day. Out of the 25 NO_x monitors in operation from 2012 through 2021, only 19 were used to calculate area-wide NO_x trends. The NO_x monitors not included in the area-wide trends due incomplete data were Mustang Bayou, Oyster Creek, Houston Texas Avenue, Harvard, Deer Park, and North Loop.

All valid hours and years of NO_x data were used to calculate yearly median and 95th percentile NO_x trends. The 95th percentile was examined to show trends at the highest NO_x levels while the median was examined to show the central tendency of NO_x concentrations in the HGB area. Results are shown in Figure 3-1: *Ozone Season NO_x Trends in the HGB Area*. From 2012 through 2021, 95th percentile NO_x only showed modest decreases of 3% and median NO_x showed an increase of 2%. There were decreases in NO_x for both statistics from 2012 through 2017. After 2017, NO_x trends flattened and even increased in some years. There is a low for both 95th percentile and median NO_x in 2020, but in 2021 NO_x concentrations increased and the median in 2021 was the highest measured in the past ten years. There were no large changes in NO_x in 2014 and 2015, evidence that the ozone changes in those years were driven by meteorology and not emissions changes.

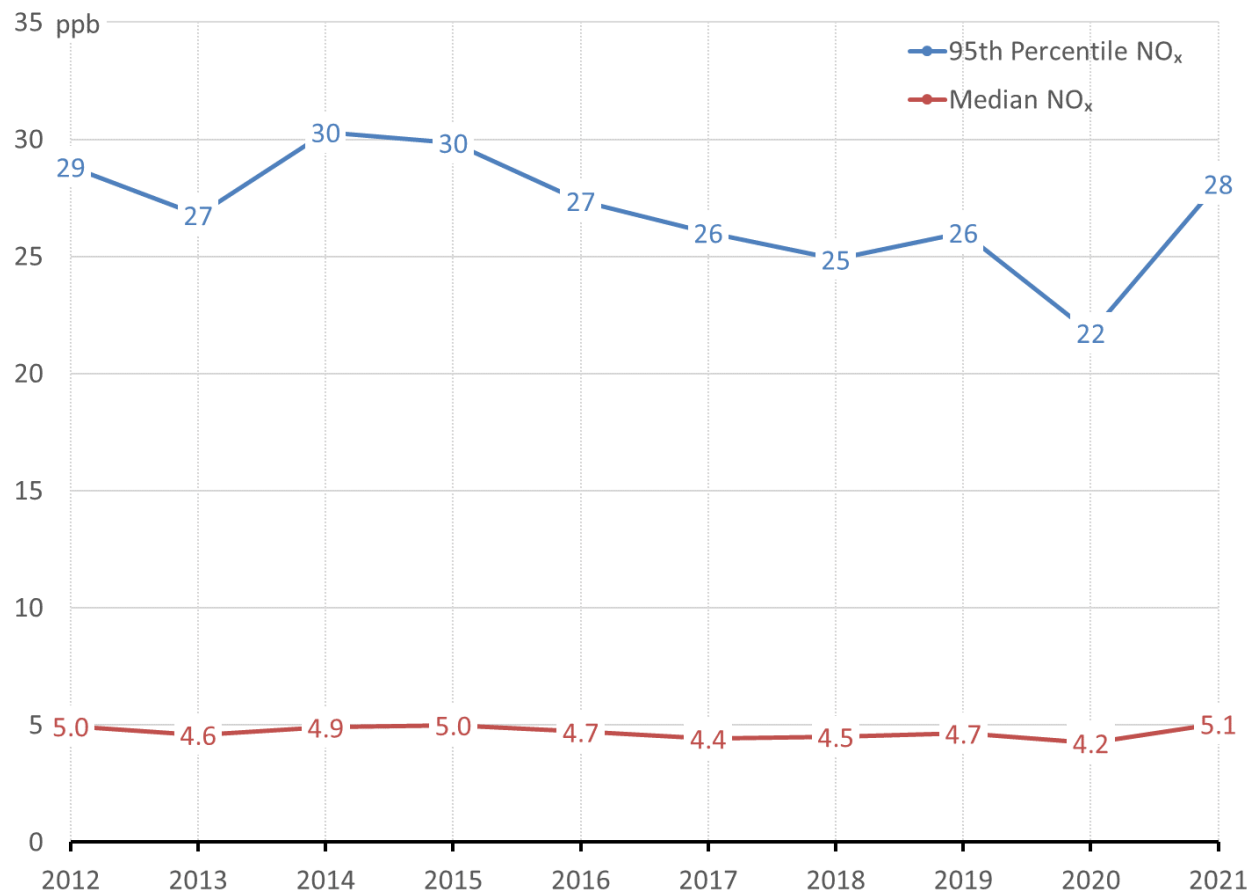


Figure 3-1: Ozone Season NO_x Trends in the HGB Area

The median and 95th percentile NO_x concentrations for the HGB area were also investigated on a monthly time scale. Results are shown in Figure 3-2: *Monthly NO_x Trends in the HGB Area*. Note the scale for the median is different than the scale for the 95th percentile trends. The monthly trends show the seasonality in NO_x concentrations, with high concentrations typically recorded in the cooler months. This is because these cooler months have less sunlight, which causes less NO_x to react to form other chemical species such as ozone. Trends for the median and 95th percentile NO_x are overall very similar. The decrease in 2020 is very apparent in March and April 2020. Although 2020 NO_x concentrations are lower in other months as well, they are not the lowest observed over the past ten years.

Another trend seen in almost all months is the increase in 2021. Both the median and 95th percentile NO_x had increases in almost all months of 2021. The late summer months observed the largest increases in NO_x. This indicates that the increase in 2021 was not due to one large scale event but rather a change that appears to be developing over the course of 2021.

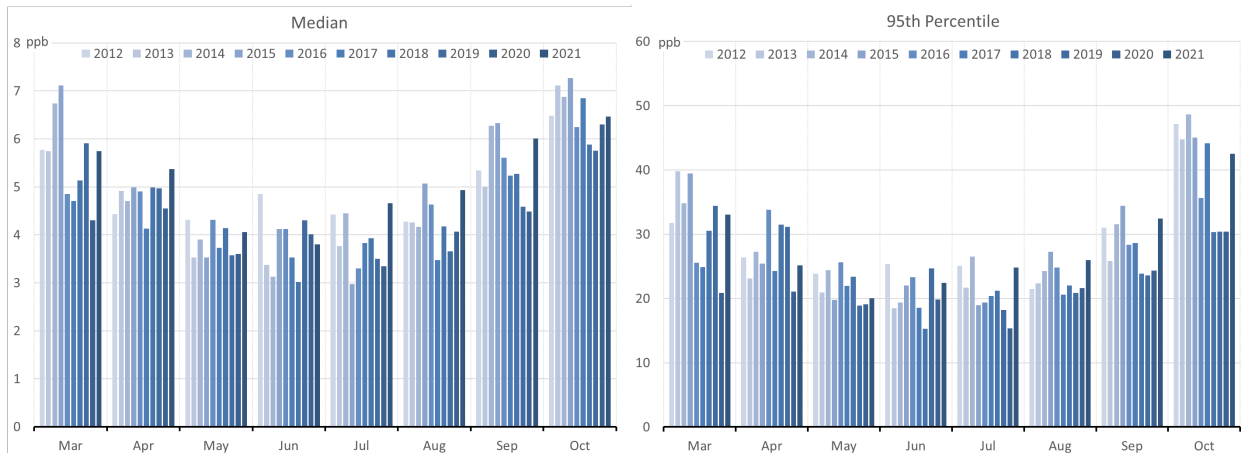


Figure 3-2: Monthly NO_x Trends in the HGB Area

Diurnal trends in ozone season NO_x for the HGB area are displayed in Figure 3-3: *Ozone Season Hourly NO_x Trends in the HGB Area*. Hourly trends for both the median and 95th percentile ozone season NO_x show that NO_x peaks in the morning around 6:00 local standard time (LST), which is equivalent to 7:00 local daylight time (LDT). This coincides with the start of morning rush hour. There is a smaller peak in the afternoon for the evening rush hour. The lower afternoon peak is due to higher mixing layer heights, which allow more room for NO_x to mix, causing monitors to measure lower concentration of NO_x.

The morning period shows some decreases in NO_x for both the median and 95th percentile. Morning concentrations in 2020 were lower compared to all other years. While there was some increase in 2021 NO_x during the morning hours, the larger increases in NO_x in 2021 appear to occur during hours outside of rush hour. This indicates possible increases from another source in addition to mobile sources. Median NO_x values in 2021 seem to have increased more compared to 95th percentile values, indicating that, while the highest concentrations have decreased, lower-level NO_x values are increasing.

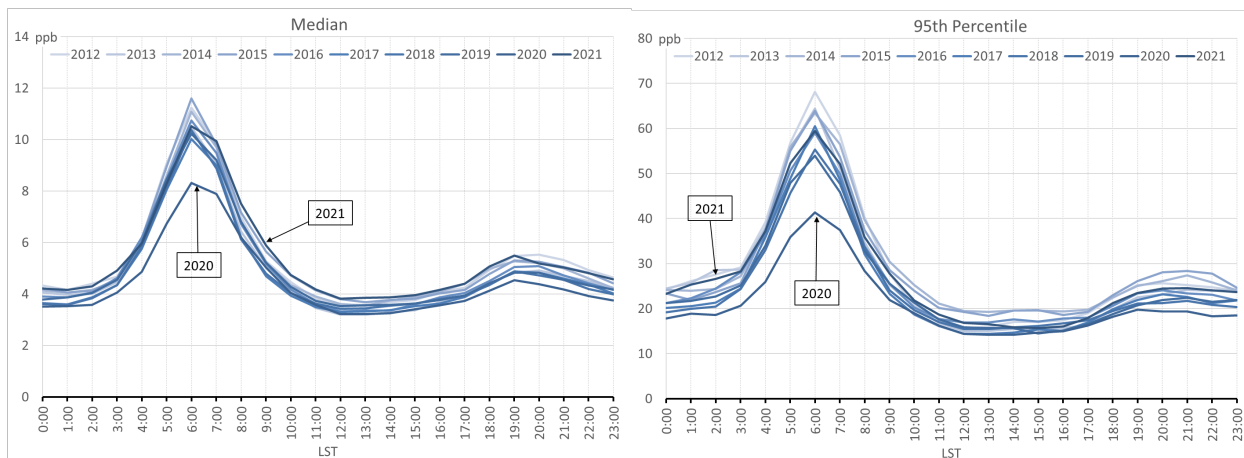


Figure 3-3: Ozone Season Hourly NO_x Trends in the HGB Area

To determine if the area-wide increases were throughout the HGB area, or only at specific monitors, the NO_x trends by monitor are shown in Figure 3-4: *Ozone Season*

NO_x Trends by Monitor in the HGB Area. The results show variable trends across the HGB area, with some monitors showing increases and others showing decreases. Over half of the NO_x monitors measured the lowest NO_x concentrations in ten years in 2020. Monitors that measure higher NO_x concentrations showed increases in NO_x from 2012 through 2021. The highest 95th percentile NO_x concentrations occur at the Southwest Freeway monitor, while the highest median NO_x concentrations occur at Clinton. The difference is likely due to emissions sources. Southwest Freeway is a near road monitor and likely measures large spikes in NO_x concentrations that occur during the morning rush hour whereas Clinton is in a more urban and industrial area and likely measures elevated NO_x concentrations throughout the day. Overall, the 95th percentile concentrations show more decreases compared to the median, further evidence that the highest concentrations are decreasing faster than mid-range NO_x concentrations.

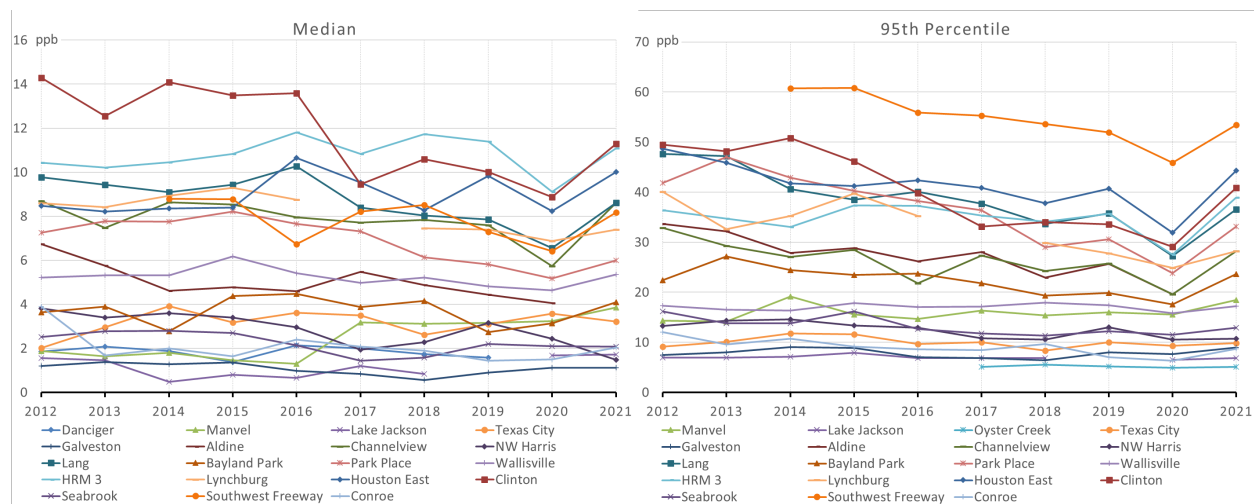


Figure 3-4: Ozone Season NO_x Trends by Monitor in the HGB Area

NO_x changes are more apparent when viewed on a map. A bivariate color scale was developed to show 2021 NO_x concentrations and how they have changed from 2012. Results for the median and 95th percentile NO_x concentrations are displayed in Figure 3-5: *2021 Ozone Season NO_x Concentrations and the Change from 2012 Values in the HGB Area.* In the map color scale, monitors with a high NO_x concentration and a NO_x increase are shown in brown, monitors with low NO_x concentrations and a NO_x increase are shown in red, monitors with a high NO_x concentration and a NO_x decrease are shown in blue, and monitors with a low NO_x concentration and a NO_x decrease are shown in light gray.

The maps show that there are more decreases overall when looking at the 95th percentile NO_x compared to the median NO_x, as evidenced by more monitors in blue on the 95th percentile NO_x map. Some monitors that typically see low NO_x concentrations such as Lake Jackson and Texas City, have seen NO_x increases over the past ten years. Some of the Houston Ship Channel monitors with the highest NO_x concentrations also show the greatest variability. Some of the largest NO_x changes, both increases and decreases, have occurred at Clinton, Houston East, and HRM3, which are all Houston Ship Channel monitors that also measure some of the largest NO_x concentrations in the area. For these monitors, the variation in NO_x trends is an indication that the increases in 2021 are due to a localized NO_x source rather than an increase in mobile sources.

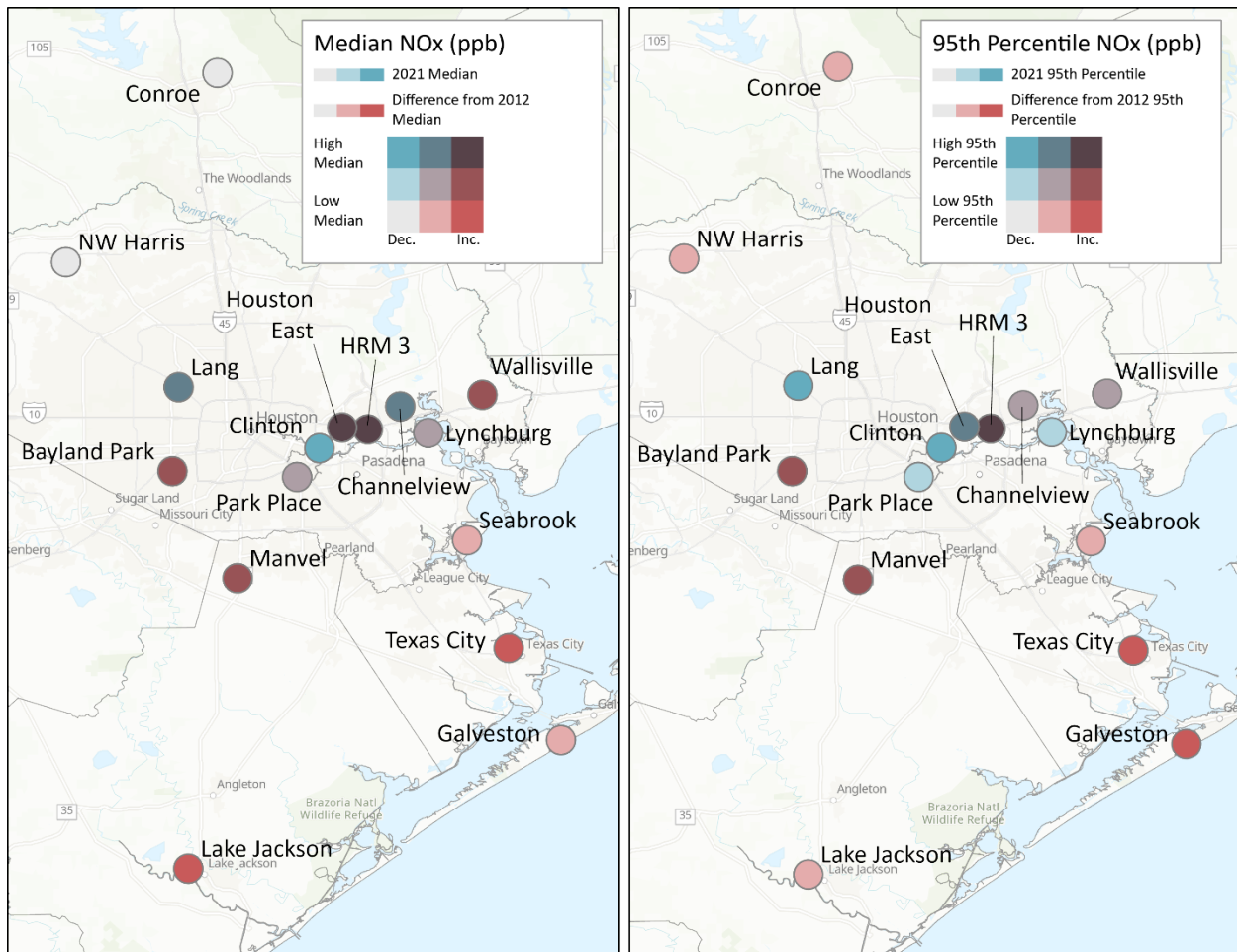


Figure 3-5: 2021 Ozone Season NO_x Concentrations and the Change from 2012 Values in the HGB Area

3.2 AMBIENT VOC COMPOSITION AND TRENDS

VOC concentrations can enhance ozone production in combination with NO_x and sunlight. VOC is emitted from numerous sources including large industrial process, automobiles, solvents, paints, dry-cleaning, fuels, and even natural sources such as trees. VOC is an important precursor to ozone formation, particularly in the HGB area, where the Houston Ship Channel, a large source of industrial VOC emissions, is located. Not all VOC species have the same ozone production potential. A subset of VOC called highly reactive volatile organic compounds (HRVOC) are more likely to produce large amounts of ozone (Kleinman et al. 2002, Ryerson et al. 2003, Webster et al. 2007). Because of their ozone formation potential, six of these HRVOC are regulated in Texas. These HRVOC include ethylene, propylene, 1-butene, c-2-butene, t-2-butene, and 1,3-butadiene.

3.2.1 Ambient VOC and HRVOC Trends

Two types of monitors record VOC data in the HGB area: automated gas chromatograph (auto-GC), which record hourly data; and canisters, which record 24-hour data. Due to the reactive nature of VOCs, the hourly auto-GC measurements are preferred when assessing trends. The HGB area currently has 15 auto-GC monitors.

There is one additional auto-GC monitor, Danciger (CAMS 0618), that was in operation in 2012 but ceased operations prior to 2021. These monitors measure both total non-methane organic carbon (TNMOC), which is a surrogate for total VOC, and speciated VOC concentrations, which include HRVOCs.

To focus on the VOC concentrations that affect ozone formation, this analysis uses only ozone season data. To remove effects of incomplete data on VOC trends, the data were first checked for validity. Only monitors that had eight or more valid years of data for the ozone season from 2012 through 2021 were used in this analysis. A year was considered valid if there were at least 75% valid days of data during the ozone season and a day was considered valid if there were at least 75% of valid hours of data recorded for that day. Out of the 16 auto-GC monitors in operation from 2012 through 2021, only 11 were used to calculate area-wide TNMOC and HRVOC trends. The auto-GC monitors not included in the area-wide trends due to incomplete data were Oyster Creek, CView Water Tower, Galena Park, HRM 7, and HRM 16.

All valid hours and years of data were used to calculate yearly median and 95th percentile TNMOC and HRVOC trends. The 95th percentile was examined to show trends at the highest levels while the median was examined to show the central tendency of both TNMOC and HRVOC concentrations in the HGB area. Ozone season trends for ambient TNMOC and HRVOC concentrations are presented in Figure 3-6: *Ozone Season Median and 95th Percentile TNMOC and HRVOC Trends in the HGB Area*. TNMOC and HRVOC are displayed on two different scales due to their differing units of measurement. TNMOC is recorded in parts per billion carbon (ppbC) and HRVOC is recorded in parts per billion by volume, which is more commonly referred to as ppb.

The 95th percentile TNMOC and HRVOC increased from 2012 through 2021 by 4% and 14%, respectively. Median values show less change, with a decrease of 2% in median TNMOC and an increase of 11% in median HRVOC. Increases occurred mostly in 2021. Prior to 2021, both TNMOC and HRVOC appeared to be slowly decreasing, with the lowest values observed in 2017 and 2020. Increases observed in 2021 are larger for HRVOC compared to TNMOC.

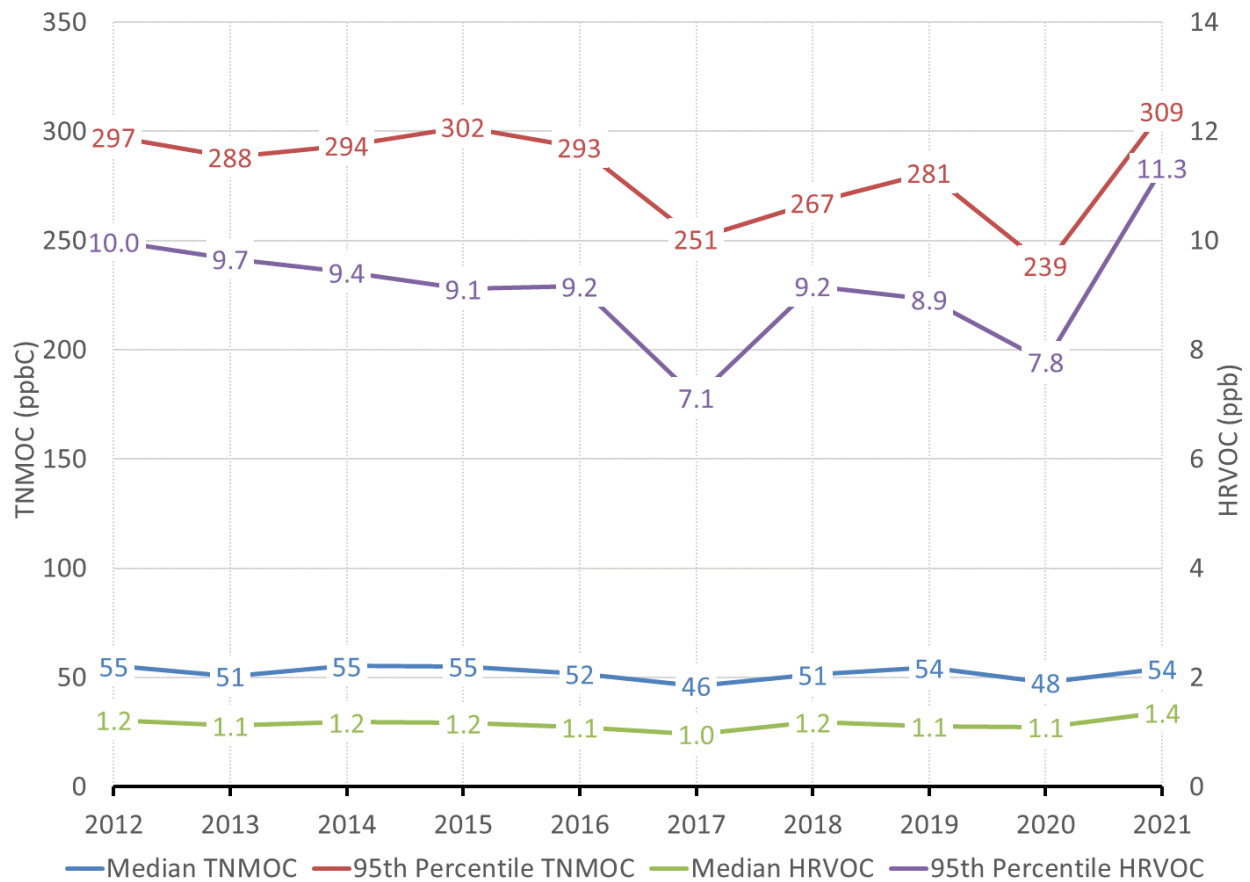


Figure 3-6: Ozone Season Median and 95th Percentile TNMOC and HRVOC Trends in the HGB Area

The median and 95th percentile TNMOC and HRVOC concentrations for the HGB area were also investigated on a monthly time scale. Results are shown in Figure 3-7: *Monthly TNMOC (top) and HRVOC (bottom) Trends in the HGB Area*. There is less seasonality in both TNMOC and HRVOC concentrations compared to NO_x, although September and October do see higher concentrations compared to other months. Median and 95th percentile TNMOC trends appear to be similar by month. Similar to the NO_x trends, most months in 2021 show an increase in TNMOC indicating that the increase is not related to a specific event, but rather something occurring throughout 2021.

While overall trends in HRVOC seems similar between the median and the 95th percentile, there are some differences. It appears that the 95th percentile is increasing in 2021 at a faster rate. The 95th percentile HRVOC values in March are the highest values measured across all months from 2012 through 2021. It is possible that these values were caused by some event in this month; however, the other months observed increases in 2021 as well, although not as large as those observed in March.

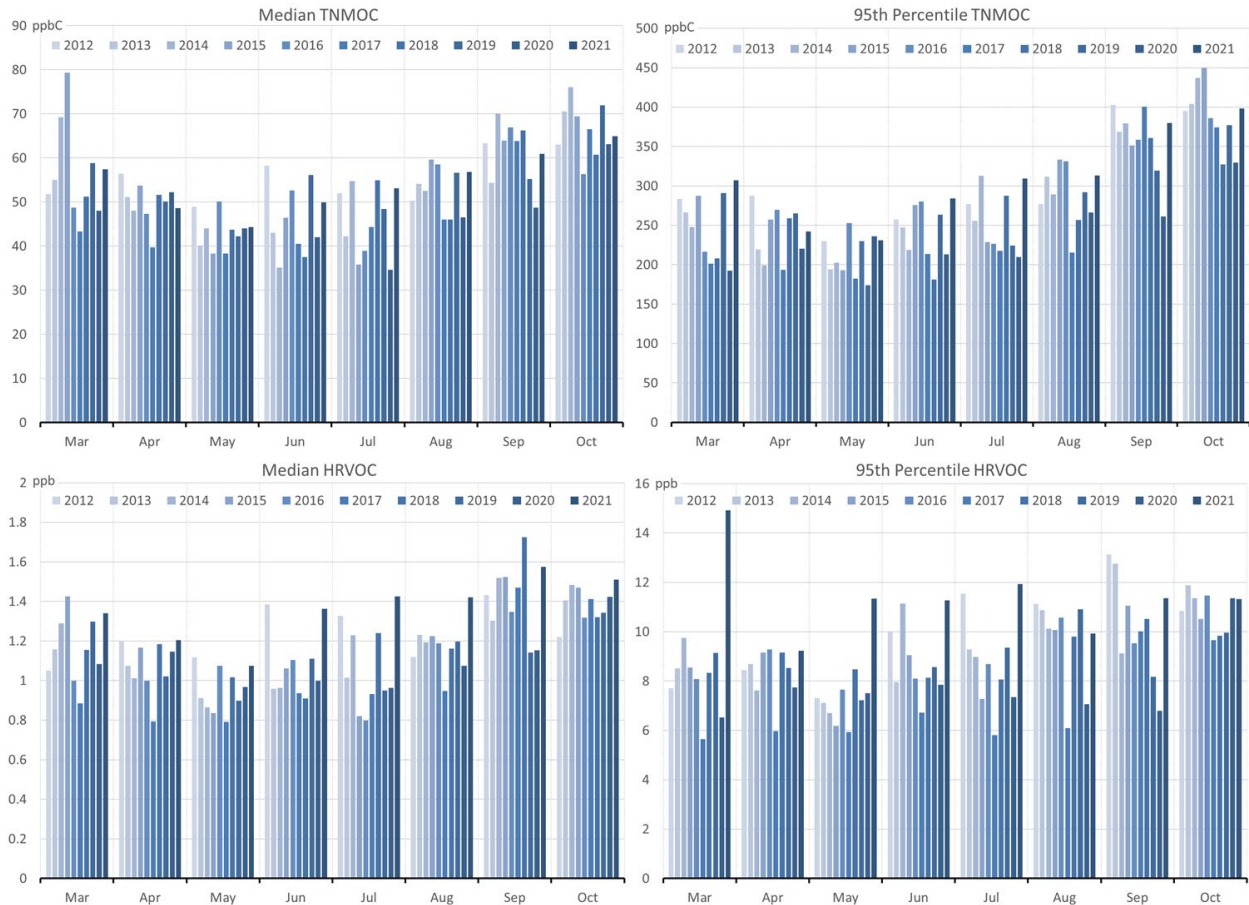


Figure 3-7: Monthly TNMOC (top) and HRVOC (bottom) Trends in the HGB Area

Diurnal trends in ozone season TNMOC and HRVOC for the HGB area are displayed in Figure 3-8: *Ozone Season Hourly TNMOC (top) and HRVOC (bottom) Trends in the HGB Area*. Hourly trends in median TNMOC and median HRVOC show a morning peak similar to that of NO_x , at around 6:00 LST. Hourly trends in 95th percentile TNMOC and 95th percentile HRVOC are slightly different. While 95th percentile TNMOC and HRVOC often peak around 6:00 or 7:00 LST, some years show the peak during nighttime hours. Unlike NO_x , which is mostly from mobile sources, larger VOC concentrations in the HGB area are more likely from point sources, meaning that high VOC concentrations can be measured throughout the day or night. Since VOC are reactive in the presence of sunlight, the higher concentrations are more likely be measured overnight.

Both median and 95th percentile TNMOC and HRVOC show low morning values in 2020. Both median and 95th percentile TNMOC increased for many hours in 2021, but some earlier years showed higher concentrations. Both median and 95th percentile HRVOC, however, showed increases for almost every hour in 2021. It appears that HRVOC are increasing more in 2021 than TNMOC.

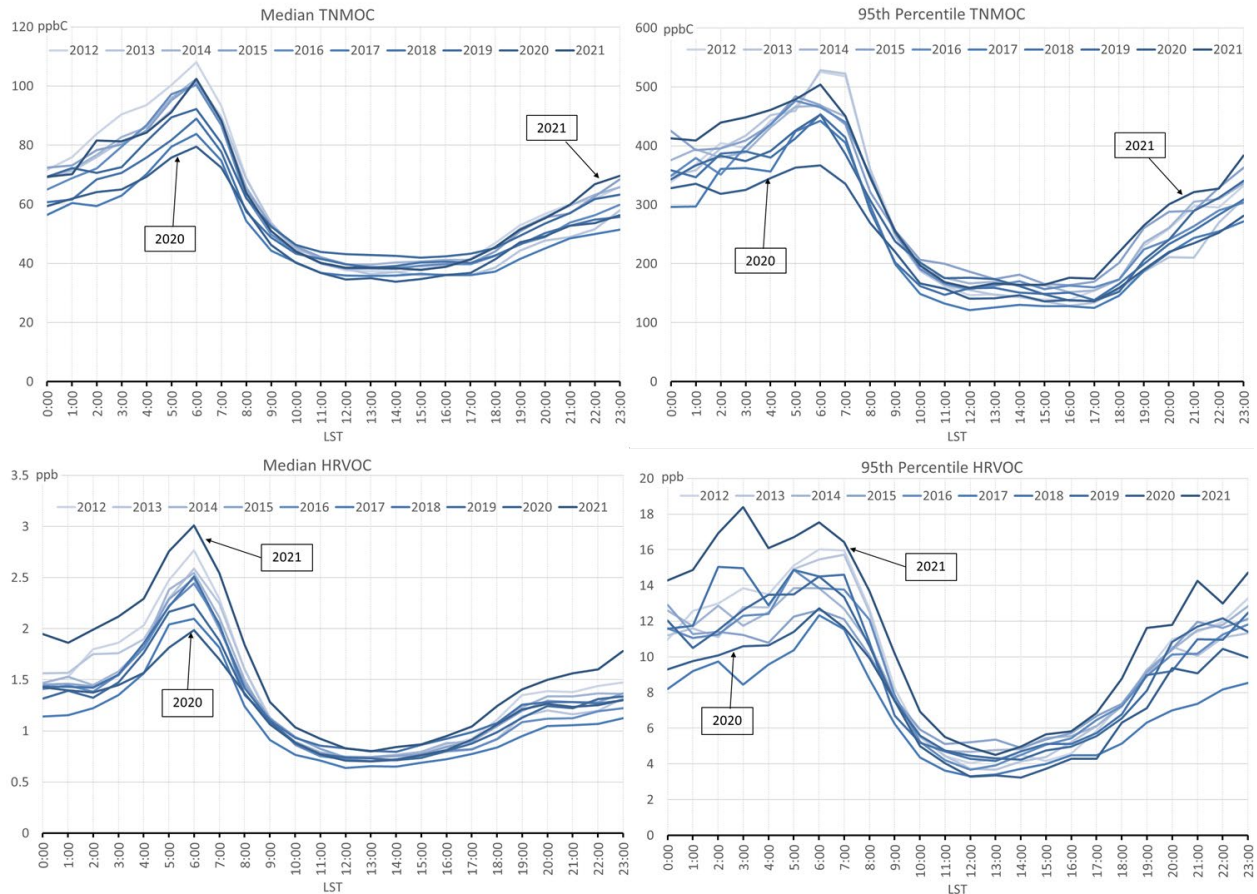


Figure 3-8: Ozone Season Hourly TNMOC (top) and HRVOC (bottom) Trends in the HGB Area

To determine if the area-wide increases were throughout the HGB area, or only at specific monitors, the TNMOC and HRVOC trends by monitor are shown in Figure 3-9: *Ozone Season TNMOC (top) and HRVOC (bottom) Concentrations by Monitor in the HGB Area*. The results show variable trends across the HGB area, with some monitors showing increases and others showing decreases. Many auto-GC observed some of the lowest TNMOC concentrations in 2020, especially in the 95th percentile concentrations. Eight auto-GC monitors measured their lowest 95th percentile TNMOC concentration from the 10 years analyzed in 2020. When looking at HRVOC concentrations, there is still a decrease in 2020, but it is not as widespread as the TNMOC concentrations. This indicates that the cause for VOC decreases in 2020 was not from sources that typically emit large amounts of HRVOC in the Houston Ship Channel area.

Some of the largest overall TNMOC decreases occurred at Channelview, which measured much higher TNMOC in 2012 compared to 2021. Other monitors, such as Milby Park, HRM 3, and Clinton, showed increases in TNMOC from 2012 to 2021. Some of the highest median TNMOC values in 2021 occurred at HRM 3, Clinton, and Milby Park. Those same monitors, with the addition of Cesar Chavez, observed the highest 95th percentile concentrations in 2021.

Individual monitor trends appear different for HRVOC compared to those for TNMOC. HRM 3, for example, showed an increase in TNMOC, but an overall decrease in HRVOC concentrations. Milby park observed much larger HRVOC increases in 2021 compared to TNMOC and measured the highest 95th percentile HRVOC concentration over the 10 years analyzed in 2021. The monitors with the highest median HRVOC in 2021 are Milby Park, HRM 3, and Lynchburg. When looking at 95th percentile HRVOC concentrations, Lynchburg measures much higher HRVOC in addition to Milby Park. The differences between the 95th percentile and the median indicate that the monitors with higher 95th percentile HRVOC concentrations may observe more episodic concentrations compared to the monitors with higher median HRVOC concentrations.

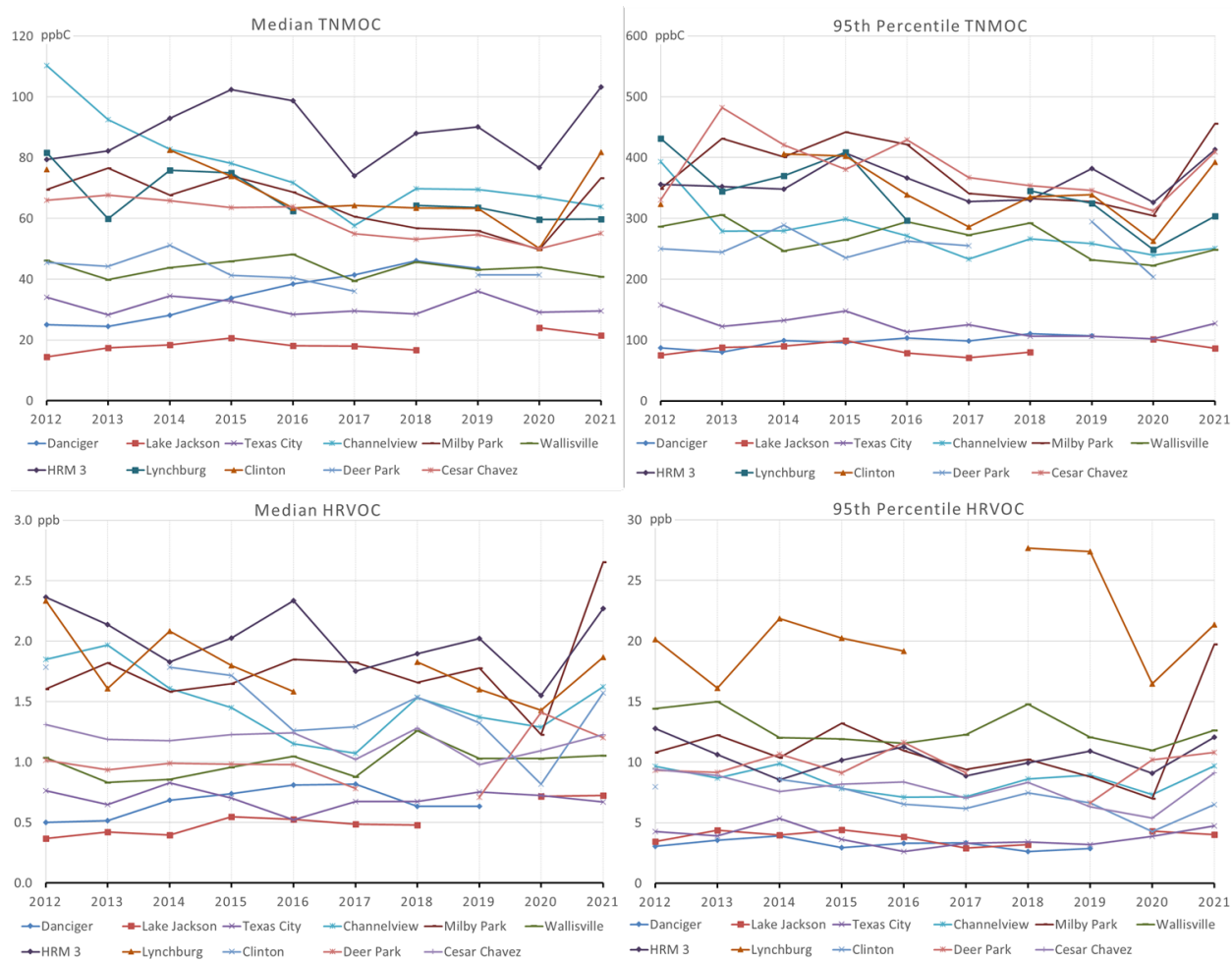


Figure 3-9: Ozone Season TNMOC (top) and HRVOC (bottom) Concentrations by Monitor in the HGB Area

TNMOC and HRVOC changes are more apparent when viewed on a map. To show not only TNMOC and HRVOC concentrations, but how they have changed from 2012 through 2021, a bivariate color scale was developed to show the 2021 ozone season TNMOC and HRVOC concentrations compared to how much they have changed from 2021. Results for the median and 95th percentile TNMOC and HRVOC concentrations are displayed in Figure 3-10: *2021 Ozone Season TNMOC and HRVOC Concentrations and the Change from 2012 Values in the HGB Area*. In the map color scale, monitors

with a high VOC concentration and a VOC increase are shown in brown, monitors with low VOC concentrations and a VOC increase are shown in red, monitors with a high VOC concentration and a VOC decrease are shown in blue, and monitors with a low VOC concentration and a VOC decrease are shown in light gray. Only Houston Ship Channel monitors are shown in the map since those monitors typically measure the highest VOC concentrations.

The maps show the varying increases and decreases by location and statistic. When looking at TNMOC, there appears to be high concentrations as well as increases in both the median and the 95th percentile at HRM 3, Milby Park, and Clinton. While the median TNMHC values decreased at Cesar Chavez, the 95th percentile values increased. Overall, it seems that the TNMOC is increasing in the central and western portions of the Houston Ship Channel but decreasing in the eastern portions.

These changes are different when looking at the HRVOC concentrations. HRVOC concentrations decreased at HRM 3. Both the median and 95th percentile HRVOC concentrations increased at Milby Park and Deer Park, and the 95th percentile concentrations also increased at Channelview and Lynchburg. Wallisville showed an increase in median HRVOC but a decrease in 95th percentile HRVOC. Overall, there appear to be increases in the highest concentrations of HRVOC in the central Houston Ship Channel, and there appears to be localized increases near Milby Park. The variable patterns between TNMOC and HRVOC indicate that some changes are due to VOC other than HRVOC.

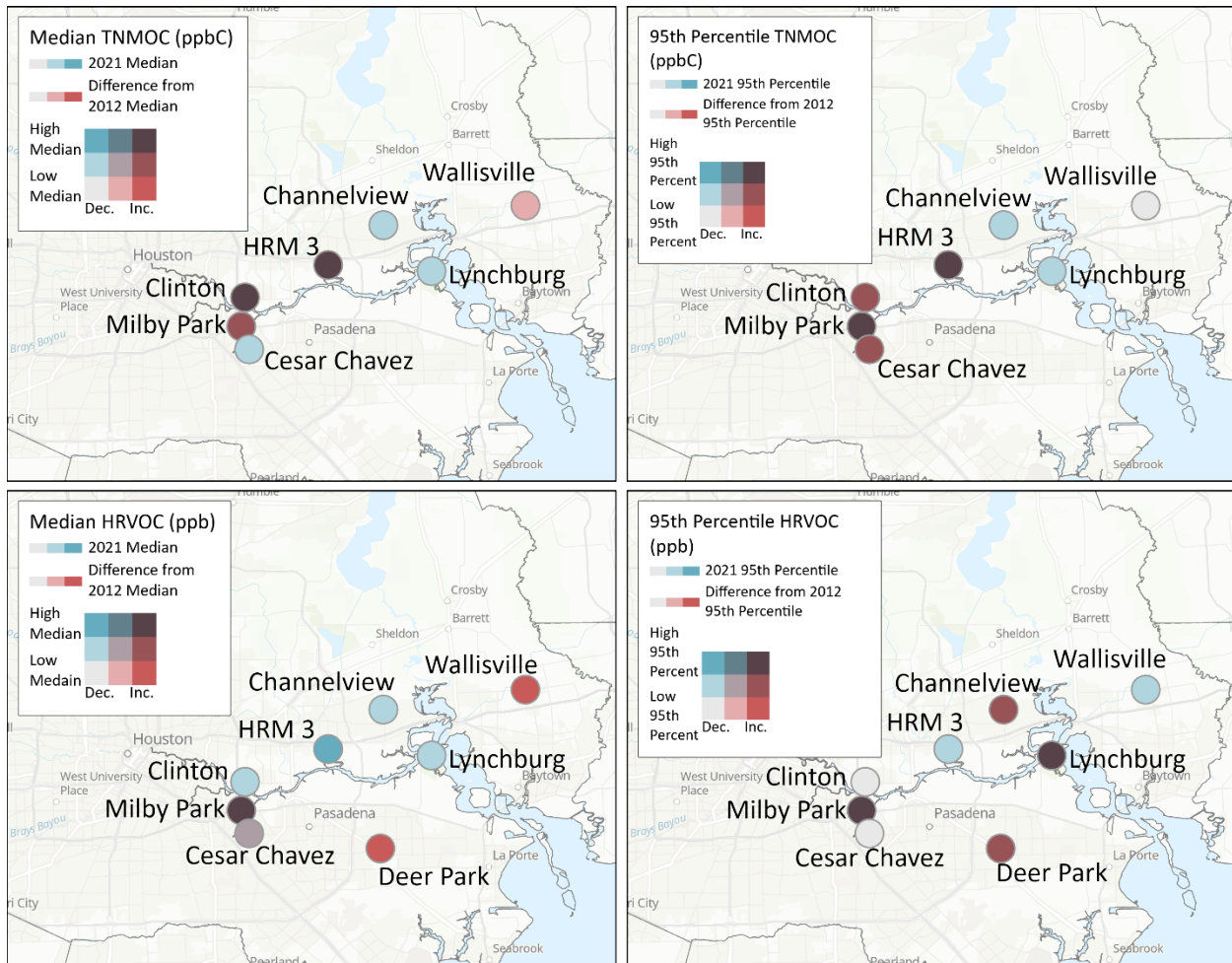


Figure 3-10: 2021 Ozone Season TNMOC and HRVOC Concentrations and the Change from 2012 Values in the HGB Area

3.2.2 HRVOC Concentrations by Wind Direction

Analysis of HRVOC concentrations by wind direction can be used to determine potential areas that could be the cause of increasing HRVOC concentrations in the Houston Ship Channel. To investigate HRVOC concentrations by wind direction, the individual HRVOC species concentrations in ppb are first multiplied by the wind speed in miles per hour. Weighting the concentrations by wind speed normalized large HRVOC concentrations that were measured due to slow wind speeds. Winds with speeds less than one mile per hour were removed because wind direction has larger uncertainty at slower wind speeds. Only days with 75% valid HRVOC data for the ozone season in 2021 were used in this analysis. The analysis focused on 2021 data since there were large HRVOC increases at several monitors during this year.

After weighting the HRVOC species by wind speed, they were then grouped into ten degree shifting wind bins based on the wind direction for each hour. Finally, the geometric mean wind speed weighted HRVOC concentrations was calculated for each wind bin. Geometric mean is calculated by first calculating the log of the wind speed weighted HRVOC concentration, then calculating the average of those values, and

finally taking the exponent of that average. This type of statistic is better for finding the central tendency of exponentially skewed data, such as HRVOC data.

The results for the auto-GC monitors in the Houston Ship Channel are displayed in Figure 3-11: *Geometric Mean Wind Speed Weighted HRVOC Concentrations by Shifting Wind Bin for the 2021 Ozone Season in the HGB Area*. The scale for each auto-GC is variable, meaning the largest points on the image should be used to assess the locations of possible HRVOC rather than concentrations. The maps were divided into the eastern Ship Channel on the right and the western Ship Channel on the left. The boundaries of various industry in the Houston Ship Channel are shaded in pink.

Results for the eastern portion of the Ship Channel point to several sources of HRVOC, most notably ethylene and propylene. Wallisville and HRM 7 both point to the area south of HRM 7 as a large source of both ethylene and propylene. Wallisville also shows a large ethylene source to the east, towards the Chevron facility, but since there is no other monitor in that area, it could be multiple other sources in that direction as well. The other more centralized auto-GC, including Lynchburg, Channelview, CView Water Tower, HRM 3, HRM 16, and Deer Park, all indicate the existence of a large source of propylene and to a lesser extent ethylene. This source appears to be in the area south of Lynchburg, southeast of CView Water Tower, and northeast of HRM16. It is difficult to pinpoint an exact source in this location due to the numerous facilities in the area. There is another possible ethylene source located to the southeast of HRM 3, north-northwest of Deer Park, and west-northwest of HRM 16, but again, with the numerous facilities in the area, an exact source cannot be determined.

In the western portion of the Ship Channel, Galena Park, Clinton, and Cesar Chavez show higher ethylene in the direction of the eastern Ship Channel. This area also has larger amounts of butenes and 1,3-butadiene compared to the eastern portion of the Ship Channel. There appears to be a large HRVOC source of mostly butenes to the southeast of Galena Park. There also appears to be a large 1,3-butadiene source to the southwest of Milby Park and the north of Cesar. As with the eastern portion of the Ship Channel, the numerous sources in the western portion of the Ship Channel make it difficult to pinpoint an exact source for the various HRVOC. It is probable that the multiple sources all have some amount of HRVOC emissions, which when combined can cause high concentrations in the area.

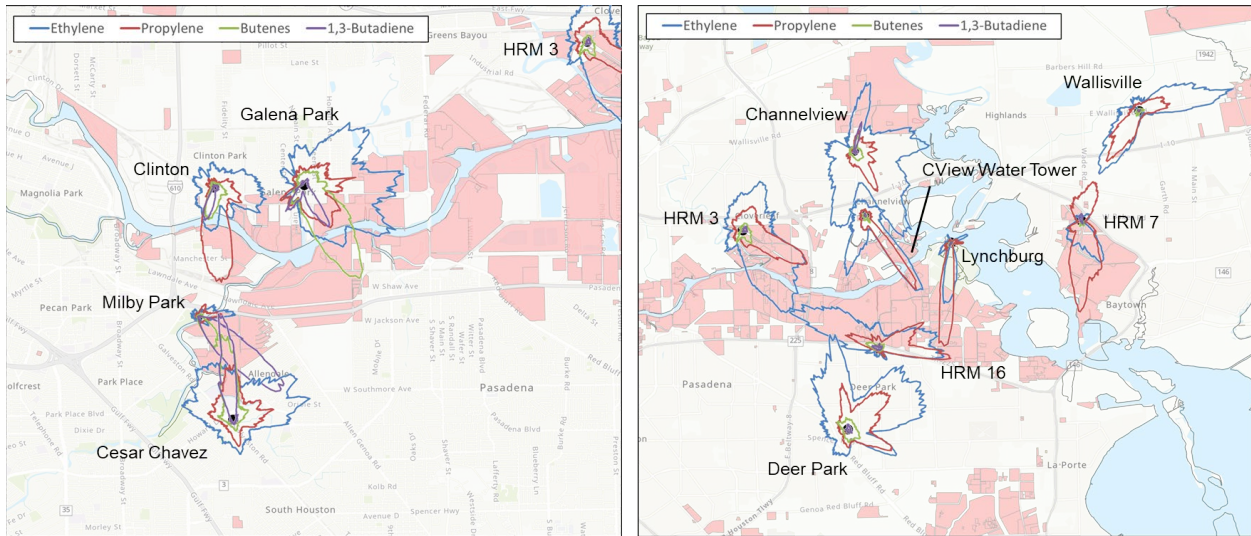


Figure 3-11: Geometric Mean Wind Speed Weighted HRVOC Concentrations by Shifting Wind Bin for the 2021 Ozone Season in the HGB Area

3.2.3 VOC Composition Trends

Auto-GC monitors measure up to 51 individual VOC species. Identifying trends in these species can show if there are changes in VOC other than HRVOC that are causing increases at certain monitors in the Houston Ship Channel.

Because not all VOC have the same ozone formation potential, VOC concentrations were weighted by the maximum incremental reactivity (MIR) (Carter 2010). To weight the VOC concentration, the MIR value in grams of ozone per grams of VOC is multiplied by the molecular weight of the VOC, then divided by the molecular weight of ozone. The VOC concentration is then multiplied by the resulting value to give a MIR weighted VOC concentration. VOC with similar properties were combined into 17 groups. The groups and the VOC within each group are defined in Table 3-1: *VOC Group Definitions*.

Table 3-1: VOC Group Definitions

VOC Group	VOC Species
1,3-Butadiene	1,3-Butadiene
Alkanes	2,2,4-Trimethylpentane, 2,2-Dimethylbutane, 2,3,4-Trimethylpentane, 2,3-Dimethylpentane, 2,4-Dimethylpentane, 2-Methylheptane, 2-Methylhexane, 3-Methylheptane, 3-Methylhexane, n-Decane, n-Heptane, n-Hexane, n-Nonane, n-Octane
Aromatics	Benzene, Ethylbenzene, Isopropylbenzene, n-Propylbenzene
Butanes	Isobutane, n-Butane
Butenes	1-Butene, cis-2-Butene, trans-2-Butene
C2C3	Acetylene, Ethane, Propane
Cyclos	Cyclohexane, Methylcyclohexane, Methylcyclopentane
Ethylene	Ethylene
Isoprene	Isoprene
Other	2-Methyl-2-Butene, Cyclopentane, n-Undecane
Pentanes	Isopentane, n-Pentane

VOC Group	VOC Species
Pentenes	1-Pentene, cis-2-Pentene, trans-2-Pentene
Propylene	Propylene
Styrene	Styrene
Toluene	Toluene
Trimethylbenzenes	1,2,3-Trimethylbenzene, 1,2,4-Trimethylbenzene, 1,3,5-Trimethylbenzene
Xylenes	m/p-Xylene, o-Xylene

After grouping the VOC species, the data were checked for completeness. Only valid days and years for the ozone season from 2012 through 2021 were used in this analysis. A complete day was any day with at least 75% valid hours and a complete year was any year with at least 75% complete days for the ozone season. The median was then calculated for each VOC group at each auto-GC monitor. Results are shown in Figure 3-12: *Ozone Season VOC Composition in the HGB Area from 2012 through 2021*. The monitors are ordered from the western most monitor to the eastern most monitor.

The top left bar chart shows that when looking at concentration-based composition, most monitors are dominated by two and three single bond carbon (C2C3) compounds followed by pentanes and then butanes. These VOC species have low reactivity. The composition changes when it is weighted by reactivity, as shown in the top right bar chart. Once weighted by reactivity the dominant species become the four groups that compose HRVOC, although this varies by monitor. It is easier to see the more dominant reactivity weighted VOC groups when looking at the concentrations as a percentage of the total, as shown in the bottom left bar chart. This percentages show that HRVOC can contribute anywhere from 20% to 50% of the total VOC composition. Monitors that are further away from the urban area, such as Danciger and Lake Jackson have more isoprene, a biogenic species that is primarily from trees. After HRVOC, pentanes appear to be the next largest VOC group. This is easier to see when grouping the MIR weighted VOC concentrations by species instead of monitor, as shown in the bottom right image. When grouping by species, the HGB area is dominated by ethylene and propylene followed by penances and butanes.

Comparing total VOC concentrations across monitors show that the monitors near the Houston Ship Channel measure much larger VOC concentrations compared to those in Brazoria or Galveston Counties. HRM 7 measured the largest VOC concentrations in the area and has an unusually high amount of propylene. This monitor only has data for 2021 so it is unclear if this is due to something unique to 2021 or if these levels of propylene are routine.

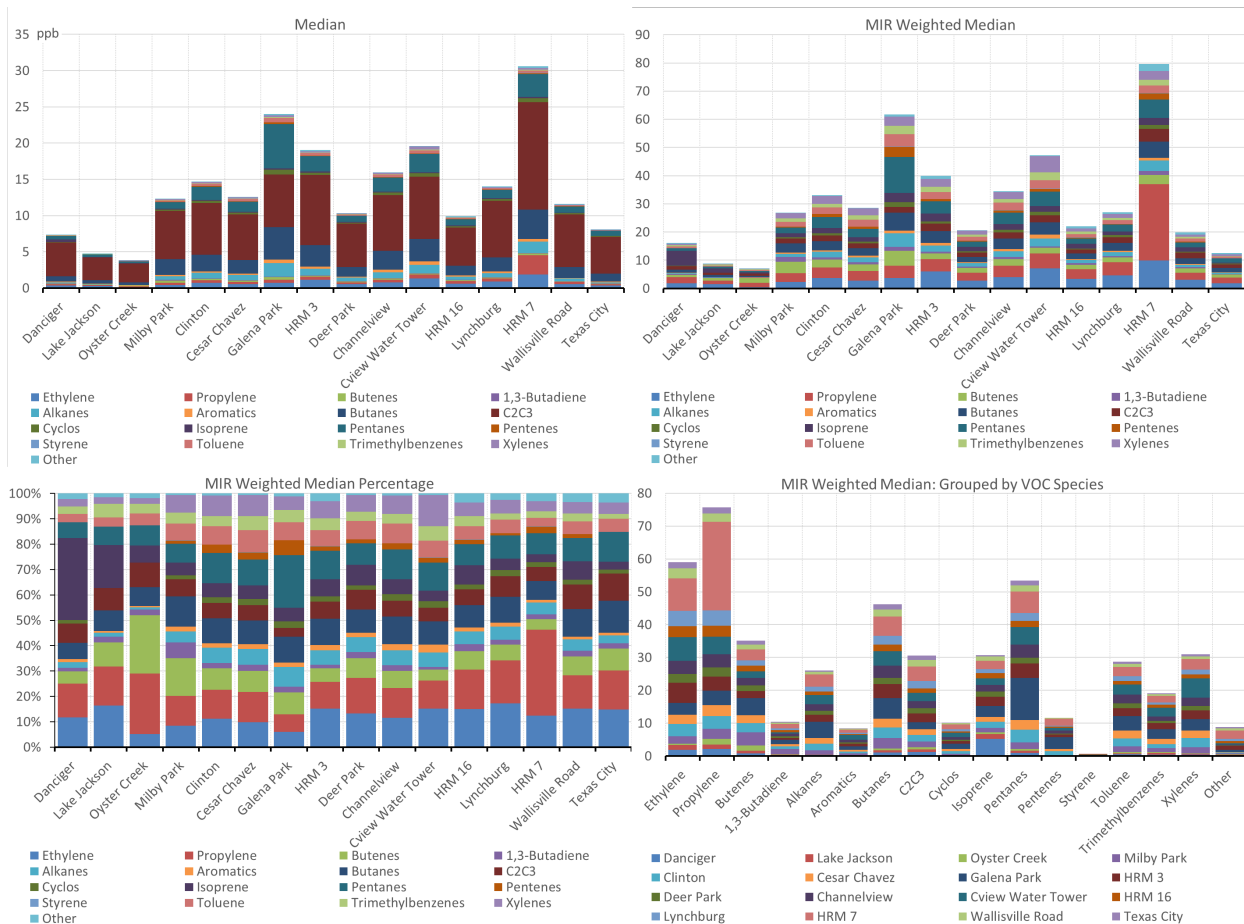


Figure 3-12: Ozone Season VOC Composition in the HGB Area from 2012 through 2021

VOC compositions were also investigated by year to determine if the compositions have changed over time. The median MIR weighted composition by year at each auto-GC with more than eight-years of valid ozone season data are shown in Figure 3-13: *Ozone Season MIR Weighted VOC Composition Trends in the HGB Area*. The scale on the Brazoria and Galveston County auto-GCs (Danciger, Lake Jackson, and Texas City) are different than the scale on the Houston Ship Channel auto-GCs. Increases at Milby Park appear to be driven by increases in HRVOC in 2021. The increases at HRM 3 in 2021 are driven by increases in the other VOC groups and ethylene. The only VOC groups that showed a decrease at HRM 3 over the 10 years analyzed were propylene, butenes, and 1,3-butadiene. While total concentrations at each monitor vary from year to year, overall, the composition for each year appears to be relatively consistent. This indicates that HRVOC remain the largest VOC group with high ozone formation potential in the HGB area.

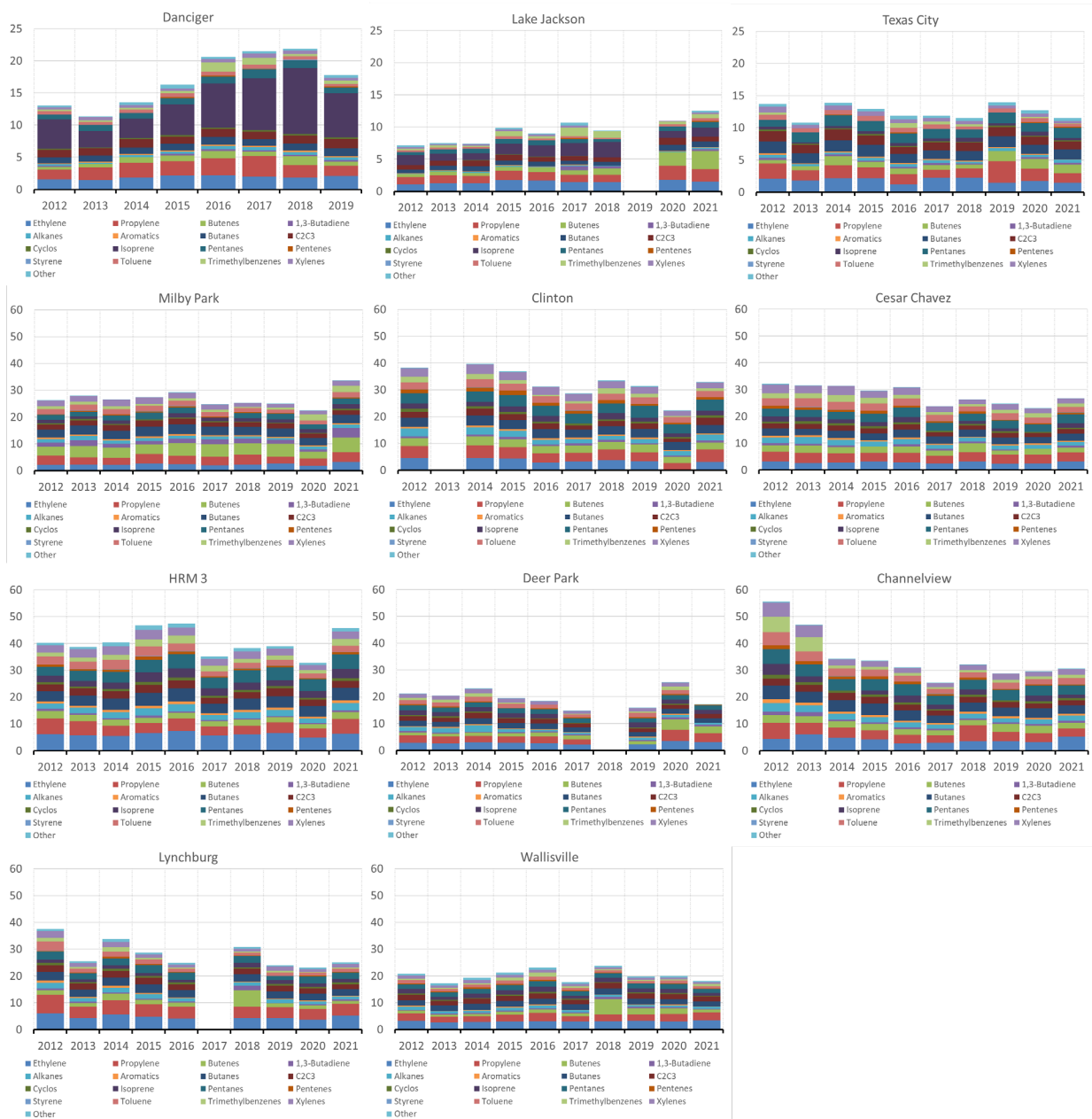


Figure 3-13: Ozone Season MIR Weighted VOC Composition Trends in the HGB Area

3.3 OZONE PRECURSOR EMISSIONS

In addition to trends in ambient concentrations of ozone and ozone precursors, trends in ozone precursor emissions inventories were also investigated. The categories of on-road, non-road, EGUs, and point sources have historically been primary sources of anthropogenic NO_x and VOC emissions in ozone nonattainment areas.

3.3.1 On-Road and Non-Road Emissions Trends

From the late 1990s to the present, federal, state, and local measures have resulted in significant NO_x and VOC reductions from on-road and non-road sources within the HGB area. The Texas Commission on Environmental Quality (TCEQ) funded a study by

the Texas Transportation Institute (TTI) to estimate on-road emissions trends throughout Texas from 1999 through 2050 using the 2014a version of the Motor Vehicle Emission Simulator (MOVES2014a) model (TTI 2015). On-road emissions in the HGB area are estimated to have large decreases from 1999 through 2021 and beyond, even as daily VMT is estimated to increase. This reduction in on-road NO_x and VOC is projected to continue as older, higher-emitting vehicles are removed from the fleet and are replaced with newer, lower-emitting ones.

A similar pattern is reflected in a TCEQ non-road emissions trends analysis using the Texas NONROAD (TexN) model. Non-road emissions are estimated to decrease from 1999 through 2021 and beyond even as the number of non-road engines, based on equipment population, has increased. As with the on-road fleet turnover effect, reductions in non-road NO_x and VOC emissions are projected to continue as older, higher-emitting equipment is removed from the fleet and replaced with newer, lower-emitting equipment.

3.3.2 Point Source Emissions Trends

Data were pulled from the State of Texas Air Reporting System (STARS) to investigate emissions from sources that meet the reporting requirements under the TCEQ emissions inventory rule (30 Texas Administrative Code (TAC) §101.10). The emissions trends analysis uses ten years of data from 2012 through 2021.

Emissions trends in tons per year (tpy) by site for NO_x, VOC, and HRVOC in the HGB area are displayed in Figure 3-13: *HGB Area Point Source NO_x Emissions by Site*, Figure 3-14: *HGB Area Point Source VOC Emissions by Site*, and Figure 3-15: *HGB Area Point Source HRVOC Emissions by Site*. Because the HGB area has so many point sources, only the top emitters are displayed on each chart. All other point source emissions in the HGB area were added together and displayed as the Sum of All Others. All figures are formatted with the largest emitter as the bottom section of the bar.

Figure 3-14 shows that the top 10 reporting sites accounted for 52% of the total point source NO_x emissions in the HGB area in 2021. Each of these sites reported total NO_x emissions exceeding 800 tpy in 2021, with the largest emitter, NRG Texas Power LLC - WA Parish Electric Generating Station,² reporting over 5,000 tons of NO_x in 2021. Overall, NO_x emissions have increased 7% from 2012 through 2021. This correlates with the ambient NO_x trends for the HGB area, which showed little change from 2012 through 2021.

² Source names are the combined company and site names from STARS.

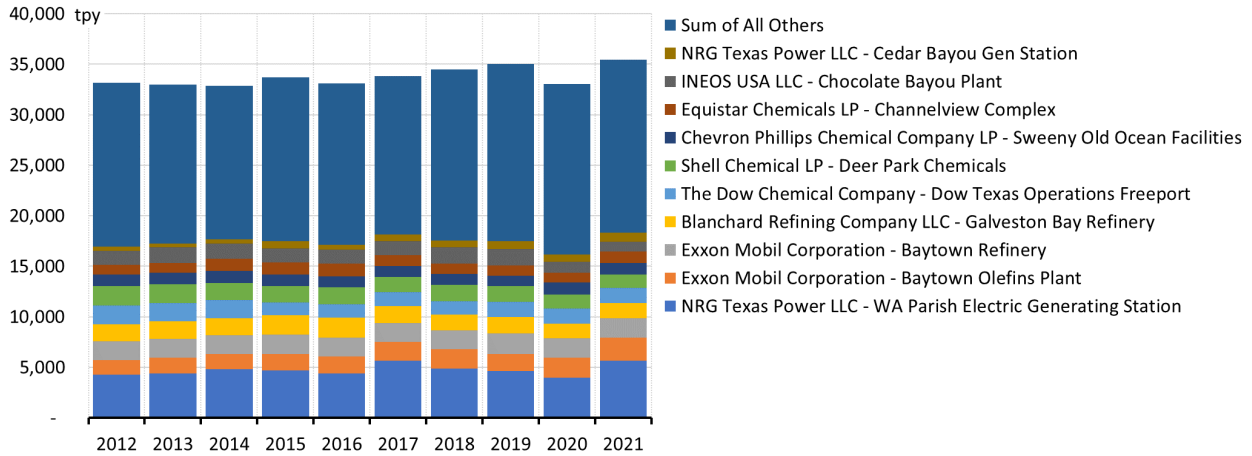


Figure 3-14: HGB Area Point Source NO_x Emissions by Site

Figure 3-15 shows that the top 11 reporting sites accounted for 41% of the total point source VOC emissions in the HGB area in 2021. Each of these sites reported total VOC emissions exceeding 500 tpy in 2021, with the largest emitter, Exxon Mobile Corporation - Baytown Refinery, reporting over 2,000 tons of VOC in 2021. Overall, VOC emissions decreased 14% from 2012 through 2021, through the 11 sites with the largest VOC emissions showed almost no change. Trends from the top 11 VOC sources correlate with the ambient VOC trends, but overall trends in VOC emissions show more decline than ambient TNMHC trends.

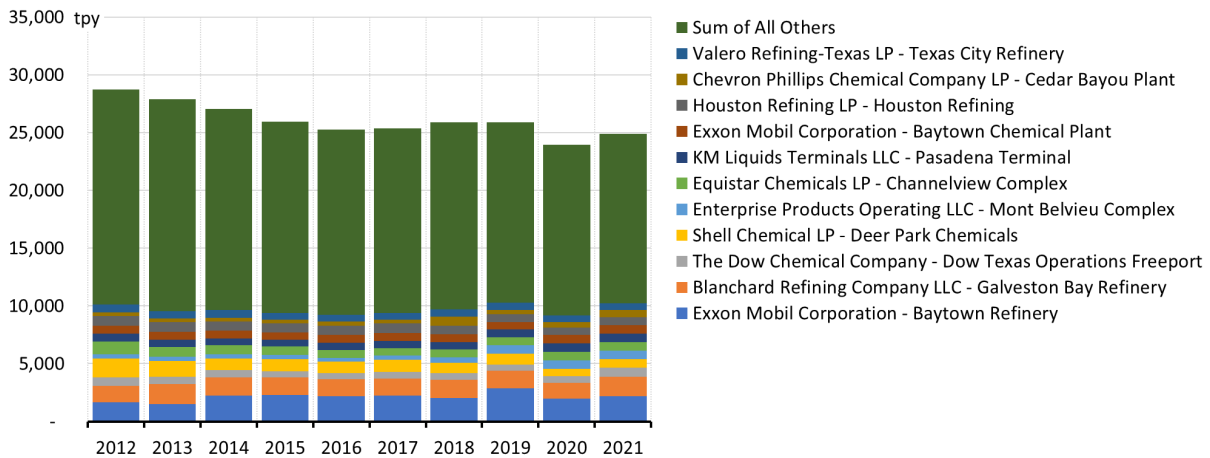


Figure 3-15: HGB Area Point Source VOC Emissions by Site

Figure 3-16 shows that the top nine reporting sites accounted for 51% of the total point source HRVOC emissions in the HGB area in 2021. Each of these sites reported total HRVOC emissions exceeding 100 tpy in 2021, with the largest emitter, the Dow Chemical Company - Dow Texas Operations Freeport, reporting over 300 tpy of HRVOC in 2021. Overall, HRVOC emissions decreased 3% from 2012 through 2021, with increases occurring after 2013. This correlates with the ambient HRVOC trends for the HGB area, which also show little change from 2012 through 2021.

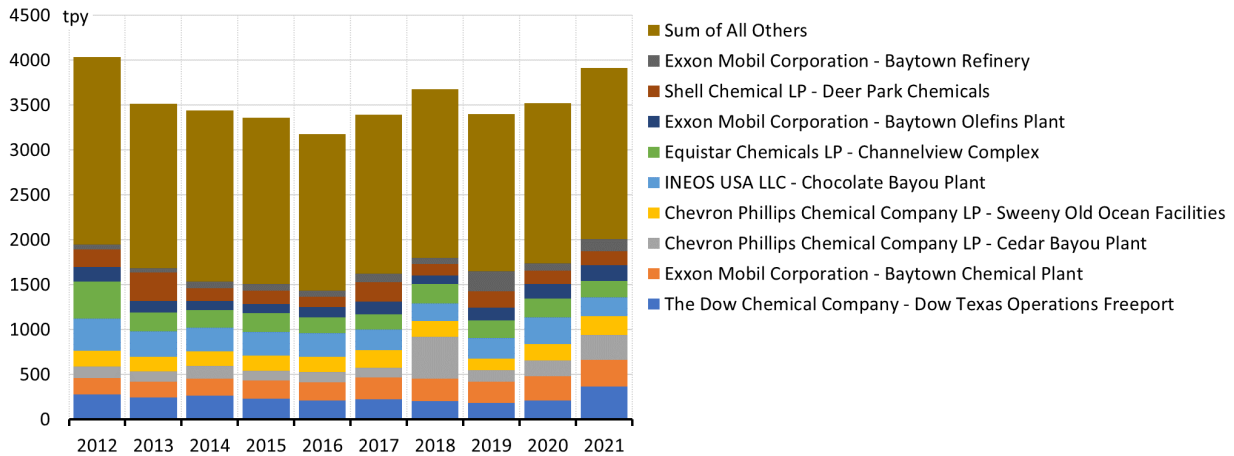


Figure 3-16: HGB Area Point Source HRVOC Emissions by Site

3.3.3 Point Source Locations

The location of the point source emissions for NO_x , VOC, and HRVOC is important to determine the impacts of these emissions on ozone formation. Sources located downwind of monitors that historically record high ozone concentrations would have less of an effect on ozone formation in the area compared to sources located upwind of those monitors.

The large amount and geographic extent of point sources in the HGB area causes many of the points to overlap on a map, obscuring the display. To provide a clearer representation of the spatial distribution of emissions, maps for NO_x , VOC and HRVOC are each displayed at four various zoom levels. Maps of the 2021 NO_x , VOC, and HRVOC emissions are displayed in Figure 3-17: *Maps of the 2021 Point Source NO_x Emissions in the HGB Area*, Figure 3-18: *Maps of the 2021 Point Source VOC Emissions in the HGB Area*, and Figure 3-19: *Maps of the 2021 HRVOC Point Source Emissions in the HGB Area*. For all three pollutants, the top left map displays emissions for the entire HGB area, the top right map displays emissions for the Houston Ship Channel, the bottom left map displays emissions for Lake Jackson, and the bottom right map displays emissions for Mont Belview. The maps show the large concentration of emissions in the Houston Ship Channel, as well as large sources of emissions in Texas City and Lake Jackson. In addition to those areas, NRG Texas Power LLC - WA Parish Electric Generating Station, which is in the west portion of the HGB area, is also a large NO_x source in the HGB area.

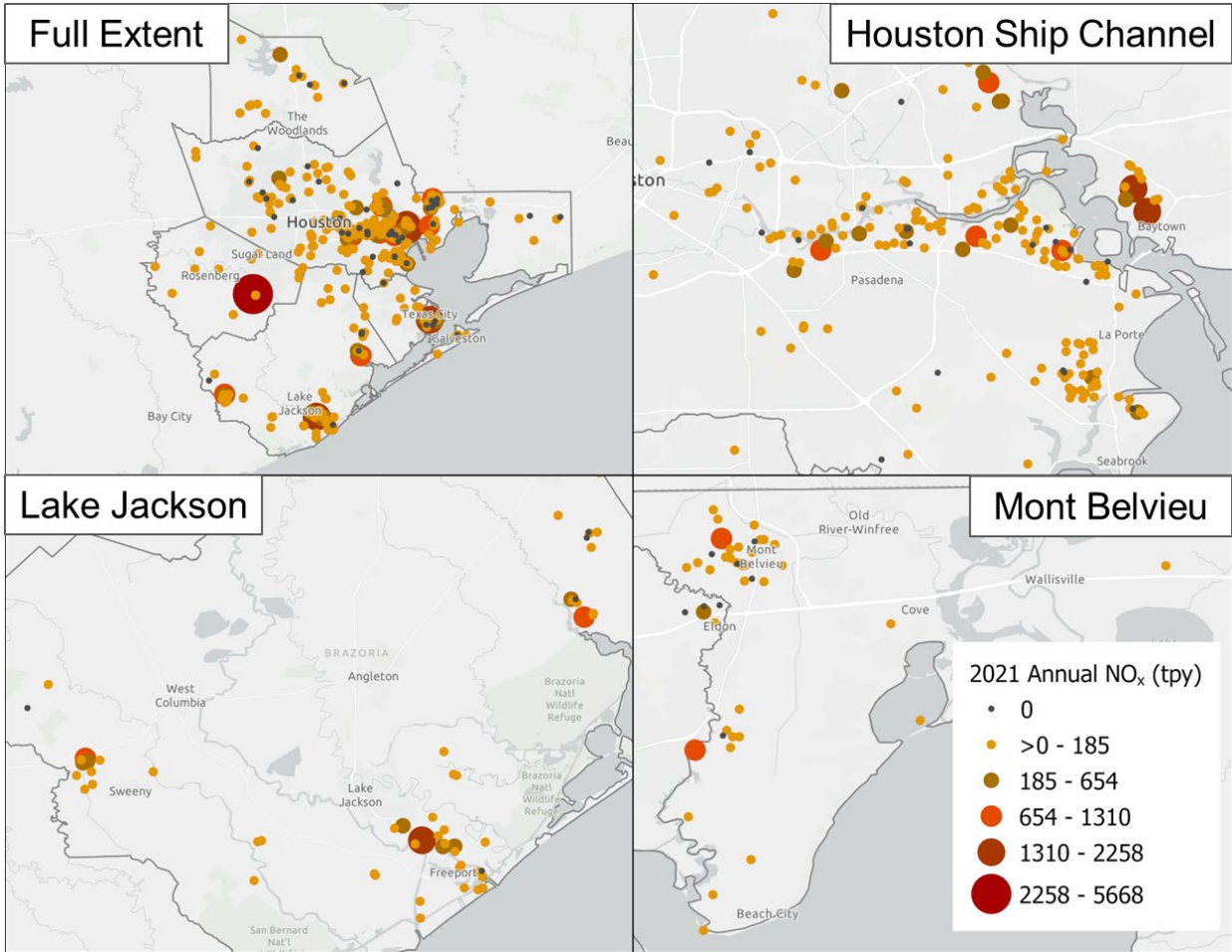


Figure 3-17: Maps of the 2021 Point Source NO_x Emissions in the HGB Area

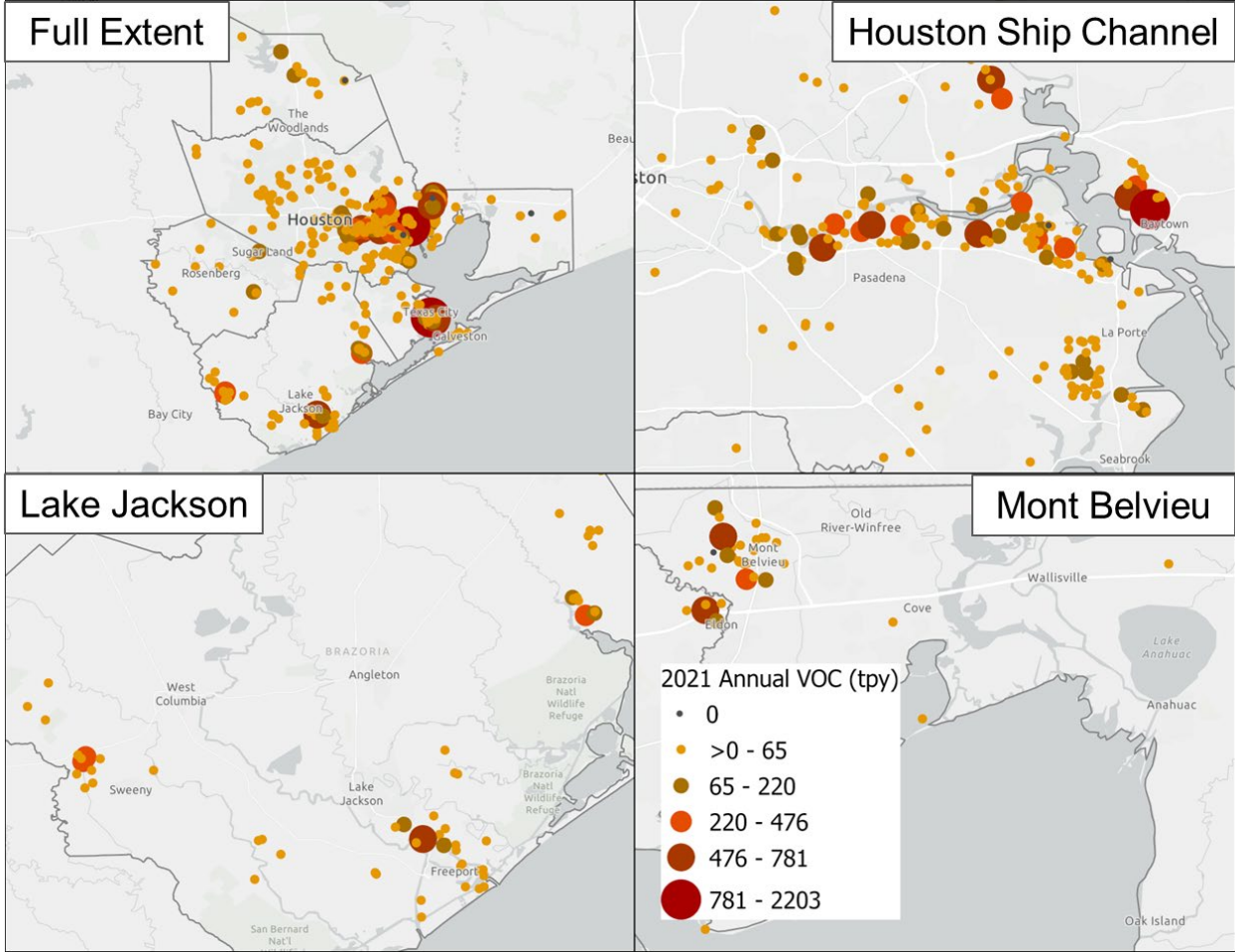


Figure 3-18: Maps of the 2021 Point Source VOC Emissions in the HGB Area

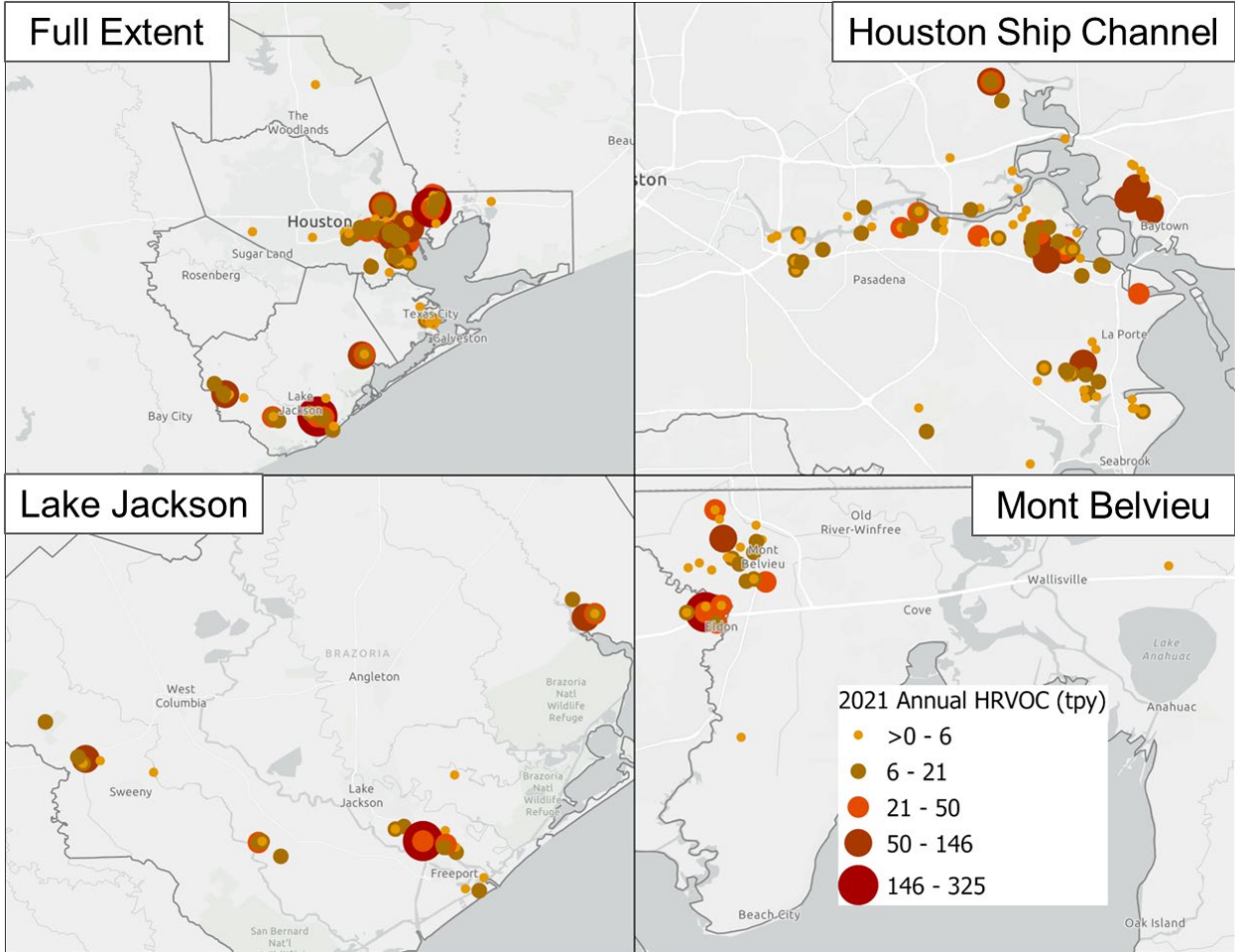


Figure 3-19: Maps of the 2021 HRVOC Point Source Emissions in the HGB Area

CHAPTER 4: OZONE CHEMISTRY

This section will explore ozone chemistry by investigating the volatile organic compound (VOC) and nitrogen oxides (NO_x) limitations as well as the ozone formation on weekdays versus weekends in the Houston-Galveston-Brazoria (HGB) area. A detailed analysis of ozone chemistry indicates which precursors are most important to ozone formation in the HGB area.

4.1 VOC AND NO_x LIMITATIONS

The VOC and NO_x limitation of an airshed indicates how ozone will change in response to reductions of either VOC or NO_x. A NO_x limited regime occurs when the radicals from VOC oxidation are abundant, and therefore ozone formation is more sensitive to the amount of NO_x present in the atmosphere. In these regimes, controlling NO_x would be more effective in reducing ozone concentrations. In VOC limited regimes, NO_x is abundant, and therefore ozone formation is more sensitive to the number of radicals from VOC oxidation present in the atmosphere. In VOC limited regimes, controlling VOC emissions would be more effective in reducing ozone concentrations. Areas where ozone formation is not strongly limited by either VOC or NO_x are considered transitional and controlling either VOC or NO_x emissions would reduce ozone concentrations in these regions. A paper by Dickens (2022) contains more detail on ozone chemistry, although the paper focuses on the Lake Michigan Air Directors Consortium region.

VOC-to-NO_x ratios are calculated by dividing hourly total non-methane organic carbon (TNMOC) concentrations in parts per billion carbon (ppbC) by hourly NO_x concentrations in parts per billion (ppb) by volume, more commonly referred to as ppb. The value of the ratio then determines the limitation of the air mass. While ratio definitions for VOC limited, NO_x limited, or transitional atmospheric conditions vary, this analysis uses the cut points described in the Environmental Protection Agency's (EPA) photochemical assessment monitoring stations (PAMS) training workshop (Hafner and Penfold, 2018). Ratios less than 5 ppbC/ppb are considered VOC limited, ratios above 15 ppbC/ppb are considered NO_x limited, and ratios between 5 ppbC/ppb and 15 ppbC/ppb are considered transitional. Calculation of VOC-to-NO_x ratios are limited by the number of collocated auto-GC and NO_x monitors available in the area. In addition, auto-GC monitors are often source-oriented, and therefore do not necessarily reflect the conditions of the whole area.

The analysis used seven monitors in the HGB area that have collocated VOC and NO_x data: Channelview, Clinton, Lynchburg, HRM 3, Wallisville, Oyster Creek, and Deer Park. These monitors do not typically measure high ozone values, meaning the VOC/NO_x ratios may not represent the chemical regime that is present at the ozone design value setting monitors. Trends at Deer Park only go through 2018, because the NO_x monitor at that site ceased operations after that year. Because Oyster Creek started operation in December 2016, trends at that monitor start in 2017. All monitors are in the area around the Houston Ship Channel except Oyster Creek, which is in Brazoria County near Lake Jackson. Ratios were calculated for each hour of the day for the ozone season and then aggregated to determine the median ratio for each year. Results are shown in Figure 4-1: *Median VOC-to-NO_x Ratios During the Ozone Season in the HGB Area.*

Most monitors show slight variations in VOC-to-NO_x ratios but only one monitor, Channelview, had a noticeable trend. Although ratios at Channelview have remained in the transitional regime over the past ten years, the ratios have trended from closer to NO_x-limited in 2012 to closer to VOC limited in 2021. Lynchburg Ferry has one year that was VOC limited, 2017, which may be due to missing data and does not necessarily represent the true conditions at that monitor during that year.

Most monitors in the Houston Ship Channel show a transitional regime, so either NO_x or VOC reductions would reduce ozone concentrations. The Clinton monitor measures ratios that, while still transitional, are closer to VOC limited. This could be due to the monitor location, which is on the western edge of the ship channel and close to downtown Houston. This would mean that the Clinton monitor measures more urban emissions compared to the other monitors, which measure more industrial emissions. Another monitor to note is the Oyster Creek Monitor, which measures transitional conditions but is close to NO_x limited. The Oyster Creek monitor is the only monitor analyzed that is not in Houston but is closer to the coast. This monitor observes much lower NO_x emissions since it is not close to the Houston urban core.

VOC-to-NO_x ratios were also investigated by hour to determine how diurnal variability effects the chemical composition of the atmosphere. Hourly medians for the ozone season from 2012 through 2021 at each monitor are shown in Figure 4-2: *Median Hourly VOC-to-NO_x Ratios During the Ozone Season from 2012 through 2021 in the HGB Area*. Diurnal patterns show that overnight hours are typically NO_x limited or close to NO_x limited. Daytime hours are typically within the transitional regime for all monitors in the HGB area. The only monitor that measured VOC limited conditions during the early morning hours is Clinton, which, as mentioned above, measures more urban emissions.

Since morning hours are when the peak VOC and NO_x are often observed, those hours were investigated more closely. The frequency that the VOC-to-NO_x ratio was either VOC limited, transitional, or NO_x limited was determined using the hours of 5:00 LST though 8:00 LST for the ozone season in the HGB area. Results are shown in Figure 4-3: *Frequency of VOC Limited, NO_x Limited, and Transitional Regimes During Ozone Season Mornings from 2012 through 2021 in the HGB Area*. The results show that, for most of the monitors, the morning hours are transitional most of the time, with a smaller number of hours measuring either VOC limited or NO_x limited conditions in approximately similar amounts. The three monitors that have different patterns are Clinton, Wallisville, and Oyster Creek. Oyster Creek, which is further from the urban area, measures more hours with NO_x limited and transitional conditions. There is a similar pattern at Wallisville, which is on the eastern end of the Houston Ship Channel. Clinton measured more VOC limited conditions, further indication that areas closer to urban emissions measure more VOC limited conditions.

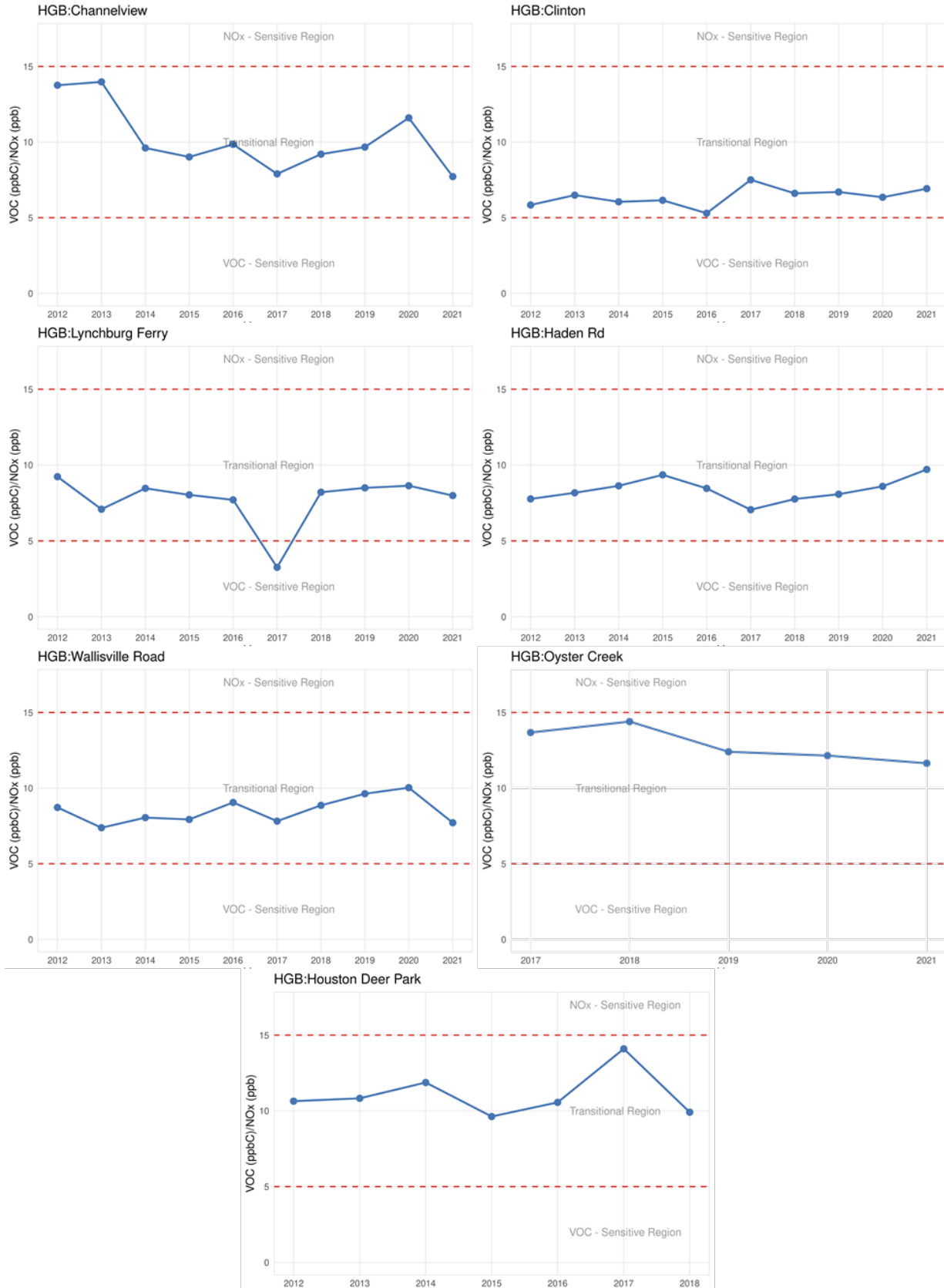


Figure 4-1: Median VOC-to-NO_x Ratios During the Ozone Season in the HGB Area

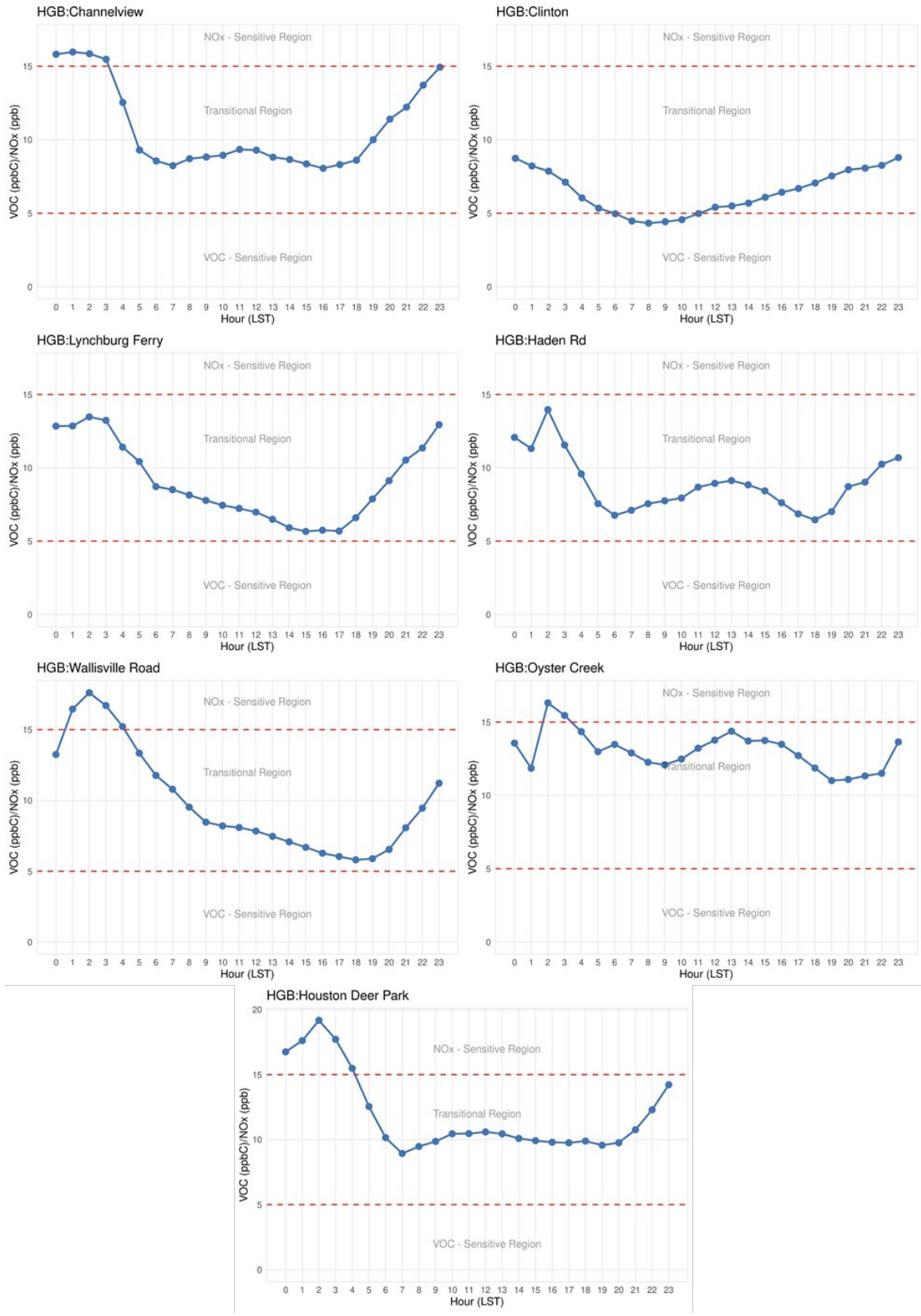


Figure 4-2: Median Hourly VOC-to-NO_x Ratios During the Ozone Season from 2012 through 2021 in the HGB Area

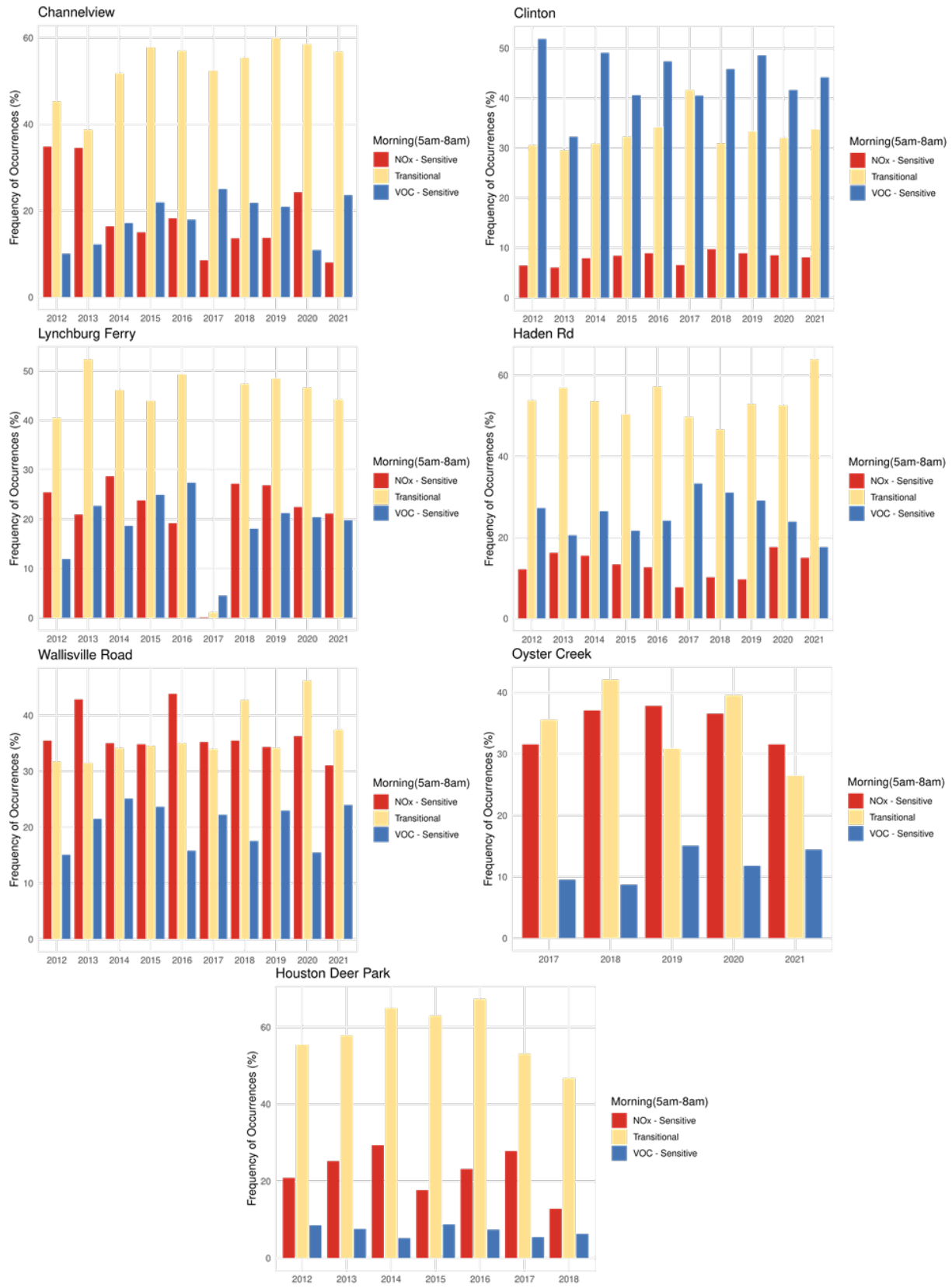


Figure 4-3: Frequency of VOC Limited, NO_x Limited, and Transitional Regimes During Ozone Season Mornings from 2012 through 2021 in the HGB Area

Overall, the VOC-to-NO_x ratio analysis indicates that monitors located closer to the urban core measure ratios closer to VOC limited conditions, monitors near more industrial areas measure closer to transitional conditions, and monitors in more suburban area measure closer to NO_x limited conditions. These findings are corroborated by other research that shows a NO_x limited regime over much of the HGB area and a VOC limited regime in the Houston Ship Channel (Goldberg et al. 2022). It appears that the atmospheric chemistry surrounding many monitors in the HGB area has not changed from 2012 through 2021. Some combination of VOC and NO_x controls would possibly be effective in reducing ozone concentrations in the HGB area. Even in transitional areas, controls on either VOC or NO_x may not give result in equal reductions in ozone, one species may reduce ozone at greater rates than the other, even in transitional areas.

4.2 WEEKDAY VERSUS WEEKEND ANALYSIS

Ozone concentrations tend to vary by day of the week. Changes in ozone and its precursors by day of the week can be used to indicate an area's ozone chemistry as well as precursor emissions sources. Theoretically, if NO_x concentrations were lowered on weekends, it would be due to less mobile-source NO_x emissions in the absence of a morning rush hour on the weekends. If ozone also changed on the weekends compared to the weekdays, then it would be evidence that changing NO_x concentrations in turn effects ozone concentrations, indicating that the area is NO_x limited.

The weekday versus weekend effect on ozone was investigated in several different ways. First, the number of eight-hour ozone exceedance days (by day of the week) from 2012 through 2021 was investigated. Various levels of ozone exceedances were used to determine if there is a varying day of the week pattern at different ozone concentrations. Results are shown in Figure 4-4: *Number of Eight-Hour Ozone Exceedance Days by Day of the Week in the HGB Area from 2012 through 2021*.

The results show that, over the past ten years, Sunday had the lowest number of eight-hour ozone exceedance days at all levels, and Wednesday had the highest total number of eight-hour ozone exceedance days. There appears to be some weekend effect; however, that effect seems more pronounced on Sunday compared to Saturday. Saturday does have fewer low-level ozone exceedance days, but at levels of 76 ppb and above, Saturday has a similar number of exceedance days compared to Monday, Tuesday, and Thursday.

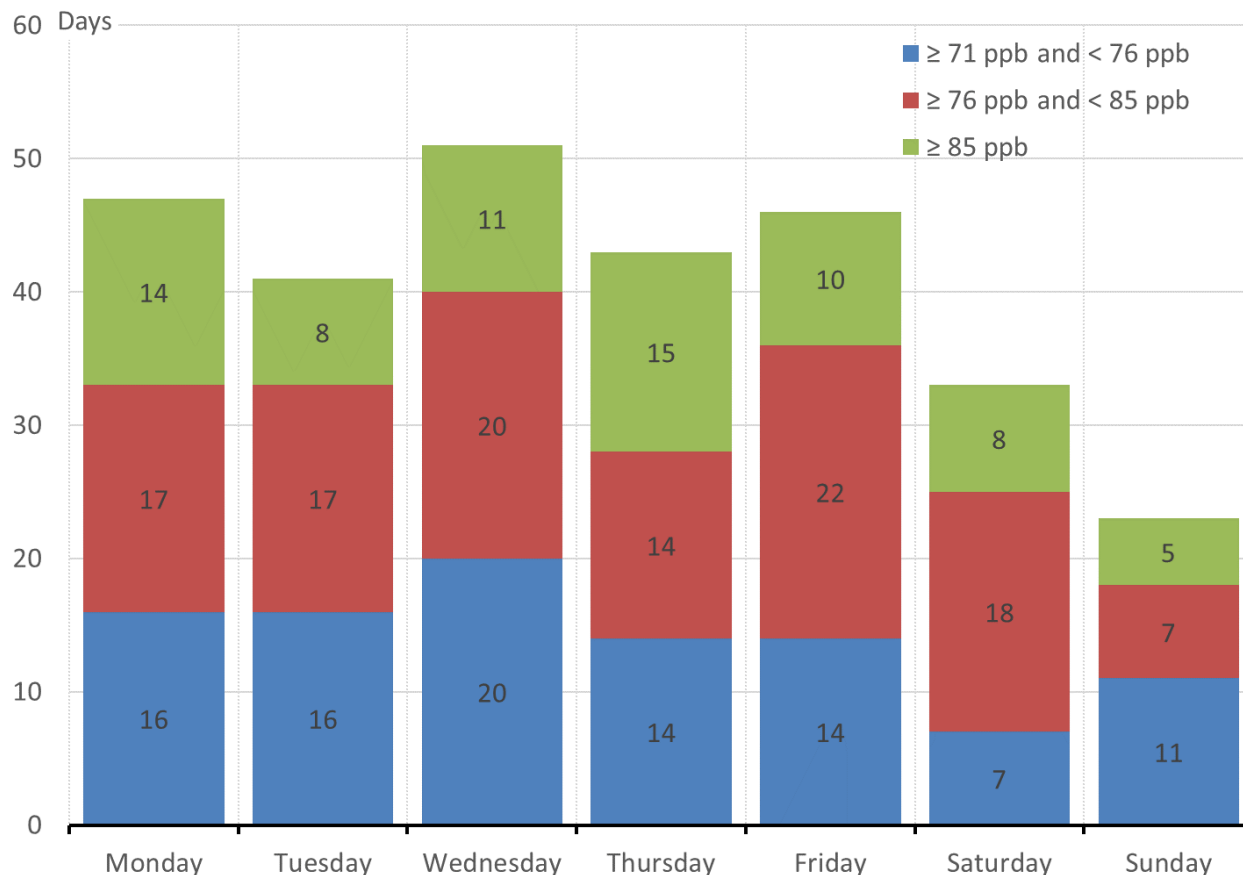


Figure 4-4: Number of Eight-Hour Ozone Exceedance Days by Day of the Week in the HGB Area from 2012 through 2021

These patterns in eight-hour ozone exceedance days by day of the week suggest changes in emissions from the weekdays relative to the weekends do influence ozone concentrations in the HGB area. To examine this further, the average number of eight-hour ozone exceedance days on the weekdays and the weekends from 2012 through 2021 was calculated at each monitor location. Those values were then mapped using kriging interpolation to determine if there were any location-based changes in ozone exceedance days on the weekdays versus the weekends. Only ozone monitors in operation in 2021 and with more than eight years of data were analyzed. Results are presented in Figure 4-5: *Average Ozone Exceedance Days on the Weekdays versus the Weekends from 2012 through 2021 in the HGB Area*. Only two monitors have an increase in the average number of ozone exceedance days, Aldine and North Wayside. The Clinton monitor showed almost no change from the weekdays to the weekend. Overall, almost all monitors observe a reduction in the average number of ozone exceedance days on the weekdays versus the weekends.

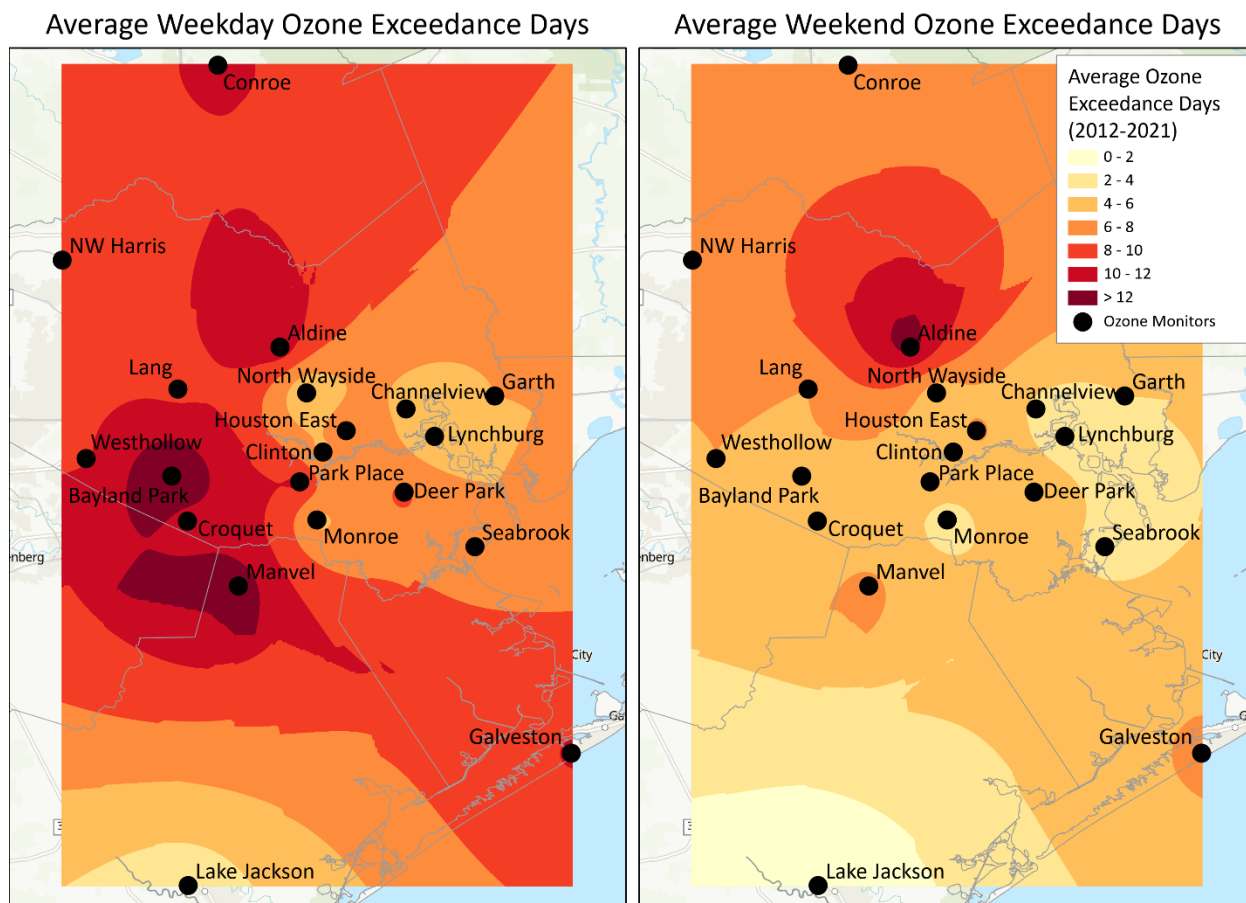


Figure 4-5: Average Ozone Exceedance Days on the Weekdays versus the Weekends from 2012 through 2021 in the HGB Area

To examine possible causes for the weekend effect, eight-hour ozone, NO_x, TNMOC, and VOC concentrations were investigated by day of the week. Since it is typically the highest values that change due to the weekend effect, this analysis investigates the 95th percentile concentrations. Only valid ozone season days and years from 2012 through 2021 were used in the analysis. A valid day is any day with at least 75% complete data and a valid year is any year with at least 75% valid days during the ozone season. All valid hours for each parameter were used to calculate the 95th percentile values. Results are shown in Figure 4-6: *Ozone Season 95th Percentile Concentrations by Day of the Week from 2012 through 2021*. All monitors with valid days and years were used in this analysis, caution should be used if comparing across monitors rather than across days of the week. The weekdays in the graphics are represented by blue bars while the weekends are represented by red bars.

Most monitors have a slight decrease in concentrations on the weekends compared to the weekdays with Sundays typically having the lowest eight-hour ozone concentrations. It appears that the increase of exceedance days on the weekends at Aldine was driven by Saturday concentrations as the Sunday concentrations are lower compared to other days of the week. Monitors that see less of a weekend effect tend to be those near more urban or industrial areas such as North Wayside, Lang, Harvard, Lynchburg, Garth, Houston East, and Clinton.

The weekend effect is clearly seen when looking at the NO_x concentrations. Almost all monitors observe a large decrease in 95th percentile NO_x on the weekends compared to the weekdays, with some monitors showing almost 50% less NO_x on the weekends. The only NO_x monitor that shows almost no change on the weekends is Galveston.

Although some monitors show a decrease in TNMOC on the weekends, the change from day to day seems negligible. There is even less change from weekday to weekends when looking at HRVOC. Although VOC can come from mobile sources, it appears that ambient VOC concentrations in the HGB area are driven more by point sources, which show little variability by day of the week.

Overall, it appears that ozone in most of the HGB area decreases on the weekends, which is driven largely by reductions in NO_x concentrations. The change in ozone levels on weekends is much smaller than the change in NO_x. This indicates that changes in ozone are not proportional to changes in precursor concentrations.

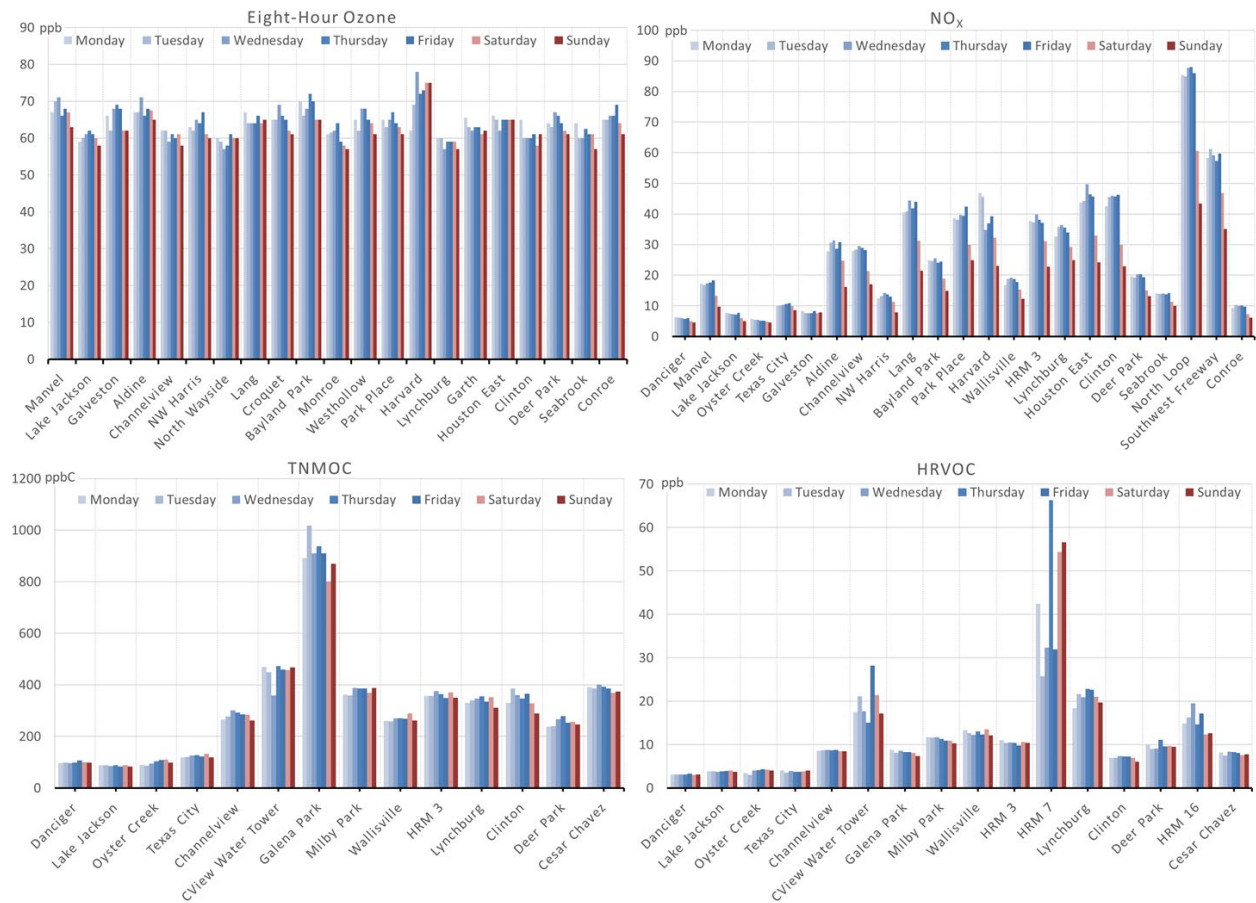


Figure 4-6: Ozone Season 95th Percentile Concentrations by Day of the Week from 2012 through 2021

CHAPTER 5: METEOROLOGY AND ITS AFFECT ON OZONE

Meteorological factors play an important role in ozone formation. Meteorological conditions can affect how ozone precursors react, where ozone is formed, and how much ozone is accumulated in an area. This section will look at these various meteorological factors at both the local-scale and the large-scale, or synoptic-scale, to determine their effects on ozone formation in the Houston-Galveston-Brazoria (HGB) area.

5.1 TEMPERATURE

Temperature can play an important part in the ozone formation process. Warmer temperatures often indicate sunny, cloudless days, which are ideal days for ozone formation. To investigate the role of temperature on ozone formation in the HGB area, the area-wide daily maximum temperature in degrees Fahrenheit (°F) was compared to the area-wide daily-maximum eight-hour (MDA8) ozone concentrations in parts per billion (ppb). This analysis only used ozone season data from 2012 through 2021. Only monitors with at least eight complete years of valid data were used. A day was considered valid when at least 75% of hours had a valid temperature and a year was considered valid when it had at least 75% of valid days. Results are displayed in Figure 5-1: *Ozone Season Daily-Maximum Temperature versus MDA8 Ozone in the HGB Area from 2012 through 2021*.

The results show that there is a positive relationship between temperature and ozone; however, at higher temperatures there is more variability in the data, with both high and low ozone levels recorded during days with high temperatures. In the graphic, days with MDA8 ozone concentrations greater than 70 ppb are highlighted in red. Over the past ten years, no days with eight-hour ozone values above 70 ppb occurred with temperatures less than 73 degrees Fahrenheit (°F). This indicates that, while high ozone occurs during times with high temperatures, other conditions are needed for high ozone to form in the HGB area.

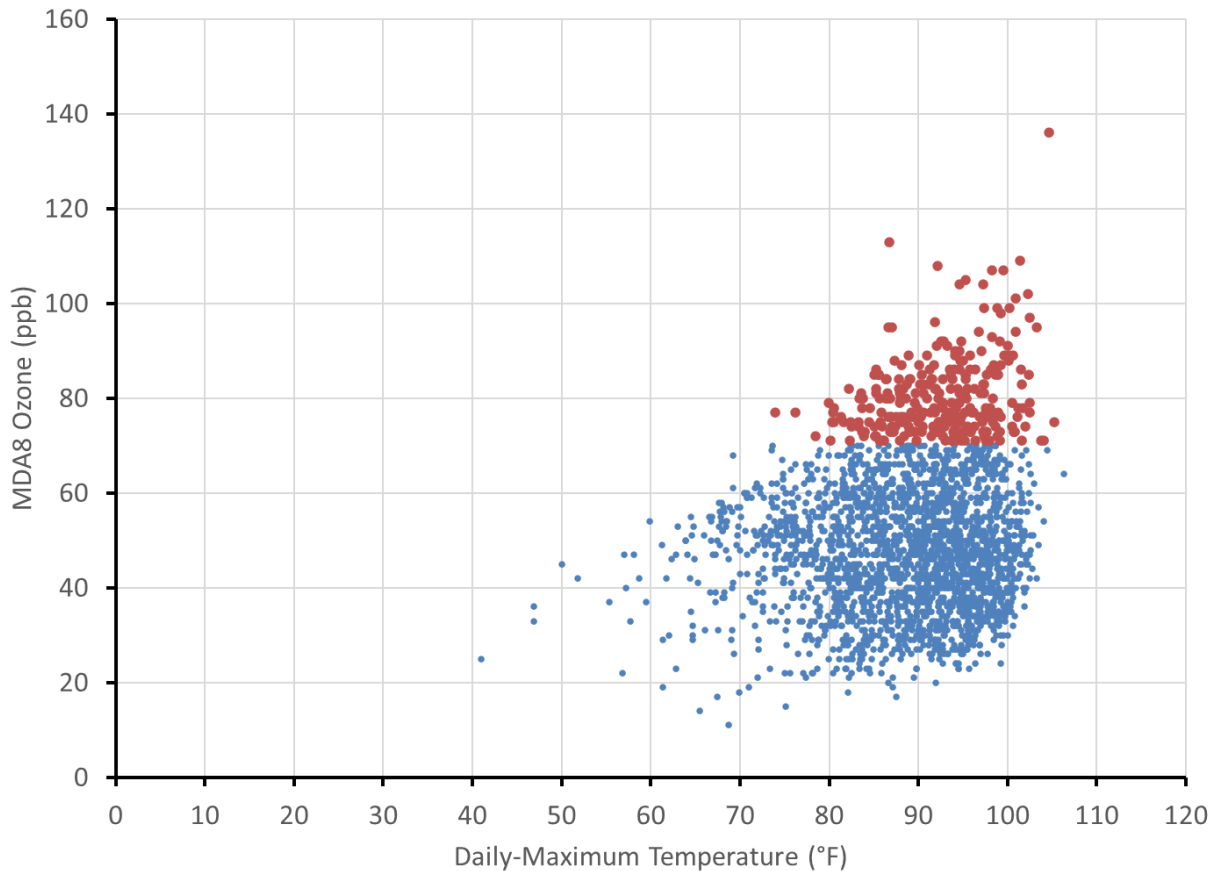


Figure 5-1: Ozone Season Daily-Maximum Temperature versus MDA8 Ozone in the HGB Area from 2012 through 2021

5.2 RELATIVE HUMIDITY

Relative humidity is another meteorological factor that correlates with ozone formation. The average mid-day (10:00 LST through 15:00 LST) relative humidity was compared to the MDA8 ozone value for each monitor with at least eight years of valid ozone season data from 2012 through 2021. A mid-day time scale was chosen because this time was shown to have a larger correlation with ozone concentrations (Wells et al. 2021). A day was considered valid when at least 75% of hours had a relative humidity value and a year was considered valid when it had at least 75% of valid days. Results are displayed in Figure 5-2: *Ozone Season Average Mid-Day Relative Humidity versus MDA8 Ozone in the HGB Area from 2012 through 2021*.

Results show a negative correlation between average mid-day relative humidity and MDA8 ozone. Low relative humidity indicates less moisture in the air. This correlation suggests that as the air is more saturated with moisture, less ozone is formed. Days with MDA8 ozone concentrations greater than 70 ppb are highlighted in red. Except for Galveston, which is located on the coast, most monitors measure higher ozone values when the average mid-day relative humidity is less than 60%. Typically, drier air follows cold fronts as they move through the HGB area, and several researchers have shown that post frontal conditions can be conducive to ozone formation in the HGB area (Lefer 2010; Rappenglueck 2008).

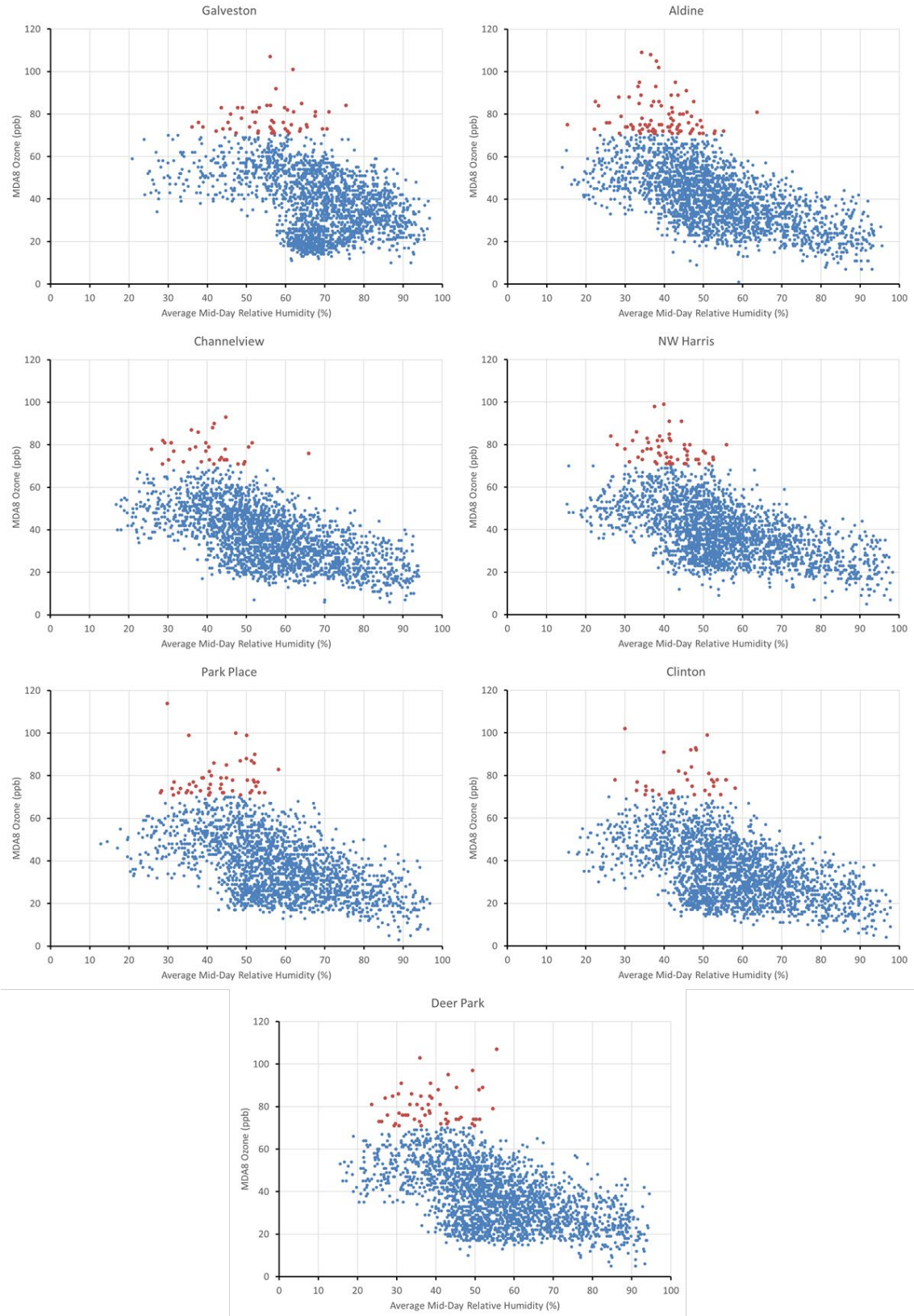


Figure 5-2: Ozone Season Average Mid-Day Relative Humidity versus MDA8 Ozone in the HGB Area from 2012 through 2021

5.3 SOLAR RADIATION

Since ozone requires sunlight to form, solar radiation, which is a measure of the energy emitted by the sun, and its correlation with ozone concentrations was investigated. To summarize solar radiation values, the average solar radiation during daylight hours was investigated. The hours used, 10:00 LST through 17:00 LST, are the hours that would typically go into an MDA8 ozone value. Only ozone season data from monitors with at least eight-years of valid solar radiation data from 2012 through 2021 were used. A day was considered valid when at least 75% of hours had a relative humidity value and a year was considered valid when it had at least 75% of valid days. Results are displayed in Figure 5-3: *Ozone Season Average Daytime Solar Radiation Versus MDA8 Ozone in the HGB Area from 2012 through 2021*. The results show the positive correlation between solar radiation and ozone, with higher ozone values occurring at higher levels of solar radiation.

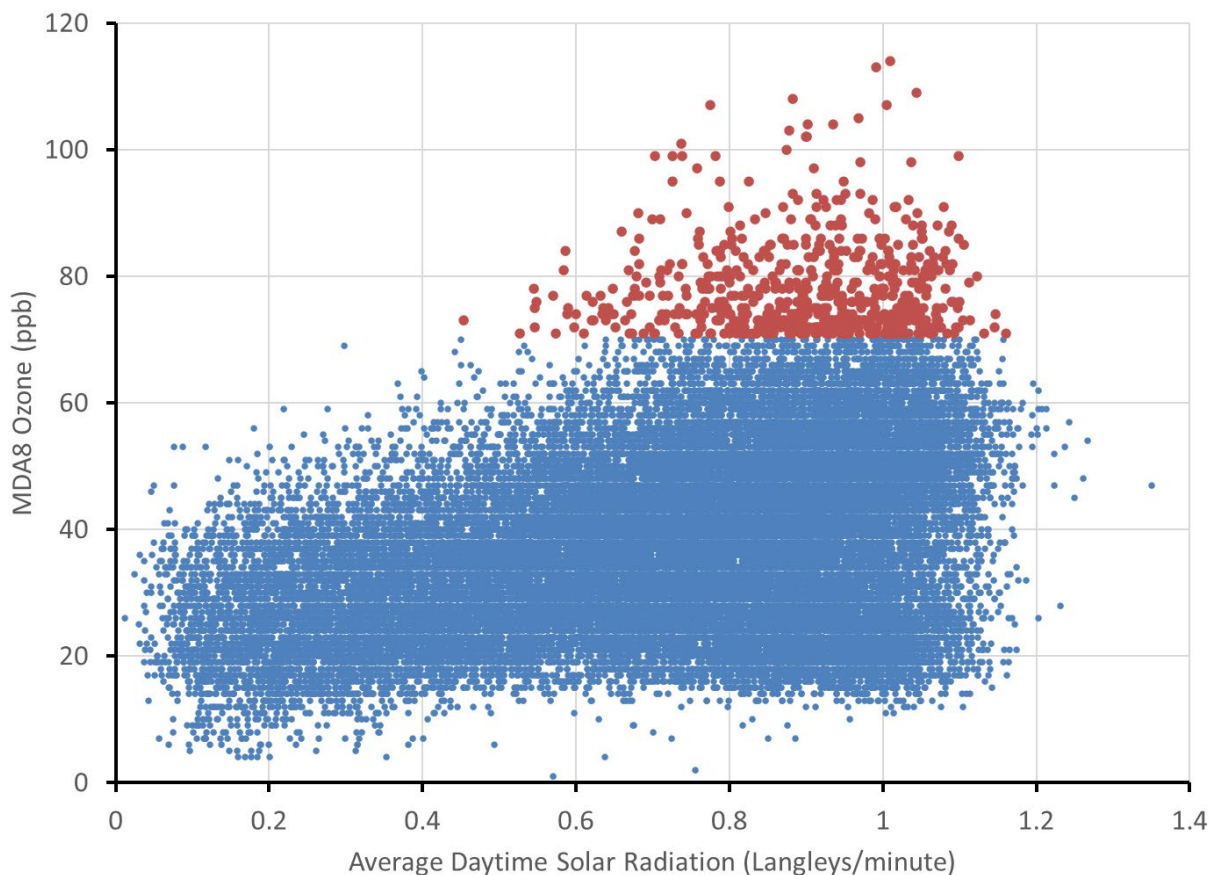


Figure 5-3: Ozone Season Average Daytime Solar Radiation Versus MDA8 Ozone in the HGB Area from 2012 through 2021

5.4 WINDS

Winds are characterized by wind speed and wind direction. Winds can play an important role in ozone formation. Studies have shown that in the HGB area, the highest ozone concentrations are associated with stagnant winds and a land-sea breeze recirculation that typically encompasses all directions over a 24-hour period (Li et al. 2020, Vizuetete et al 2022). Low wind speeds can allow accumulation of ozone and its

precursors, and high wind speeds can lead to dispersion of ozone and its precursors. Changing wind directions can cause recirculation of pollutants in an area, bring about transported ozone from other areas, or bring precursor concentrations from sources upwind to areas downwind. This section will investigate the characteristics of the winds in the HGB area and determine how those winds affect ozone and its precursors.

5.4.1 Wind Speed

Typically, higher ozone concentrations are observed on days with lower wind speeds. Lower wind speeds, many times due to a surface-level high-pressure system in the area, give ozone precursors more time to mix and react, and ozone can quickly accumulate due to limited dispersion. High wind speeds ventilate an area, essentially diluting ozone and its precursors.

To determine the effect of wind speeds on ozone formation, the average morning (07:00 LST through 10:00 LST) resultant wind speed in miles per hour (mph) was calculated from all monitors with at least eight years valid ozone season days from 2012 through 2021. Morning hours were used because these hours were shown to have a larger correlation with ozone concentrations (Wells et al. 2021). A day was considered valid when at least 75% of hours had a relative humidity value and a year was considered valid when it had at least 75% of valid days. Wind speeds were then compared to the MDA8 ozone from the HGB area.

Results are shown in Figure 5-4: *Ozone Season Average Morning Resultant Wind Speed Versus MDA8 Ozone in the HGB Area from 2012 through 2021*. Days with an MDA8 ozone concentration greater than 70 ppb are highlighted in red. The results show that higher ozone is formed when average morning resultant wind speeds are less than about ten miles per hour (mph); however, slower wind speeds don't always produce high ozone. This indicates that there are meteorological factors in addition to wind speed that are involved in ozone formation in the HGB area.

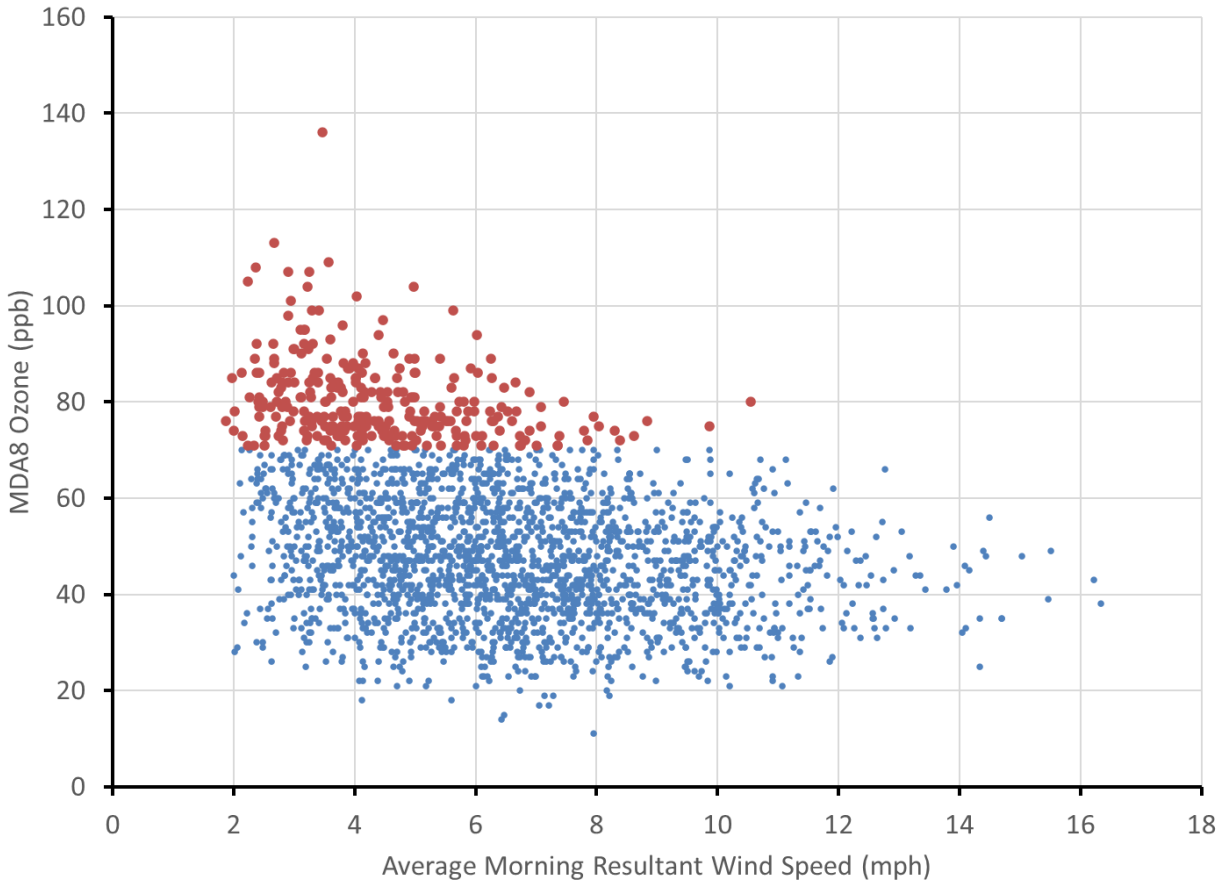


Figure 5-4: Ozone Season Average Morning Resultant Wind Speed Versus MDA8 Ozone in the HGB Area from 2012 through 2021

Typically, meteorological patterns do not show trends but there have been recent worldwide declines in surface winds speeds, a phenomenon known as terrestrial stilling (Deng et al. 2022). To investigate if this is occurring in the HGB area, the average morning resultant winds speeds for the ozone season, as calculated above, were plotted according to date. The results are shown in Figure 5-5: *Average Morning Resultant Wind Speed in the HGB Area from 2012 through 2021*. When plotted by date, there does appear to be a slow decline in average morning resultant wind speeds from 2012 through 2021. Since slow winds are correlated with higher ozone concentrations, the slowing of wind speeds over time may have further implications on ozone in the HGB area. The area may need to do more to reduce ozone if meteorological conditions become more conducive to ozone formation over time.

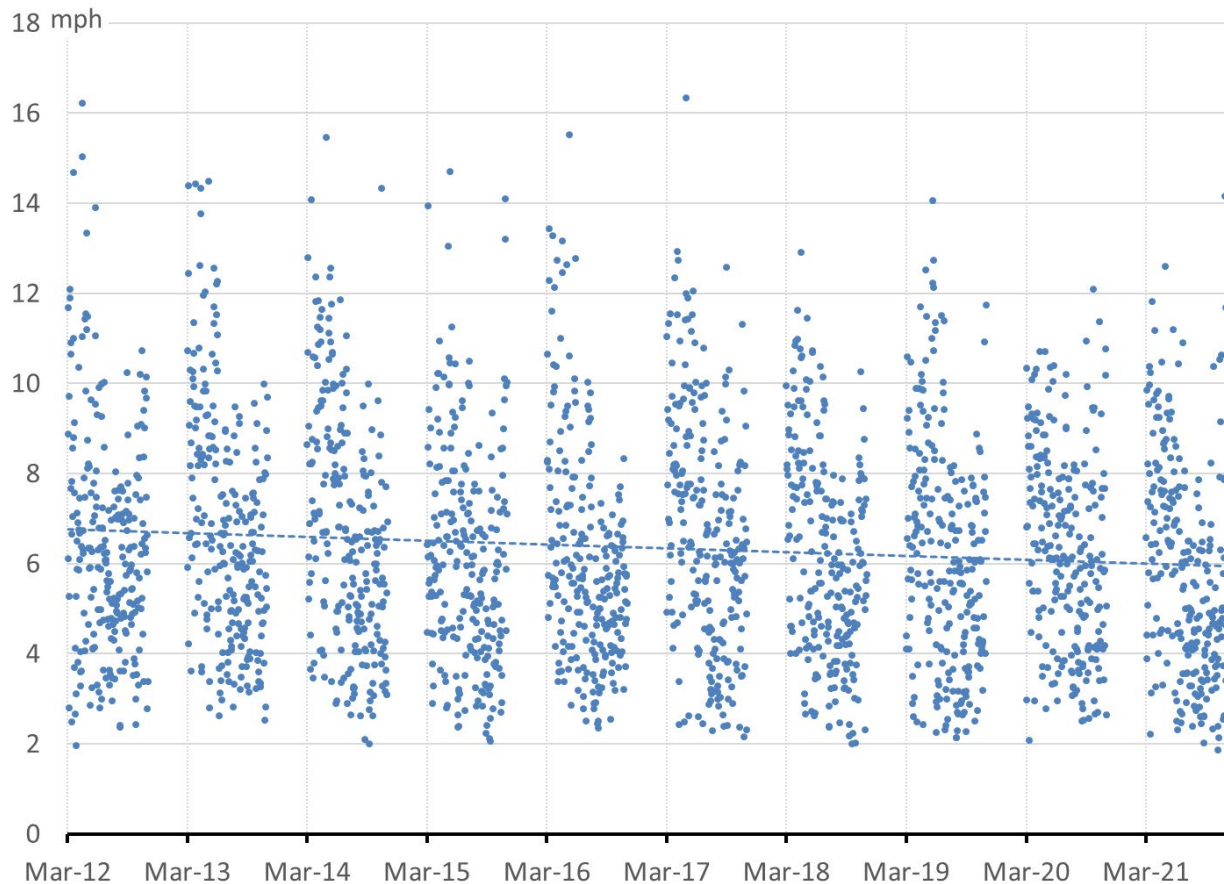


Figure 5-5: Average Morning Resultant Wind Speed in the HGB area from 2012 through 2021

5.4.2 Surface Winds on High Ozone Days

Wind roses and surface-level back trajectories were both used to examine the surface level wind patterns on high ozone days. These types of analysis are informative because they consider both wind speed and wind direction. While a wind rose will show a summary of general wind patterns, a surface-level back trajectory plots the location of an air parcel every five minutes, showing the path of winds on high ozone days.

Wind roses were calculated for the ozone season from 2012 through 2021 at five monitors in the HGB area: Aldine, Clinton, Bayland Park, Manvel, and Galveston. Aldine, Bayland Park, and Manvel were chosen since those monitors frequently measure the highest ozone concentrations, Clinton was chosen to represent air near the Houston Ship Channel, and Galveston was chosen to represent coastal air. Only ozone season days with at least 75% complete data were used in the calculation. Days were further separated into high and low ozone days. Results are shown on the maps in Figure 5-6: *Ozone Season Wind Roses on High and Low Ozone Days in the HGB Area from 2012 through 2021*. The lighter colors on the wind roses represent faster wind speeds.

Wind roses show that the direction of prevailing winds does change depending on the monitor location and between high and low ozone days. On low ozone days, most

monitors show faster winds primarily from the south and southeast, with the Clinton monitor also showing winds from the southwest. On high ozone days, the winds are slower at most monitors with a more variable direction. Bayland Park and Manvel both continue to mostly show southeast winds, but Aldine has more west winds in addition to the southeast winds, and Clinton has more winds from the northeast. Galveston is different than the other monitors in that it still shows faster wind speeds on high ozone days, but the slower winds do show a northwest component, indicating possible influence of the urban area.

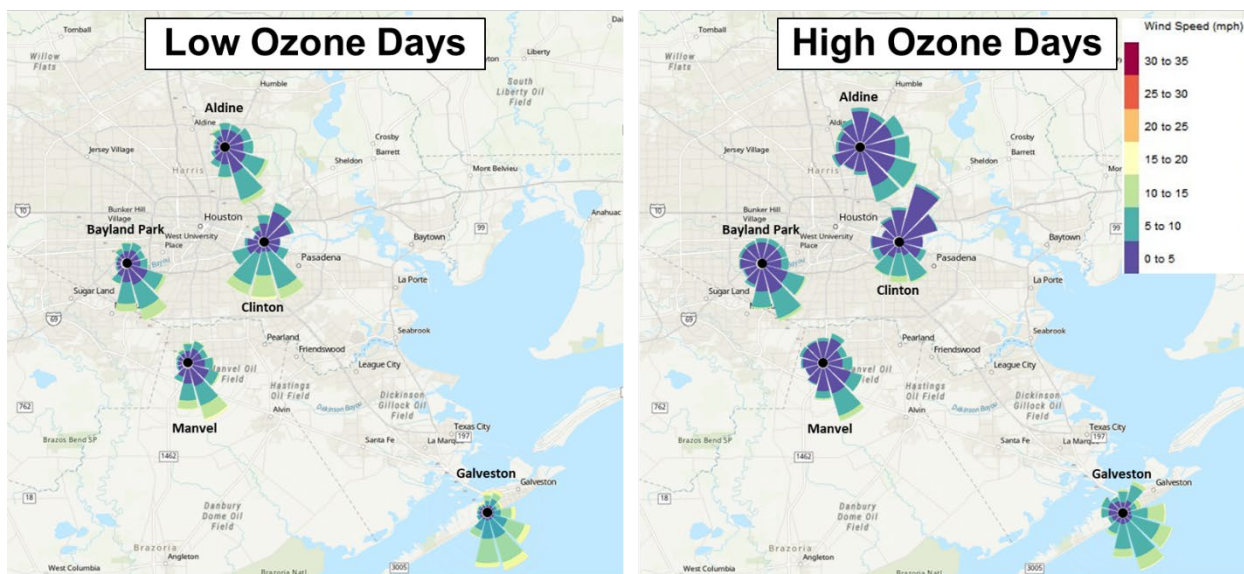


Figure 5-6: Ozone Season Wind Roses on High and Low Ozone Days in the HGB Area from 2012 through 2021

Surface-level back trajectories are calculated using a Lagrangian model that calculates the location of an air parcel using inverse distance square weighted wind speed and wind direction. This model uses no vertical mixing in the calculation of trajectories. The trajectory calculation uses five-minute resolution meteorological data from all Texas Commission on Environmental Quality (TCEQ) ground-based meteorological monitors in the HGB area, essentially putting the trajectory height at 10 meters above ground level (mAGL).

For this analysis, surface-level back trajectories were calculated for every ozone exceedance day at four monitors in the HGB area from 2017 through 2021. The monitors investigated were Aldine, Bayland Park, Deer Park, and Manvel. Aldine, Bayland Park and Manvel were selected because those monitors frequently measure the highest ozone concentrations and Deer Park was chosen to represent air in the area near the Houston Ship Channel. Trajectories were calculated starting at the hour of maximum one-hour ozone for the day at each respective monitor and then were run backwards for four hours. Some exceedances days may have missing meteorological data so not all exceedance days may have a corresponding trajectory.

The surface-level back trajectories are displayed in Figure 5-7: *Surface-Level Back-Trajectories at on Ozone Exceedance Days at Four Monitors in the HGB Area from 2017 through 2021*. The blue dots on the map represent the estimated location of each air

parcel at five-minute intervals. Although the monitors show various wind patterns on ozone exceedance days, they all show slow wind speeds. Often the winds on these ozone exceedance days stay within Harris County, except for Manvel, which is in Brazoria County. For many ozone exceedance days, the winds appear to come from in the direction of the Houston Ship Channel, before slowly moving across the urban area and ending at the downwind monitor.

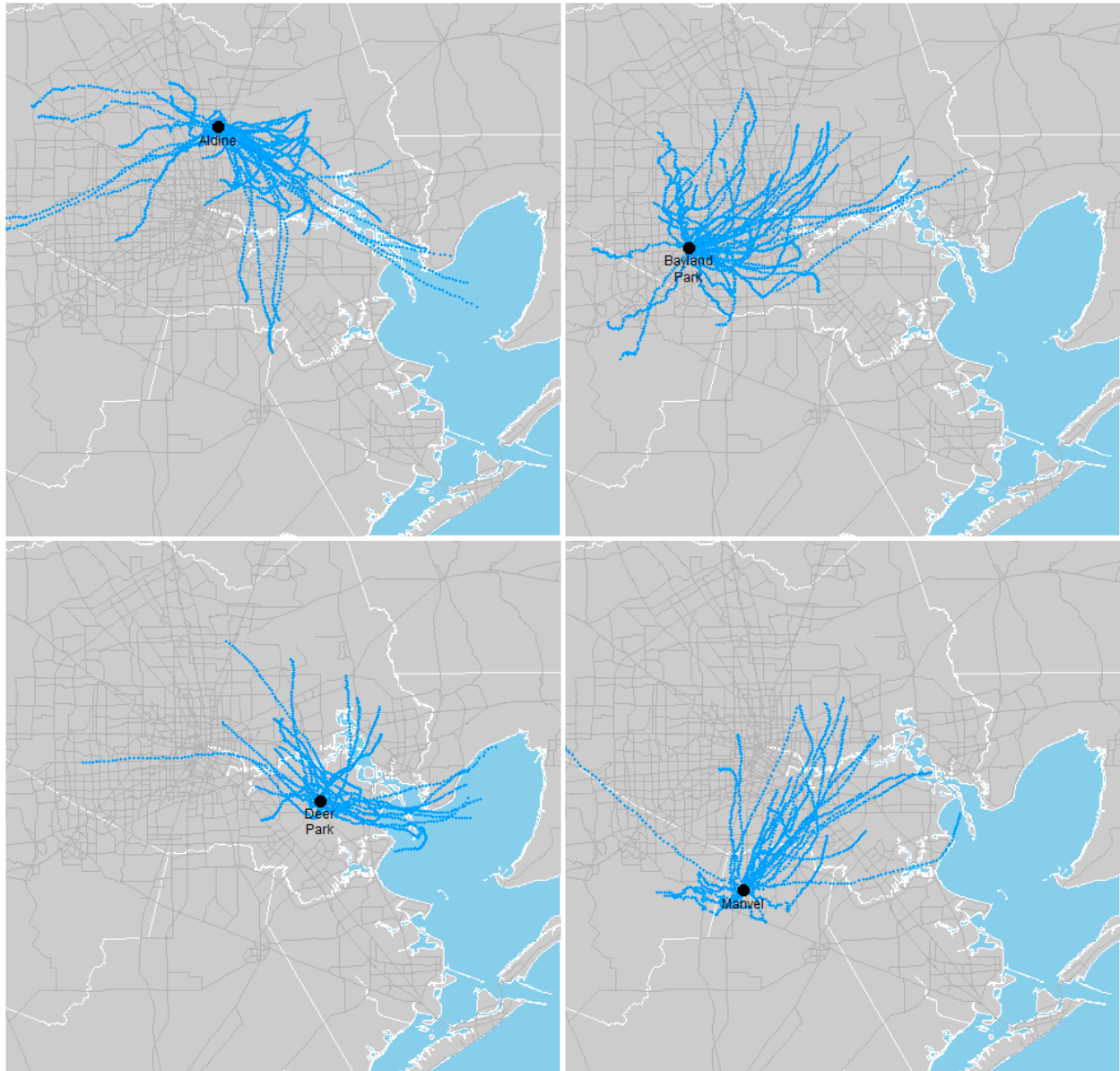


Figure 5-7: Surface-Level Back-Trajectories at on Ozone Exceedance Days at Four Monitors in the HGB Area from 2017 through 2021

5.4.3 Upper-Level Winds

While surface winds can show how ozone is formed locally, upper-level wind characterization can indicate potential sources that transport ozone into the area from other regions. Upper-level winds are examined using the HYSPLIT model which was developed by the National Oceanic and Atmospheric Administration's (NOAA) Air

Resources Laboratory (ARL) (Stein et al. 2015, Rolph et al. 2017). HYSPLIT back trajectories were computed for each day of the ozone season from 2012 through 2021. The 72-hour back trajectories were started at 12:00 LST at the center of the HGB area using an altitude of 500 mAGL and North American Mesoscale Forecast System (NAM) 12 kilometer (km) gridded meteorological data.

Trajectories with similar patterns were then combined to distinguish mean transport patterns into the HGB area. This analysis used a HYSPLIT clustering algorithm to group multiple trajectories based on trajectory size and shape. The total spatial variance (TSV) was used to determine seven clusters for the HGB area. To further investigate what transport patterns lead to high or low ozone in the HGB area, various ozone statistics were calculated for each trajectory cluster.

Results of the analysis are displayed in Figure 5-8: *Mean of 72-Hour HYSPLIT Back Trajectory Clusters and Ozone Exceedance Days for the Ozone Season in the HGB Area from 2012 through 2021*. The trajectories shown in the map are just the centerline of each cluster, meaning individual trajectories in each cluster may vary. The results also show the percent of total trajectories within each cluster as well as the number of ozone exceedance days associated with each cluster.

About 64% of the trajectories from clusters one, four, five and six are from the south and southeast and pass over the Gulf of Mexico. The longer Gulf of Mexico clusters four and five are associated with the lowest number of ozone exceedance days, zero and two respectively. This indicates that winds on those days are faster and bring clean air from the Gulf of Mexico through the HGB area, causing low ozone values. The other two Gulf of Mexico clusters one and six do have some ozone exceedance days, 28 and 26 respectively, but both are shorter, indicating slower winds for these clusters. Cluster one also appears to end near the Yucatan Peninsula in Mexico, which could be associated with transport from that area.

About 19% of trajectories are associated with cluster three, which is the shortest cluster and is associated with the largest number of ozone exceedance days at 120 days. This cluster appears to form a half circle and passes from the southeast over the Gulf of Mexico before turning northward and passing over the Texas-Louisiana border area. This indicates that days in this cluster have extremely slow winds that are possibly recirculating. While there may be some transport from industry near the Texas-Louisiana area, it is more likely that these trajectories are associated with local pollutants that accumulate and recirculate over the HGB area.

The last two clusters two and seven are associated with continental air from the north and northeast and account for about 18% of trajectories. These clusters have less ozone exceedance days, 30 and 45 respectively, compared to cluster 3, but more compared to the Gulf of Mexico Clusters. Cluster two is longer than cluster seven and is in turn associated with less ozone exceedance days. These continental clusters indicate that ozone on these days is possibly from continental transport from both within and outside of Texas.



Figure 5-8: Mean of 72-Hour HYSPLIT Back Trajectory Clusters and Ozone Exceedance Days for the Ozone Season in the HGB Area from 2012 through 2021

The other ozone statistics for each cluster are shown in Table 5-1: *Eight-Hour Ozone Statistics in ppb by HYSPLIT Cluster*. Overall, ozone statistics follow the same general pattern that was observed with the ozone exceedance days with some minor variations. It appears that the highest ozone concentration was associated with cluster seven,

although higher ozone concentrations more frequently occur in cluster three. At least 25% of days in cluster three and cluster seven are associated with ozone levels above the NAAQS, as indicated by the 75th percentile values of 74 ppb and 71 ppb respectively. Although cluster five is associated with the lowest ozone concentrations on average, clusters one and six, which both pass over the Gulf of Mexico, have lower minimum eight-hour ozone values, 15 ppb and 14 ppb respectively.

Table 5-1: Eight-Hour Ozone Statistics in ppb by HYSPLIT Cluster

Statistic	1	2	3	4	5	6	7
Count	446	163	347	166	142	450	165
Mean	47	59	63	46	37	47	63
Standard Deviation	14	12	16	11	10	13	16
Minimum	15	19	19	25	20	14	22
25%	36	52	52	38	30	39	53
50%	45	58	63	44	36	46	62
75%	56	67	74	53	44	54	71
Maximum	113	104	109	84	69	86	136

Overall, the HYSPLIT cluster analysis indicates that the highest ozone levels in the HGB area are most frequently associated with slow, recirculating local winds. There are also high ozone days associated with continental transport from the north and northeast. Air from the Gulf of Mexico is most often associated with low ozone concentrations, but on days with slower winds, air from this direction may also produce high ozone.

5.4.4 Ozone Concentrations versus Winds

Wind speed and direction are also used to determine potential sources for ozone. One method to perform this type of source attribution involves the use of bivariate polar plots (Uria-Tellaetxe and Carslaw 2014). Bivariate polar plots show how pollutant concentrations vary with wind speed and wind direction at certain receptor location. These types of plots help to figure out the type of source based on wind-speed dependence analysis. Bivariate polar plots use the Conditional Probability Function (CPF) to identify potential sources. CPF calculates the probability that, for a particular wind direction, the concentration of species is greater than a specified value. The value specified is usually expressed as a percentile of the species of interest. Bivariate polar plots are constructed by partitioning wind speed, wind direction, and pollutant concentration data into wind speed and wind direction bins. Mean pollutant concentration is then calculated for each bin. CPF is the ratio of number of samples in a given bin having some defined high concentration, to the total number of samples in that bin. The CPF analysis shows which wind direction and wind speed intervals are dominated by high concentrations.

This analysis used one-hour ozone, resultant wind speed, and resultant wind direction data for the ozone season from 2012 through 2021 at Aldine, Bayland Park, Clinton, Manvel, and Galveston. Aldine Bayland Park, and Manvel were chosen since those monitors frequently measure the highest ozone concentrations, Clinton was chosen to represent air near the Houston Ship Channel, and Galveston was chosen to represent coastal air. The conditional probability was then calculated for the 95th percentile. This value corresponds to one-hour ozone concentrations greater than or equal to 80 ppb at

Aldine, Bayland Park, and Manvel, 73 ppb at Clinton, and 75 ppb at Galveston. For easier interpretation of the results, the bivariate polar plots were then displayed on a map of the HGB area. The results are shown in Figure 5-9: *One-Hour Ozone Bivariate Polar Plots for the Ozone Season from 2012 through 2021 at Select Monitors in the HGB Area*. The plots at the various monitors are not the same scale. In the plots, the warmer (redder) colors represent wind direction and speeds that are more likely to have high one-hour ozone concentrations. The higher wind speeds are further from the center of the plots, with each light gray ring representing a wind speed increment of 2 mph at Aldine and Bayland Park, and 5 mph at Clinton, Manvel, and Galveston.

The plots show that, except for Galveston, the highest ozone concentrations occur at the slower wind speeds from 2 mph to 8 mph. At Galveston, high ozone occurs with both slower wind speeds but also faster wind speeds above 15 mph. The faster winds speeds and high ozone at Galveston is an indication that the highest ozone at that monitor likely originates from the HGB urban area. The direction with the highest ozone values varies by monitor but it appears that the highest ozone originates in the direction of the Houston Ship Channel. This correlates well with the surface trajectories on high ozone days which also show winds originating in the Houston Ship Channel then moving across the urban area before ending up at the monitor with the highest ozone concentration.

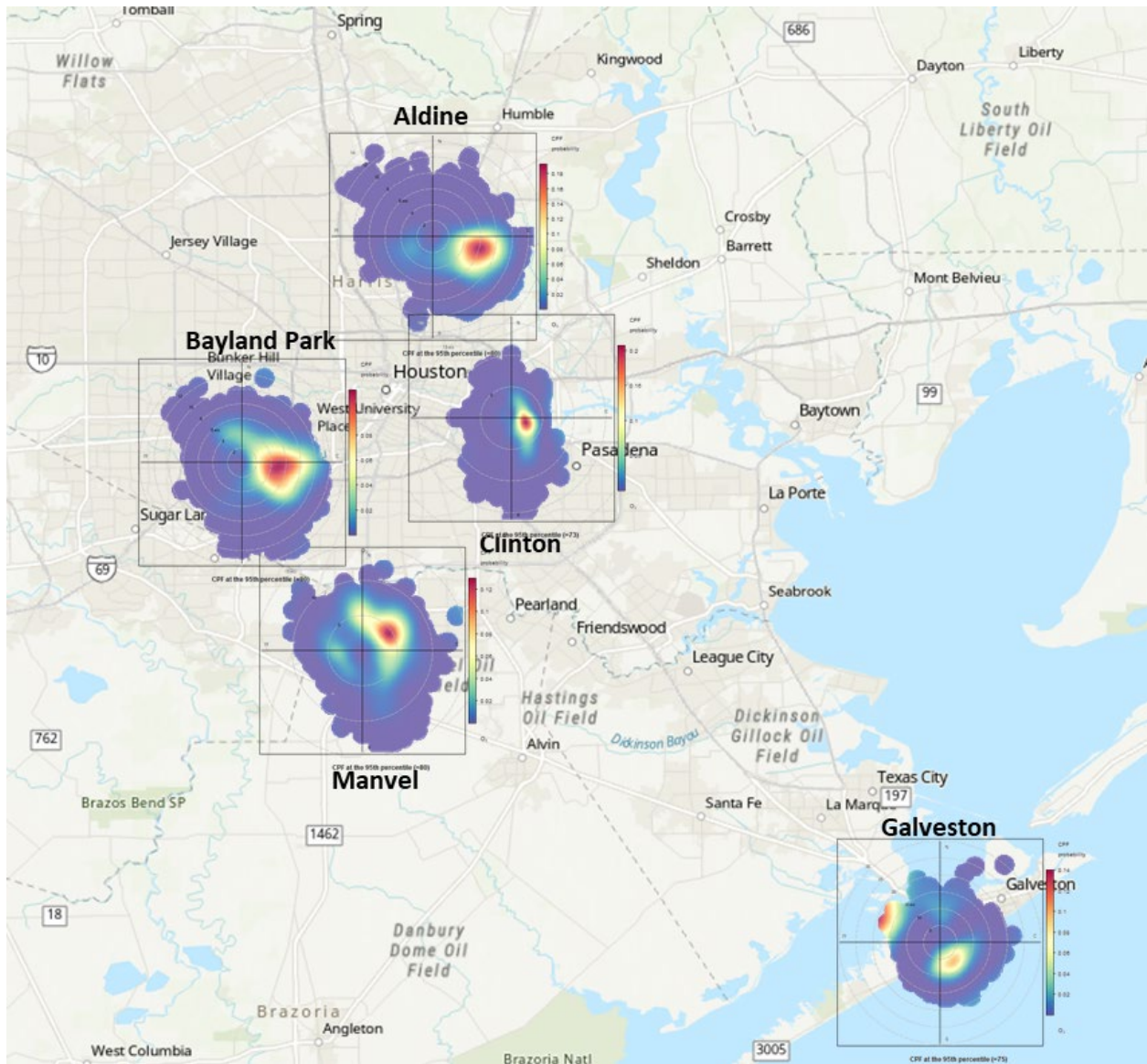


Figure 5-9: One-Hour Ozone Bivariate Polar Plots for the Ozone Season from 2012 through 2021 at Select Monitors in the HGB Area

5.5 METEOROLOGICALLY ADJUSTED OZONE CONCENTRATIONS

Meteorological conditions play an important role in ozone formation. Year-to-year variability in meteorological conditions in turn cause variability in ozone concentration trends. Although design values consider this variability by averaging the fourth-highest MDA8 ozone over three-years, this is often not enough to account for years with extreme meteorological conditions such as low winds speeds, drought, or extremely high temperatures. Investigating meteorological influences on ozone trends allows analysis of how ozone concentrations respond to changes in emissions rather than changes in the meteorology.

Meteorologically adjusted MDA8 ozone values represent what the ozone would have been if meteorological effects on ozone concentrations are removed. Without the influence of meteorology, changes observed in ozone concentrations are more likely

due to emissions changes rather than extreme meteorological events. The Environmental Protection Agency (EPA) has developed a statistical model that uses local weather data to adjust the ozone trends according to the meteorology for that year (Wells et al. 2021). These trends compare the average, 90th percentile, and 98th percentile MDA8 ozone from May through September to the meteorologically adjusted average, 90th percentile, and 98th percentile MDA8 ozone from May through September. The EPA calculated these trends for each ozone monitor in the HGB area from 2012 through 2021 (EPA 2022). Although results for all statistics were examined, only the 98th percentile trends will be discussed in this document since it most closely relates with the ozone values that are used in the design value calculations. The 98th percentile is approximately the eight-largest MDA8 value for the year.

Trends at four monitors with the highest fourth-highest MDA8 ozone were first investigated. The results are shown in Figure 5-10: *Meteorologically Adjusted 98th Percentile MDA8 Ozone for May through September at Select Monitors in the HGB Area*. The results show how for each year, meteorology can affect each monitor differently. Croquet appears to measure higher ozone when adjusted for meteorology for the past several years. This means the ozone at that monitor should have been higher, but meteorological variables at that monitor caused it to be lower. It also shows that the fourth-highest MDA8 ozone at Croquet in 2021 increased due to meteorology.

All four monitors show lower ozone in 2014 and higher values in 2015 due to meteorology. The four monitors show that there is little trend in adjusted or unadjusted ozone concentrations from 2012 through 2021. Manvel is the only monitor of the four to show a slight decrease in ozone trends, even when adjusted for meteorology. These results match well with those from a study that used a generalized additive model (GAM) to correct ozone trends for meteorology (Mountain 2022). That study found decreases in ozone for the past ten years slowed when adjusting for meteorology.

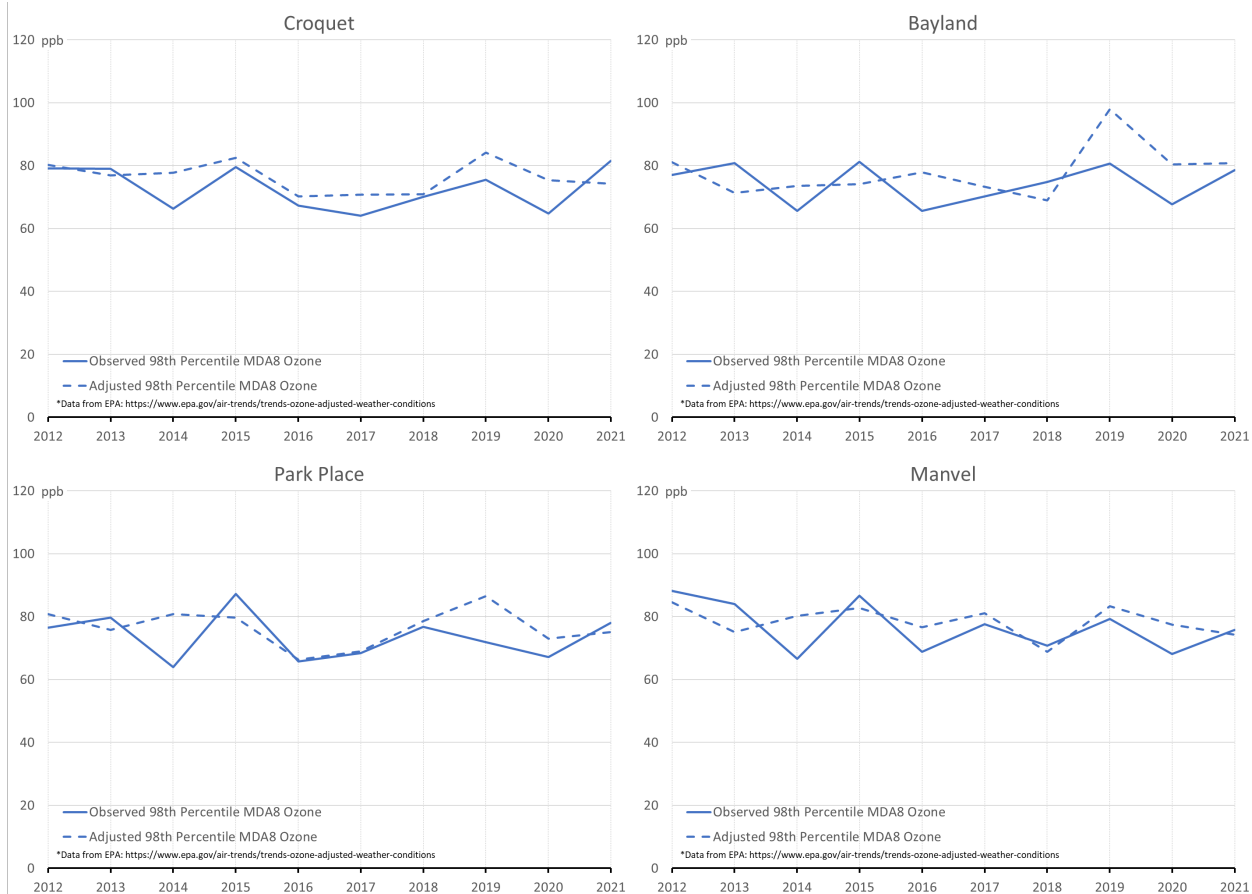


Figure 5-10: Meteorologically Adjusted 98th Percentile MDA8 Ozone for May through September at Select Monitors in the HGB Area

To aggregate the results further, for each year the maximum, median, and minimum 98th percentile MDA8 value was calculated from all monitors within the HGB area. This allows for easier examination of the results across all monitors. The results for the 98th percentile are displayed in Figure 5-11: *Meteorologically Adjusted Ozone Trends for May through September in the HGB Area*. These trends confirm that the low ozone in 2014 and the high ozone in 2015 were largely influenced by the meteorology. Another year with large meteorological influences was 2019, when observed ozone appears to be lower mostly due to meteorology. There seems to be some meteorological effects on ozone in 2020. Overall, there was little effect of meteorology on ozone in 2021.

From 2012 through 2021 the trends show only small decreases in ozone, both measured and meteorologically adjusted. Overall trends are very flat, even more so when ozone is adjusted for meteorology. This suggests that recent decreases observed in ozone concentrations are more likely due to yearly changes in meteorology rather than emissions changes. This correlates well with the flat trends observed in both NO_x and VOC concentrations.

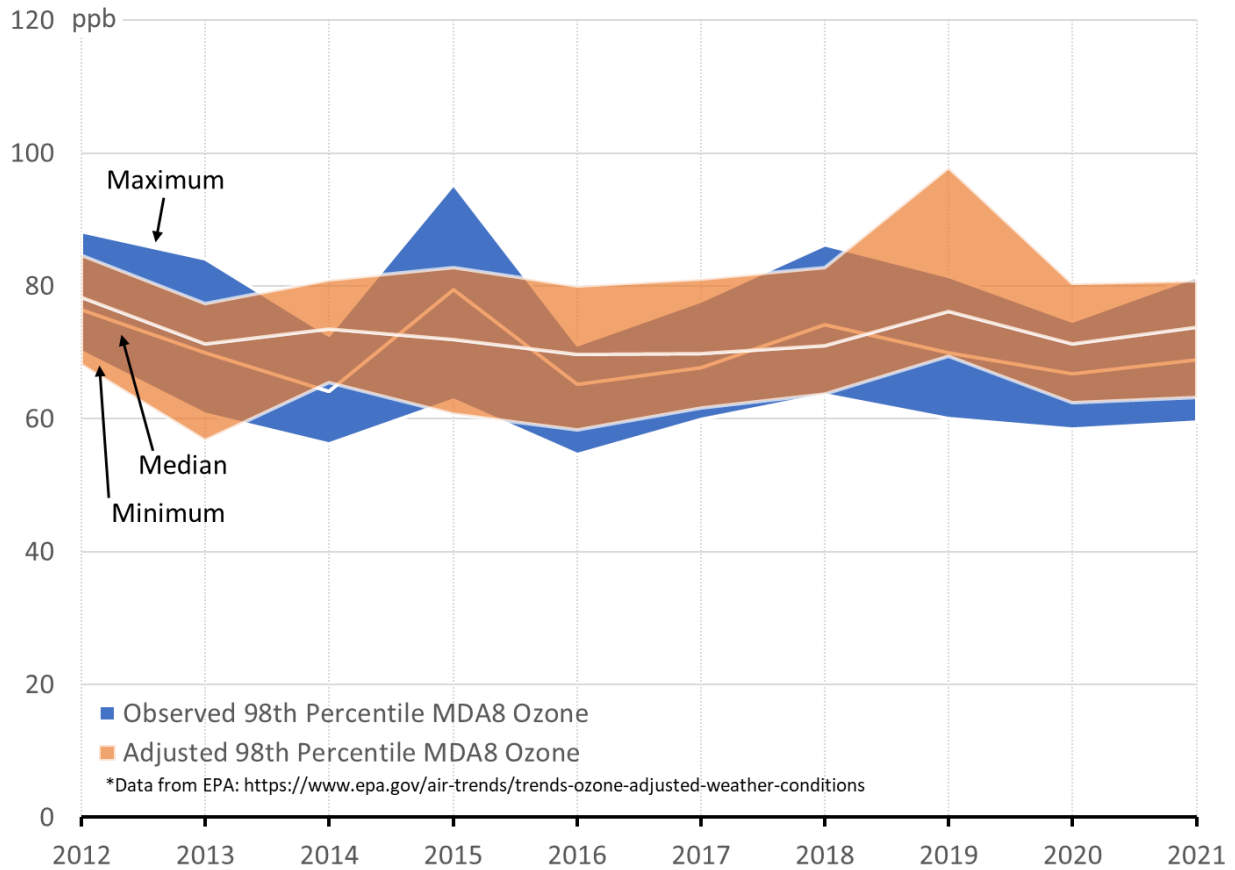


Figure 5-11: Meteorologically Adjusted Ozone Trends for May through September in the HGB Area

Another way to investigate the meteorological adjusted ozone trends is to examine the difference between the meteorologically adjusted and the observed 98th percentile MDA8 ozone for each year. After finding the difference at each monitor, the maximum, median, and minimum difference was calculated for the area. Positive differences indicate that the ozone that year was higher because of meteorology and negative differences indicated that the ozone that year was lower because of the meteorology. Results are shown in Figure 5-12: *Difference Between Meteorological Adjusted and Observed 98th Percentile MDA8 Ozone Concentrations from May through September in the HGB Area.*

Results show that 2015 had the largest increases in ozone due to meteorology. Since 2015, more monitors in the HGB area observe lower ozone values due to meteorology. The lowest ozone values due to meteorology appeared to have occurred in 2019. There are variable results in 2021, with the highest ozone values being higher due to meteorology, but the lower values being lower due to meteorology.

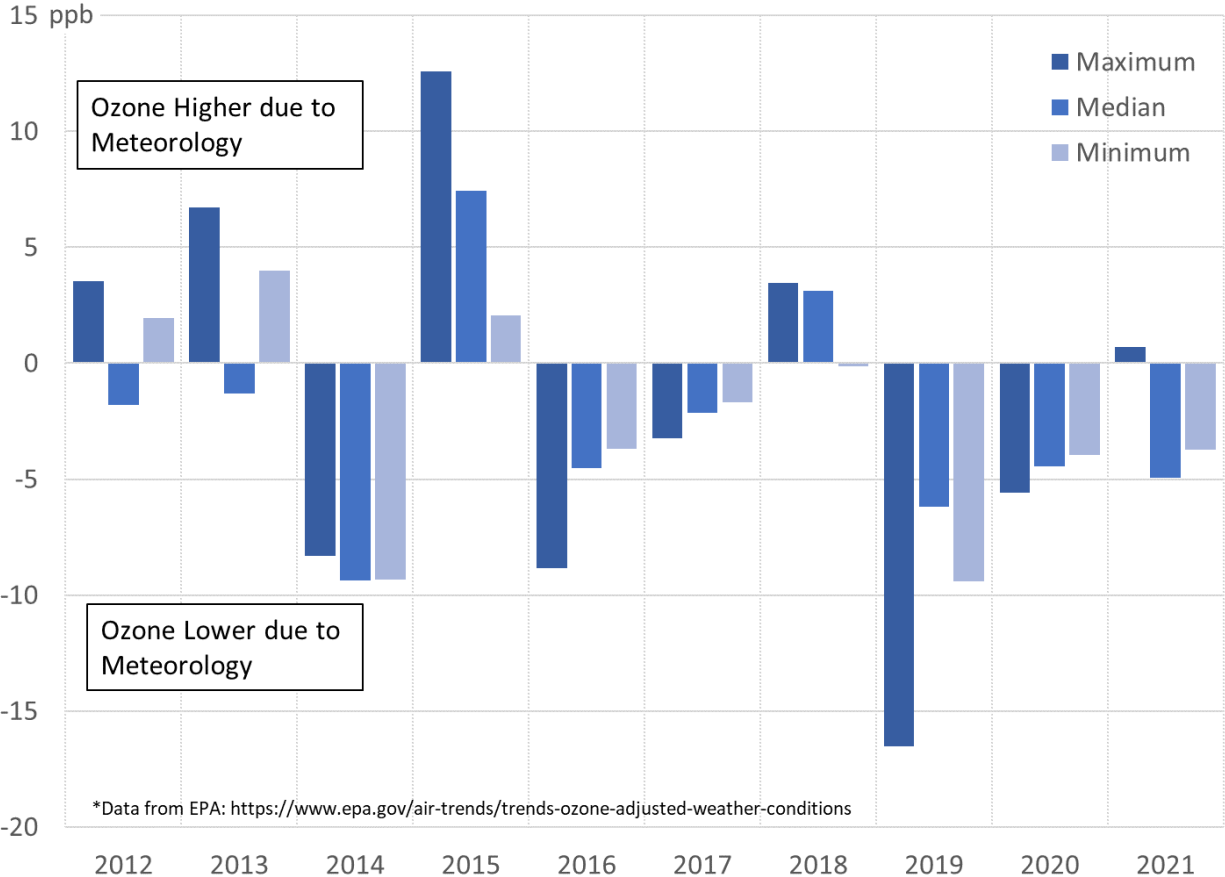


Figure 5-12: Difference Between Meteorological Adjusted and Observed 98th Percentile MDA8 Ozone Concentrations from May through September in the HGB Area

CHAPTER 6: CONCLUSIONS

This conceptual model provides a detailed examination of ozone formation in the Houston-Galveston-Brazoria (HGB) area with a focus on ozone levels above 70 parts per billion (ppb). Most of the analyses in this conceptual model focus on ten years of data from 2012 through 2021. This focus allowed the analyses to incorporate newer data and investigate recent changes in how, when, and where ozone forms in the HGB area.

From 2012 through 2021, eight-hour ozone design values in the HGB area have decreased 13%. The area monitors attainment of the 1997 eight-hour ozone National Ambient Air Quality Standards (NAAQS) of 84 ppb, but was designated as nonattainment of the 70 ppb 2015 eight-hour ozone standard. Maximum eight-hour ozone design values most recently occurred at Bayland Park in the west, but it is common for the location of the maximum design value to change over time. In previous years, the maximum eight-hour ozone design value occurred at Aldine in the north and Manvel in the southwest. Fourth-highest eight-hour ozone values, which are used to calculate design values, have remained flat.

At a threshold of 70 ppb, the ozone season in the HGB area peaks in June and again in August, with a low occurring in July. Although peak ozone occurs in June and August, high ozone concentrations can occur anytime from March through October. Much of the analysis in this conceptual model focused on the months of March through October to capture the ozone formation process during this important period.

During the ozone season, the highest one-hour ozone occurs from about 13:00 local standard time (LST) through 14:00 LST. Ozone peaks later in the day on high ozone days compared to low ozone days. Typically, ozone first peaks in areas closer to the coast and then peaks later in areas further north and west.

Regional background ozone coming into the HGB area is not well correlated with daily maximum eight-hour ozone concentrations on high ozone days. This suggests that there is both a transported and local component to ozone in the HGB area. Although it varies year-to-year, overall, estimates of local ozone production and regional background ozone in the HGB area have not changed much from 2012 through 2021. Regional background ozone and local ozone increase from low to high ozone days, but they increase proportionally, with background contributing approximately 60% and locally produced ozone contributing 40% to ozone concentrations in the HGB area. The spring season observed the highest background ozone while the late summer season observed the highest local ozone production. This indicates that the spring ozone season is characterized by high background ozone coming into the HGB area while the late-summer ozone season is characterized by more local ozone production.

Ozone is not directly emitted into the atmosphere, but rather formed through a photochemical reaction with nitrogen oxides (NO_x) and volatile organic compounds (VOC). Examination of ambient NO_x trends from 2012 through 2021 shows only modest changes across the area. Over that time, 95th percentile NO_x decreased 3% and median NO_x increased 2%. Changes in NO_x were variable across the HGB area. The largest NO_x increases occurred at monitors in the Houston Ship Channel, which

measure the largest NO_x concentrations, and at monitors in Galveston and Brazoria Counties, which measure the lowest NO_x concentrations.

VOC and highly reactive VOC (HRVOC) concentrations show variable trends. 95th percentile TNMOC and HRVOC increased from 2012 through 2021 by 4% and 14%, respectively. Median values show less change, with a decrease of 2% in median TNMOC and an increase of 11% in median HRVOC. The areawide increases, especially of HRVOC, appear to be due to large increases at select monitors in the Houston Ship Channel. Weighting VOC species by maximum incremental reactivity shows that HRVOC, pentanes, and butanes contribute the most to total VOC concentrations. HRVOC contributions to reactivity weighted VOC concentrations range from 20% to 50%. Of the HRVOC species, ethylene and propylene typically have the largest reactivity weighted concentrations.

In the past, high ozone in the HGB area was characterized by sudden rapid increases in ozone, due to either concentrated ozone plumes or large sudden releases of ozone precursors, in particular HRVOC. Trends show that these rapid increases continue to occur in the area, but at lower levels and frequency than previously observed. These rapid ozone increases are typically observed at monitors located in closer proximity to the Houston Ship Channel. In general, eight-hour ozone concentrations are correlated to rapid one-hour ozone increases, with higher daily-maximum eight-hour ozone observed on days with larger one-hour ozone increases.

From 2012 through 2021, NO_x emissions increased 7%, VOC emissions decreased 14%, and HRVOC emissions decreased 3%. While there are large point sources in Lake Jackson and at the Parish power plant (for NO_x), the Houston Ship Channel contains some of the largest emissions for NO_x, VOC, and HRVOC.

The VOC or NO_x limitation of an air mass can determine if decreases in either NO_x (NO_x limited) or VOC (VOC limited) would have a larger effect on ozone concentrations. VOC-NO_x ratios vary across the day at all sites studied, with ratios closer to NO_x limited in the early morning hours, transitioning to transitional and closer to VOC limited as motor vehicle traffic increases. The ratio differs according to location in the area, with the urban area maintaining a more VOC limited regime, industrial areas maintaining a more transitional regime, and suburban sites being more NO_x limited.

Analysis of ozone and precursors on the weekdays versus the weekends shows that ozone in most of the HGB area decreases on the weekends, driven largely by reductions in NO_x concentrations due to changes in rush hour traffic patterns. The decreasing ozone concentrations that occur with the decreasing NO_x on the weekend are an indicator that the area may benefit more from NO_x reductions compared to VOC reductions.

Meteorological conditions linked to high ozone in the HGB area include high temperatures, low relative humidity, and slow recirculating winds. On high ozone days, slow surface winds transport emissions from the Houston Ship Channel across the urban area to downwind monitors. Upper-level winds also show that the highest ozone concentrations occur with the slowest wind speeds and under conditions that contain a wind flow reversal, which would allow for increased accumulation of pollutants in the area.

Overall, high ozone in the HGB area mostly occurs from April through June and from August through October. High ozone typically occurs on hot sunny days with dry conditions and slow recirculating winds. On these days, urban emissions throughout the area combine with emissions from the Houston Ship Channel to create ozone at downwind monitors. Although the HGB area produces much of its own ozone, there are also high ozone days that are associated with continental transport from the north and northeast. The HGB area measures mostly transitional ozone chemistry, meaning reductions in either VOC or NO_x could reduce ozone concentrations; however, equal reductions in VOC or NO_x may not lead to equivalent reductions in ozone. It is likely that controlling NO_x would be more effective at influencing the HGB area design value than controlling VOC, although ozone formation may respond to VOC (in particular HRVOC) emission reductions in some parts of the metro area and at certain times of day.

CHAPTER 7: REFERENCES

- Berlin, Shaena R., Andrew O. Langford, Mark Estes, Melody Dong, and David D. Parrish. 2013. "Magnitude, decadal changes, and impact of regional background ozone transported into the greater Houston, Texas area." *Environ. Sci. Technol.* 47 (24): 13985-13992. <https://doi.org/10.1021/es4037644>.
- Carter, Willian P. 2010. "Updated Maximum Incremental Reactivity Scale and Hydrocarbon Bin Reactivities for Regulatory Application." Prepared for the California Air Resources Board. Contract No. 07-339. January 28, 2010.
- Census Bureau. 2022. "County Population Totals: 2020-2021." Last Modified March 1, 2022. <https://www.census.gov/data/datasets/time-series/demo/popest/2020s-counties-total.html>.
- Chan, E., R. J. Vet. 2010. "Baseline levels and trends of ground level ozone in Canada and the United States." *Atmos. Chem. Phys.* 10: 8629-8647. <https://doi.org/10.5194/acp-10-8629-2010>.
- Davis, J. M., B. K. Eder, D. Nychka, and Q. Yang. 1998. "Modeling the effects of meteorology on ozone in Houston using cluster analysis and generalized additive models." *Atmospheric Environment.* 32: 2505-2520. [https://doi.org/10.1016/S1352-2310\(98\)00008-9](https://doi.org/10.1016/S1352-2310(98)00008-9).
- Deng, K., W. Liu, C. Azorin-Molina, S. Yang, H. Li, G. Zhang, et al. 2022. "Terrestrial stilling projected to continue in the Northern Hemisphere mid-latitudes." *Earth's Future.* 10, e2021EF002448. <https://doi.org/10.1029/2021EF002448>.
- Dickens, Angela F. 2022. "Ozone Formation Sensitivity to NO_x and VOC Emissions in the LADCO Region. Technical Report." Prepared for the Lake Michigan Air Directors Consortium. September 9, 2022. https://drive.google.com/file/d/1Y_xF9v8xF4wBaE2Eyro0LHUGAb1BPhLf/view.
- Edwards, Rebecca Paulson, Oliver Sale, a Gary A. Morris. 2018. "Evaluation of El Nino-Southern Oscillation influence on 30 years of tropospheric ozone concentrations in Houston." *Atmospheric Environment.* 192, 72-83. <https://doi.org/10.1016/j.atmosenv.2018.08.032>.
- EPA. 2018. "Modeling Guidance for Demonstrating Attainment of Air Quality Goals for Ozone, PM2.5, and Regional Haze." November 2018. https://www.epa.gov/sites/default/files/2020-10/documents/o3-pm-rh-modeling_guidance-2018.pdf.
- EPA. 2022. "Trends in Ozone Adjusted for Weather Conditions." Last modified June 1, 2022. <https://www.epa.gov/air-trends/trends-ozone-adjusted-weather-conditions>.
- Ge, Sijie, Sujing Wang, Qiang Xu, Thomas Ho. 2020. "Effect of industrial flare DRE's derived by CFD and WERF on ozone pollution through CAMx simulation." *Atmospheric Environment.* 238, 117723. <https://doi.org/10.1016/j.atmosenv.2020.117723>.

Goldberg, Daniel L., Monica Harkey, Benjamin de Foy, Laura Judd, Jeremiah Johnson, Greg Yarwood, and Tracey Holloway. 2022. "Evaluating NO_x emissions and their effect on O₃ production in Texas using TROPOMI NO₂ and HCHO." *Atmos. Chem. Phys.* 22, 10875–10900. <https://doi.org/10.5194/acp-22-10875-2022>.

Hafner, Hilary R. and Bryan M. Penfold. 2018. "PAMS Data Validation and Analysis Training Material, Sonoma Technology, Inc." Prepared for the EPA. January 4, 2018. https://www.epa.gov/sites/default/files/2020-03/documents/pams_data_analysis_workbook.pdf.

Kleinman, L. I., P.H. Daum, D. Imre, Y. Lee, L.J. Nunnermacker, and S.R. Springston. 2002. "Ozone production and hydrocarbon reactivity in 5 urban areas: A cause of high ozone concentration in Houston." *Geophysical Research Letters*. 30, 1639-1642. <https://doi.org/10.1029/2001GL014569>.

Lefer, Barry, Bernhard Rappenglück, James Flynn, Christine Haman. 2010. "Photochemical and meteorological relationships during the Texas-II Radical and Aerosol Measurement Project (TRAMP)." *Atmos. Environ.* 44: 4005-4013. <https://doi.org/10.1016/j.atmosenv.2010.03.011>.

Li, Wei, Yuxuan Wang, Claudia Bernier, Mark Estes. 2020. "Identification of Sea Breeze Recirculation and Its Effects on Ozone in Houston, TX, During DISCOVER-AQ 2013." *Journal of Geophysical Research: Atmospheres*. 125, e2020JD033165. <https://doi.org/10.1029/2020JD033165>.

Mountain, Marikate. 2022. "Final Report: Meteorologically Corrected Ozone, SO₂, and PM_{2.5} Trends." Atmospheric and Environmental Research Inc. Prepared for Erik Gribbin, for the Texas Commission on Environmental Quality. December 6, 2022.

Nielsen-Gammon, John W., James Tobin, Andrew McNeel, and Guohui Li. 2005. "A conceptual model for eight-hour ozone exceedances in Houston, Texas, Part 1: Background ozone levels in eastern Texas." HARC/TERC/TCEQ report. project H12.2004.8HRA. January 29, 2005.

Rappenglück Bernhard, Ryan Perna, Shiyuan Zhong, Gary A. Morris. 2008. "An analysis of the vertical structure of the atmosphere and the upper-level meteorology and their impact on surface ozone levels in Houston, Texas." *J. Geophys. Res.* 113, D17315. <https://doi.org/10.1029/2007JD009745>.

Rolph, Glenn, Ariel Stein, and Barbara Stunder. 2017. "Real-time Environmental Applications and Display System: READY." *Environmental Modelling & Software*. 95, 210-228. <https://doi.org/10.1016/j.envsoft.2017.06.025>.

Ryerson, T.B.; M. Trainer, W.M. Angevine, C.A. Brock, R.W. Dissly, F.C. Fehsenfeld, G.J. Frost, et al. 2003. "Effect of petrochemical industrial emissions of reactive alkenes and NO_x on tropospheric ozone formation in Houston, Texas." *J. Geophys. Res.* 108(D8), 4249. <https://doi.org/10.1029/2002JD003070>.

Smith, Jim, Fernando Mercado, and Mark Estes. 2013. "Characterization of Gulf of Mexico background ozone concentrations." Presented at CMAS conference, October 2013.

Soleimanian, Ehsan, Yuxuan Wang, Mark Estes. 2022. "Long-term trend in surface ozone in Houston-Galveston-Brazoria: Sectoral contributions based on changes in volatile organic compounds." *Environmental Pollution*. 308, 119647. <https://doi.org/10.1016/j.envpol.2022.119647>.

Stein, A. F., R. R. Draxler, G. D. Rolph, B. J. B. Stunder, M. D. Cohen, and F. Ngan. 2015. "NOAA's HYSPLIT atmospheric transport and dispersion modeling system." *Bull. Amer. Meteor. Soc.* 96, 2059-2077. <https://doi.org/10.1175/BAMS-D-14-00110.1>.

Texas Commission on Environmental Quality. 2002. "Conceptual Model for Ozone Formation in the Houston-Galveston Area, Appendix A to Phase I of the Mid Course Review Modeling Protocol and Technical Support Document." December 13, 2002. https://wayback.archive-it.org/414/20210529061639/https://www.tceq.texas.gov/assets/public/implementation/air/am/docs/hgb/protocol/HGMCR_Protocol_Appendix_A.pdf.

Texas Commission on Environmental Quality. 2019a. "Appendix D: Conceptual Model for the HGB Attainment Demonstration SIP Revision for the 2008 Eight-Hour Ozone Standard." September 11, 2019. https://www.tceq.texas.gov/assets/public/implementation/air/sip/hgb/hgb_serious_A_D_2019/HGB_AD_SIP_19077SIP_Appendix%20D.pdf.

Texas Commission on Environmental Quality. 2019b. "Appendix D: Conceptual Model for the DFW Attainment Demonstration SIP Revision for the 2008 Eight-Hour Ozone Standard." September 11, 2019. https://www.tceq.texas.gov/assets/public/implementation/air/sip/dfw/dfw_ad_sip_2019/DFWAD_19078SIP_Appendix_D_pro.pdf.

Texas Transportation Institute. 2015. "Development of 2014 On-Road Mobile Source Annual, Summer, Weekday, and Winter Work Weekday Emissions Inventories for Specified Areas: Houston-Galveston-Brazoria Area." PGA Number: 582-15-52083-17.

Uria-Tellaetxe, Iratxe and David C. Carslaw. 2014. "Conditional bivariate probability function for source identification." *Environmental Modelling & Software*. 59, 1-9. <https://doi.org/10.1016/j.envsoft.2014.05.002>.

Vizuete, William, John Nielson-Gammon, Judy Dickey, Evan Couzo, Charles Blanchard, Peter Breitenbach, Quazi Z. Rasool, and Daewon Byun. 2022. "Meteorological based parameters and ozone exceedances in Houston and other cities in Texas." *Journal of the Air & Waste Management Association*. 72:9, 969-984. <https://doi.org/10.1080/10962247.2022.2064004>.

Wells, Benjamin, Pat Dolwick, Brian Eder, Mark Evangelista, Kristen Foley, Elizabeth Mannshardt, Chris Misenis, and Anthony Weishampel. 2021. "Improved estimation of trends in U.S. ozone concentrations adjusted for interannual variability in

meteorological conditions.” *Atmospheric Environment*. 248 (March): 118234.
<https://doi.org/10.1016/j.atmosenv.2021.118234>.

Webster, Mort, Junsang Nam, Yosuke Kimura, Harvey Jeffries, William Vizuete, David T. Allen. 2007. “The effect of variability in industrial emissions on ozone formation in Houston, Texas.” *Atmos. Environ.* 41: 9580-9593.
<https://doi.org/10.1016/j.atmosenv.2007.08.052>.

CHAPTER 8: DATA SOURCES

National Oceanic and Atmospheric Administration. 2022. "NAM 12 km (May 2007 - present)." Accessed September 1, 2022, <https://www.ready.noaa.gov/archives.php>.

Texas Commission on Environmental Quality. 2022. "Texas Air Monitoring Information System (TAMIS) Web Interface." Accessed September 1, 2022. <https://www17.tceq.texas.gov/tamis/index.cfm?fuseaction=home.welcome>.

Texas Commission on Environmental Quality. 2022. "Point Source Emissions Inventory." Accessed August 2022. <https://www.tceq.texas.gov/airquality/point-source-ei/psei.html>.

U.S. EPA. 2022. "Pre-Generated Data Files." Accessed September 1, 2022. https://aqs.epa.gov/aqsweb/airdata/download_files.html.